SESSION IV

RADIOIODINE REMOVAL AND RETENTION

Monday, August 2, 1976
CO-CHAIRMEN: R. D. Rivers, J. G. Wilhelm

AN AIRBORNE RADIOIODINE SPECIES SAMPLER AND ITS APPLICATION FOR MEASURING REMOVAL EFFICIENCIES OF LARGE CHARCOAL ADSORBERS FOR VENTILATION EXHAUST AIR

W. A. Emel, D. C. Hetzer, C. A. Pelletier, E. D. Barefoot, J. E. Cline

OPERATING EXPERIENCE WITH THE TESTING OF IODINE ADSORBERS ON THE AIR CLEAN UP SYSTEMS OF THE BELGIAN PWR POWER PLANTS

B. Deckers, P. Sigli, L. Trehen

HEAD-END IODINE REMOVAL FROM A REPROCESSING PLANT WITH A SOLID SORBENT

J. G. Wilhelm, J. Furrer, E. Schulte

REPORT OF THE GOVERNMENT-INDUSTRY COMMITTEE ON ADSORBERS AND ADSORPTION MEDIA

C. A. Burchsted

OPENING REMARKS OF SESSION CHARIMAN: (J. G. Wilhelm)

Thirteen years ago the first charcoals were developed which removed iodine in both organic and elemental form. Today, iodine filters for power reactor stations can be constructed with high decontamination factors, but some problems still remain unsolved. One of the most pressing at this time is the ageing and poisoning of iodine filters (which may take place within a few months, or even weeks) to such an extent that the lowest removal efficiencies acceptable for iodine filters will not be met. Four papers will be given on this subject.

Improved impregnants for activated charcoal are still the goal of R&D work. Of special interest are impregnants which allow operation at higher temperatures and better withstand poisoning. In addition, it is of interest to increase the variety of base charcoals which can be used effectively. Two papers will be presented on this subject.

A new inorganic material was developed for removal of iodine from fuel reprocessing plant effluents. Two papers will discuss the trapping of iodine on silver containing materials;one will discuss a method for recycling expensive silver zeolite adsorbers.

The low discharge levels for radioactive iodides still permissible may limit the number of nuclear plants acceptable in a nuclear park. In some countries - Germany, for example - regulations are so stringent

that determination of the chemical forms of iodine releases may be a necessary step in calculating the actual hazards from such releases; surely elemental iodine moves most easily through the ingestion path and produces most of the irradiation of the surrounding population. One paper will discuss a sampler which separates effectively airborne radioiodine species.

Two papers will discuss the reliability of tests of sample-bypass canisters in determining the current condition of large-scale filter beds. These papers will consider alternatives of performing these tests, including a convenient test kit for in-situ evaluation of full-scale filter banks with radioiodine compounds.

Another paper will discuss the effects of various additives on the evaporation of iodine from containment spray-cooling solutions. Still another will discuss a facet of the post-LOCA environment which has previously been little studied: the effect of intense radiation on the performance of iodine - trapping charcoals.

One paper will present a new filter system design which allows convenient testing of HEPA filter gaskets and renewal of adsorption media in safe and convenient fashion.

Finally, a report will be given on the March, 1976 topical meeting held by ERDA in Washington, at which preliminary data on some of the items above were given, and matters related to standards, interlaboratory comparisons of adsorber tests, and laboratory certification were discussed.

IODINE EVAPORATION FROM IRRADIATED AQUEOUS SOLUTIONS CONTAINING THIOSULFATE ADDITIVE*

A. H. Dexter, A. G. Evans, and L. R. Jones
Savannah River Laboratory
E. I. du Pont de Nemours and Co.
Aiken, S. C. 29801

Abstract

Sodium thiosulfate in concentrations of 1 wt% was shown to limit iodine evaporation to 0.5% or less in $\sim 5 \times 10^{-4}$M aqueous solutions of iodine irradiated to 10^8 rad. Potassium hydroxide in concentrations of 0.05 wt% was almost as effective. Lower concentrations of thiosulfate were ineffective: iodine was almost completely released, and a portion was converted into a form capable of penetrating several inches of activated carbon. Attempts to identify the penetrating form were unsuccessful; it may be either a particulate or an aerosol because it was removable by HEPA filters.

Introduction

This paper reports measurements of the effectiveness of sodium thiosulfate in preventing the volatilization of iodine subjected to a radiation dose of 10^8 rad. Previous studies[1] at the Savannah River Laboratory (SRL) had shown that thiosulfate was very effective in inhibiting this release in a nonradiation environment. Earlier studies at Babcock and Wilcox[2] and at Oak Ridge National Laboratory[3] evaluated the effect of radiation on thiosulfate and demonstrated that a significant fraction of the thiosulfate would survive large doses of radiation. No previous measurements have been reported on the effect of radiation on the water-iodine-thiosulfate system.

In earlier work, in the absence of radiation, small concentrations of thiosulfate were found to be very effective in reducing iodine evolution from aqueous solutions of iodine.[1] For example, in studies that used ^{131}I as a tracer, 32.8% of the iodine in a 5×10^{-5}M aqueous solution volatilized in a 5-hr period; whereas with a 8×10^{-4}M concentration of thiosulfate present as an additive, only 0.00066% of the iodine was volatilized. On the basis of Zittel and Row's work,[3] about 60 to 70% of the thiosulfate was expected to be destroyed by the combined effects of temperature and radiation at doses of 10^8 rad. However, with an excess of thiosulfate present (for example, the 16 to 1 molar ratio used in the nonradiation experiments at SRL) - the volatilization of iodine in the presence of radiation was not expected to be significantly different from that in the absence of radiation. Laboratory-scale experiments were designed to evaluate this premise.

* Work done under Contract No. AT(07-2)-1 with the Energy Research and Development Administration.

Experimental

The SRL ^{60}Co Irradiation Facility[4] which provides ∿2.7 x 10^7 rad/hr was used to irradiate aqueous solutions of KI to doses of 10^8 rad. The KI in each experiment was "tagged" with ∿1 mCI of ^{131}I, and scintillation counting equipment was used to measure the volatilization of the ^{131}I as a function of radiation dose imparted to the solution. Typically, 4ℓ of solution in a stainless steel vessel was irradiated for ∿5 hr while air flowed over the solution surface at 13 ℓ/min. The volatilized ^{131}I was transported by the flowing air and collected on activated carbon that was monitored with a scintillation counter (Fig. 1). An inventory (material balance) was made of the ^{131}I activity of all system components after each test. Pre-irradiation pH was typically about 7, and in several experiments this was increased to >10 by adding KOH. The solutions were not buffered. Solution temperature during irradiation was ∿50°C.

Results

Experimental results are given in two parts: 1) the effect of additives, and 2) the attempts to identify a penetrating form of iodine that was found during the experiments.

Influence of Additives on Iodine Evaporation

The study included experiments with: a) no additive, b) sodium thiosulfate, c) sodium thiosulfate and potassium hydroxide, and d) potassium hydroxide.

Tests With No Additive. Irradiation of a water solution containing KI (5.6×10^{-4}M) to a dose of 10^8 rad caused the evaporation of 14.6% of the iodine. This result compared with 16 to 34% evaporation of iodine[1] from a solution containing elemental iodine (∿1.5×10^{-4}M) in the absence of radiation. These results indicate that radiation converts ionic iodide to volatile iodine, most probably through OH radical attack of the iodide

$$OH + I^- \rightarrow I - OH^- \qquad (1)$$

The OH radicals result from the radiolysis of the water. Further, because the iodine evaporation is about equivalent in the two experiments, the conversion of iodide to iodine is thought to be almost quantitative.

Sodium Thiosulfate Additive. When sodium thiosulfate was added at a molarity (5.5×10^{-4}) approximately equal to that of the KI, an almost quantitative release of the iodine occurred (94% in one experiment and 96% in another). The ineffectiveness of the thiosulfate at this concentration is thought to be due to the radiolysis of thiosulfate by the reaction[2]

$$S_2O_3^{=} + 4(0) + H_2O \rightarrow 2SO_4^{=} + 2H^+ \qquad (2)$$

augmented by acid decomposition of the thiosulfate by the reaction[2]

$$S_2O_3^{=} + H^+ \rightarrow HS_2O_3^- \rightarrow HSO_3^- + S \qquad (3)$$

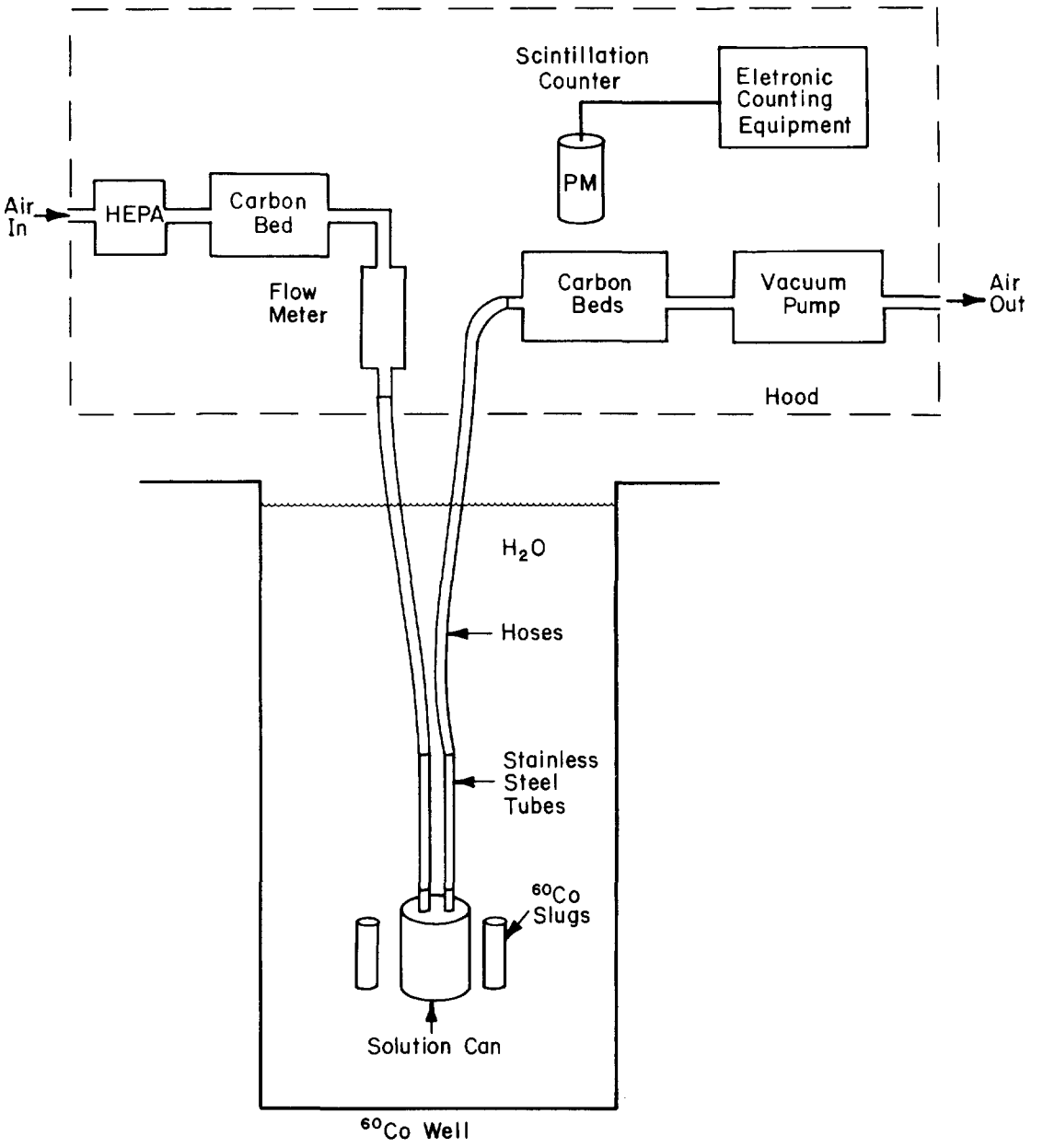

Figure 1. Schematic of iodine evaporation experiment.

However, if all of the thiosulfate were destroyed, the iodine release should be about equivalent to the non-additive release. This was not the case, and the degradation of the thiosulfate or the degradation products is assumed to actually promote the release of iodine from solution.

An unexpected result of this experiment was that about 11 to 15% of the iodine evolved was a penetrating form that passed through the 3 in. of activated carbon designed to collect the iodine. Some of this activity was stopped in a 1-ft-thick backup bed of carbon, but a large portion penetrated it.

Tests With Sodium Thiosulfate and Potassium Hydroxide. To reduce possible acid decomposition of the thiosulfate, KOH (10^{-3}M) was added to increase the pre-irradiation pH of the solution from ∿7 to >10. Some improvement was found in that iodine evaporation was reduced to 30%. The penetrating iodine was found again.

With the same KI and KOH concentrations, the thiosulfate concentration was increased to 0.1 wt%. Almost quantitative release of the iodine occurred, but there was no evidence of generation of penetrating form. When the thiosulfate concentration was increased to 1 wt% with the same KI and KOH concentrations, iodine evolution was significantly reduced to 0.044% in one experiment and 0.55% in another. There was no evidence of the penetrating form.

The first of these experiments with KOH added indicates that the KOH served to partially neutralize the reaction product ($2H^+$) of Equation 2 thus reducing acid decomposition by Equation 3. However, when the thiosulfate was increased to 0.1 wt%, the KOH was either ineffective in neutralizing the larger quantity of decomposition products ($2H^+$) or was depleted in neutralizing the lower pH solution resulting from the larger addition of thiosulfate. In the case of the 1 wt% addition of thiosulfate, sufficient thiosulfate was apparently present, even with decomposition, to maintain iodine essentially in the nonvaporizable iodide form by

$$2S_2O_3^{=} + I_2 \rightarrow S_4O_6^{=} + 2I^- \qquad (4)$$

Tests With Potassium Hydroxide Additive. The alternatives to thiosulfate as an additive for iodine retention are limited. One that has been suggested is KOH. The rationale behind the use of KOH is that it serves two purposes: 1) it promotes formation of the nonvolatile iodide by

$$3I_2 + 6OH^- \rightarrow 5I^- + IO_3^- + 3H_2O \qquad (5)$$

and, 2) it increases solution pH to prevent the OH radical attack of the iodide[5]

$$OH + I^- \rightarrow I + OH^- \qquad (1)$$

which occurs in neutral or acidic solutions. In alkaline solution, the OH radicals are dissociated by the reaction

$$OH \rightarrow H^+ + O^- \qquad (6)$$

The effectiveness of KOH as an additive was briefly examined. With the same KI concentration as previously used, experiments were performed with KOH concentrations of 10^{-3}M and 8 x 10^{-3}M (0.05 wt%). The iodine evolutions measured were 2.5 and 1.2%, respectively.

A comparison of these results with the thiosulfate results indicates that 0.05 wt% KOH is almost as effective as 1 wt% thiosulfate. In addition, the change in iodine evolution is slight for an almost 10-fold change in KOH; a 100-fold change in iodine evolution occurs for a 10-fold change in thiosulfate concentration.

The additive experiments (Table I and Fig. 2) indicate that the rate of iodine evolution is a function of radiation dose.

Penetrating Form of Iodine

As previously noted, several thiosulfate additive experiments produced significant quantities of an iodine form capable of passing through several inches of activated carbon. Tests were conducted to identify the penetrating iodine species to determine if it might occur in systems that use activated carbon for removal of radioiodine.

Nine experiments were performed in the ^{60}Co irradiation facility in an attempt to obtain a sample of the penetrating iodine for analysis and identification. The experimental equipment shown in Fig. 3 was designed to freeze out a sample. Nitrogen was also substituted for air as the flow gas to avoid freezing out oxygen. After seven such experiments with KI and thiosulfate concentrations equal to those that had previously given the penetrating iodine, the penetrating iodine was not formed in a nitrogen atmosphere. Oxygen appears to be a pre-requisite for its formation.

Two experiments were then performed with flowing air and a cold trap containing dry ice and trichloroethylene (-70°C) substituted for the liquid nitrogen trap. In both experiments, the penetrating iodine was generated, but the trap was incapable of freezing out a sample. Two experiments were performed to determine if the decomposition products of thiosulfate ($SO_4^=$ and S) were involved in the formation of the penetrating iodine. One experiment used KI plus Na_2SO_4 in the radiation field and the other used KI plus sulfur. Neither experiment produced the penetrating form of iodine.

Two additional experiments, with HEPA filters in the air stream, showed that the penetrating iodine was readily removable. This result suggests that the penetrating iodine may exist in the form of either a particulate or an aerosol. Both of these forms can pass through activated carbon beds. In the absence of a suitable analytical technique to apply to the material collected on the HEPA, identification work was halted.

TABLE I

Iodine Evaporated After Exposure to 10^8 Rad

Type Experiment	*Concentrations, wt%*			*Iodine Evaporated, %*
	KI	*$Na_2S_2O_3$*	*KOH*	
No Additive	0.010	-	-	14.6
Thiosulfate	0.010	0.014	-	94[a]
	0.010	0.014	-	96[a]
Thiosulfate and KOH	0.010	0.014	0.006	30[a]
	0.010	0.1	0.006	96
	0.010	1.0	0.006	0.044
	0.010	1.0	0.006	0.55
KOH	0.010	-	0.006	2.5
	0.010	-	0.050	1.2

a. Experiments that gave the penetrating iodine species.

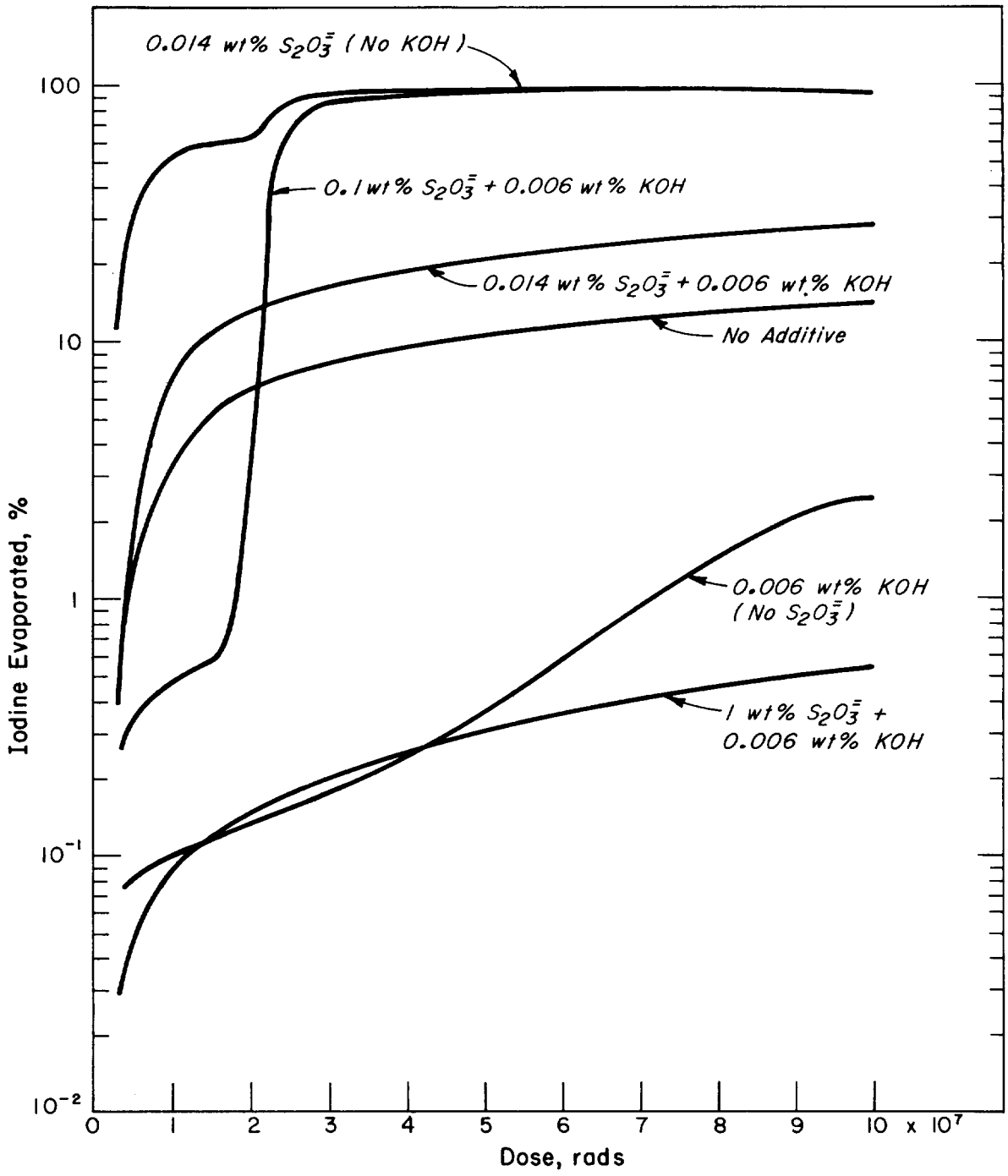

Figure 2. Effect of additive and radiation dose on iodine evaporation (5.6×10^{-4}M solution of KI).

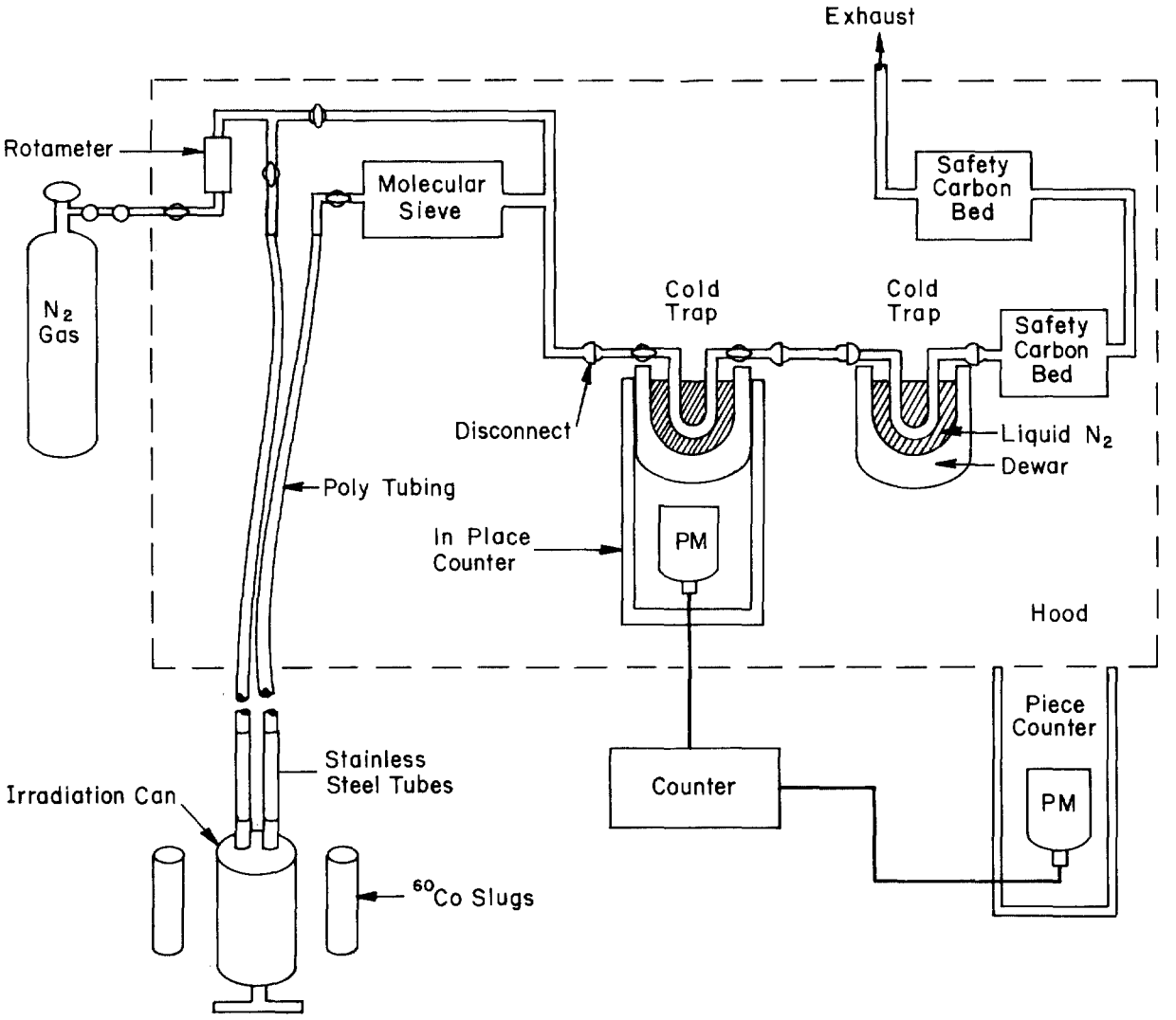

Figure 3. Schematic of iodine penetration experiment.

References

1. A. H. Dexter, A. G. Evans, and L. R. Jones. *Confinement of Airborne Radioactivity*. USAEC Report DP-1390, E. I. du Pont de Nemours and Company, Savannah River Laboratory, Aiken, S. C. (1974).

2. W. N. Bishop and D. A. Nitti. "Stability of Thiosulfate Spray Solutions." *Nucl. Tech. 10*, 436 (1971).

3. H. E. Zittel and T. H. Row. "Radiation and Thermal Stability of Spray Solutions." *Nucl. Tech. 10*, 436 (1971).

4. L. R. Jones. "Effects of Radiation on Reactor Confinement System Materials." *Twelfth AEC Air Cleaning Conference*, Oak Ridge, Tennessee, August 28-31, 1972, USAEC Report CONF-720823 Volume 2 (1972).

5. A. R. Denaro and G. G. Jayson. *Fundamentals of Radiation Chemistry*. Ann Arbor Science Publishers Inc., Ann Arbor, Michigan (1972).

DISCUSSION

RIVERS: Is the current norm for sprays pure sodium thiosulfate?

DEXTER: We don't mean to imply that the results we got are applicable to any other reactor or containment vessel. It is entirely unrelated to that, and we would not want to make any inferences as to how this sulfate would work in that kind of system. Their requirements are different from the sort of problems that we are concerned with. But to answer your question, others use both thiosulfate and caustic in sprays to knock down the iodine in the air over the reactor vessel.

DEPENDENCE OF GAS PENETRATION OF CHARCOAL BEDS ON RESIDENCE TIME AND LINEAR VELOCITY

V. R. Deitz, C. H. Blachly
Naval Research Laboratory, Washington, D.C. 20375
and
L. A. Jonas
Edgewood Arsenal, Aberdeen Proving Ground, MD 21010

Abstract

The trapping of methylradioiodide (CH_3I^{131}) was studied in packed columns of different diameters, bed depths, and at various flow velocities, using impregnated granular activated charcoals. The gradient in penetration along the axis of flow was determined after dividing the column into eight equal layers by discs of perforated stainless steel, followed by a back-up section, and counting each layer. In one series of measurements six columns were used in which the depth and the corresponding superficial linear velocity was varied 5.6 fold; the weight and volume of charcoal and the volumetric flow rate were held constant. Although the residence time was constant (0.25 sec) in all six columns, significant decreases in penetration occurred with increase in linear velocity. In other series of measurements, the diameter, depth, and weight of charcoal were held constant and the volumetric flow rate was varied over a wide range of superficial linear velocity. Differences in penetrability, as a result of varying the bed geometry, the residence time, and the flow velocity were examined in accord with recent concepts of adsorption kinetics and catalytic behavior in packed beds.

I. Introduction

During the two decades following World War I the data of adsorption included studies on the flow of gas-air mixtures through granular charcoal (1). A period then followed in which steady-state adsorption data (mostly physical adsorption) dominated the attention of many investigators (2). Within the last two decades, however, there has been renewed interest in dynamic adsorption studies due to the remarkable development of gas chromatography and the applications of adsorbents to engineering processes.

Much of the design of charcoal filters has followed in the footsteps of early jerry-built structures. The many engineering parameters have not been evaluated for their influence on the penetration of an adsorbed gas through the charcoal. This paper is concerned with the dependence of penetration of methyl iodide containing radioiodine 131 on two parameters - residence time and carrier gas velocity - using beds of impregnated charcoals. By counting the radioactivity in each of the equal volume sections into which a bed is divided, the gradient of adsorbed methyl iodide along the axis of flow can be directly determined. The results are examined in accord with recent concepts of adsorption kinetics and catalytic behavior in packed beds.

II. Theoretical

The Wheeler (3) adsorption equation for gas breaking through or penetrating a bed of charcoal, modified by Jonas et al (4) to reflect charcoal bed weights rather than bed depths, was originally derived from a continuity equation of mass balance, and can be expressed as

$$t_b = \frac{W_e}{C_o Q} \left[W - \frac{\rho_\beta Q \ell n \ (C_o/C_x)}{k_v} \right] \tag{1}$$

where t_b is the time (min) at which an exit concentration C_x ($g.cm^{-3}$) penetrates the bed when challenged by an inlet concentration C_o ($g.cm^{-3}$) at a volumetric flowrate Q ($cm^3.min^{-1}$), ρ_β is the bulk density of the charcoal bed ($g.cm^{-3}$), W is the bed weight (g), W_e is the adsorption capacity of the charcoal ($g.g^{-1}$), and k_v is the pseudo first order adsorption rate constant (min^{-1}). The critical weight of charcoal, W_c, is

$$W_c = \frac{\rho_\beta Q \ell n \ (C_o/C_x)}{k_v} \tag{2}$$

and identified as that weight of charcoal just sufficient to reduce the inlet concentration to the arbitrarily chosen exit concentration. Equations (1) and (2) apply to the kinetics of gas adsorption by activated charcoal.

Since plug flow is usually assumed for gas movement through the charcoal bed, the mean residence time τ in the bed can be shown as

$$\tau = \frac{L}{V_\ell} = \frac{V}{Q} = \frac{W}{\rho_\beta Q} \tag{3}$$

where L is the bed depth (cm), V_ℓ the superficial linear velocity ($cm\ min^{-1}$), and V the volume of the bed (cm^3). Thus, by substituting into equation (1) one obtains

$$t_b = \frac{W_e \rho_\beta}{C_o} \left[\tau - \frac{\ell n \ (C_o/C_x)}{k_v} \right] \tag{4}$$

Here, the breakthrough time t_b is shown as a function of residence time, τ.

In heterogeneous catalysis, as opposed to heterogeneous adsorption, the attenuation of C_o to C_x can be independent of time and, therefore, the kinetics of this process are studied under steady-state conditions. Under these conditions the first order equation relating the concentration attenuation is

$$\frac{C_x}{C_o} = \exp\ (-k\tau) \tag{5}$$

where k is the first order catalytic rate constant (min^{-1}).

If, in the case of gas adsorption kinetics, a finite concentration exited the bed immediately, and remained relatively steady and independent of time, equation (1) could apply to these conditions by setting t_b equal to zero. Then, for the equation

$$o = \frac{W_e}{C_o Q} \left[W - \frac{\rho_\beta Q \ell n \ (C_o/C_x)}{k_v} \right] \tag{6}$$

to be satisfied in the non-trivial case where

$$\frac{W_e}{C_o Q} \neq 0 \tag{7}$$

it is required that

$$W - \frac{\rho_\beta Q \ell n \ (C_o/C_x)}{k_v} = 0 \tag{8}$$

and

$$W = \frac{\rho_\beta Q \ell n \ (C_o/C_x)}{k_v} \tag{9}$$

From this one can show that

$$\ell n \frac{C_o}{C_x} = \frac{k_v W}{\rho_\beta Q} \tag{10}$$

or

$$\ell n \frac{C_x}{C_o} = - \frac{k_v W}{\rho_\beta Q} \tag{11}$$

and in exponential form

$$\frac{C_x}{C_o} = \exp \left(- \frac{k_v W}{\rho_\beta Q} \right) \tag{12}$$

Since we note from equation (3) that

$$\tau = \frac{W}{\rho_\beta Q}$$

we can substitute for $W/\rho_\beta Q$ in equation (12) to obtain

$$\frac{C_x}{C_o} = \exp \left(- k_v \tau \right) \tag{13}$$

Equation (13), applying to the case of a finite yet steady gas concentration exiting a charcoal bed, can be seen as equivalent in form and concept to equation (5), applying to heterogeneous catalysis, with the rate constant k_v denoting sorption and k denoting catalysis.

III. Experimental

1. Materials.

The three impregnated charcoals, 4167, 4169, and 4171, were prepared from two base charcoals, and some physical properties pertinent to the present treatment are given in Table I. The impregnation formulation (hexamethylenetetramine, iodine, and sodium hydroxide) is one of many samples reported in another paper presented at this Conference (5).

2. Equipment.

The carrier air flow was first passed through charcoal and then through a high efficiency particulate filter. In all measurements the test charcoal sample was prehumidified for 16 hours with the air flow at 95-97 RH. The methyl iodide-131 was purchased (ICN Life Sciences, Irvine, California) at suitable intervals as a liquid (1 ml) of 5 millicuries activity. The charcoals were counted in aliquots of about 13 cm^3 using a Nuclear Chicago Gas Flow Detector, Model 470 and Model 8712 decade scaler.

TABLE I: PHYSICAL PROPERTIES OF ACTIVATED CHARCOALS

	Lot 4171	Lot 4169	Lot 4167
Base Charcoal	G212-coconut	MBV-coal	G212-coconut
Particle dia. (cm)	0.172	0.256	0.172
Bulk dens. ($g.cm^{-3}$)	0.393	0.391	0.392
Spherical vol. (cm^3)	0.002664	0.008785	0.002664
Particle wt. (g)	0.002033	0.008197	0.001972
Particle dens. ($g.cm^{-3}$)	0.763	0.933	0.746
Particles per g	492	122	507
Sieve Analysis			
on 6	0	1.5	0
6-8	2.7	61.0	2.7
8-10	14.9	23.1	14.9
10-12	35.6	9.2	35.6
12-16	45.0	4.9	45.0
16-20	1.4	0.2	1.4
Pan	0.4	0.1	0.4

3. Procedure.

The data were obtained for 17 charcoal columns of constant volume (106 cm^3), each column initially being divided into eight equal sequential sections. A fixed volume flow of air plus the dose of methyliodide-131 entered the column for two hours and then the air flow alone was continued for two additional hours. Each of the eight sections (each containing 106/8 cm^3 charcoal) was evaluated in terms of its retained radioactive counts per minute (CPM) and likewise in the backup beds, which had a total depth of two inches.

4. Bed Section Penetration Calculation.

Since the bed depth was divided into eight equal sections, each section was challenged by the radioactive methyl iodide penetrating

the previous section (C_x), and the back-up beds retained all the methyl iodide penetrating the eighth section. The total methyl iodide challenge (C_o) to the bed was the sum of the radioactive counts per minute (CPM) found on all eight sections plus that on the back-up beds. The fractional penetration of each section was calculated from the retention (CPM) on each bed section and the total CPM challenge to the bed:

$$\text{Fractional Penetration for 1st Section} \quad (C_x/C_o)_1 = \frac{\text{Total CPM Challenge} - \text{CPM Retained on 1st Section}}{\text{Total CPM Challenge}} \quad (14)$$

$$\text{Fractional Penetration for nth Section} \quad (C_x/C_o)_n = \frac{\text{Total CPM Challenge} - \text{Sum of CPM Retained on } 1 + 2 + \ldots n}{\text{Total CPM Challenge}} \quad (15)$$

$$= \frac{\text{CPM Penetrating nth Section}}{\text{CPM Challenging nth Section}} \quad (16)$$

The sum of the fractional penetration and the fractional retention, either for a particular bed section, or for the arithmetic means, is unity.

IV. Results

1. Observed Data.

The experimental data are tabulated in terms of the number of radioactive counts per minute (CPM) detected in each of the equal volume sections of the column. The weight, volume, and bulk density of the packed charcoal were maintained invariant, but the bed area, bed depth, volumetric flowrate, gas residence time, and superficial linear flow velocity were varied.

Charcoal #4171 was tested at a constant volumetric flowrate of 25 liters per minute and residence time of 0.254 seconds for the vapor in the bed by varying both the bed depth and area of the charcoal bed. In these tests the superficial linear velocity ranged from 21 to 118 $cm.sec^{-1}$. In order to extend the lower limit of the linear velocity to 4.2 $cm.sec^{-1}$ one test was made at a volumetric flowrate of 5 liters per minute. The data are shown in Table II.

TABLE II: RETENTION OF CH_3I^{131} BY IMPREGNATED CHARCOAL: CONSTANT RESIDENCE TIME, VARIABLE SUPERFICIAL LINEAR VELOCITY, (LOT #4171)

TEST CONDITION	OBSERVED VALUES						
Vol. flowrate, $\ell.min^{-1}$	25.0	25.0	25.0	25.0	25.0	25.0	5.0
Bed depth (total), cm	5.33	8.03	11.3	16.1	21.6	30.0	5.33
Bed dia. , cm	5.08	4.10	3.45	2.90	2.50	2.12	5.08
Bed area , cm^2	20.27	13.20	9.35	6.61	4.91	3.53	20.27
Weight , g	41.3	41.3	41.3	41.3	41.3	41.3	41.3
Bulk density, $g.cm^{-3}$	0.393	0.393	0.393	0.393	0.393	0.393	0.393
Sup. lin. vel., $cm.sec^{-1}$	21.0	31.6	44.6	63.1	84.9	118.0	4.2
Res. time, , sec	0.254	0.254	0.254	0.254	0.254	0.254	1.27
Radioactive CPM on							
Bed section 1	36227	19358	156245	89281	80615	15796	56808
2	25248	13067	104162	58135	40954	9336	49020
3	20487	9520	75753	35709	28970	5707	28409
4	14965	7463	49995	25505	18470	3633	14451
5	10725	5133	34717	16335	11470	2325	7184
6	8301	3965	23580	10960	7323	1431	3392
7	6455	2852	15239	6789	5000	732	1685
8	4685	2206	9799	4328	3004	420	656
Back-up bed	14588	6152	17097	6486	3376	240	680
TOTAL	141681	69716	486587	253528	199182	39620	162285

Charcoal #4169 was tested at constant bed depth and area, but varying volumetric flowrates (5.5 to 50.0 ℓ min^{-1}), so that the superficial linear velocity ranged from 4.52 to 41.1 cm sec^{-1} and the residence time from 1.179 to 0.130 seconds. The data are shown in Table III.

TABLE III: RETENTION OF CH_3I^{131} BY IMPREGNATED CHARCOAL: VARIABLE RESIDENCE TIME AND SUPERFICIAL LINEAR VELOCITY (LOT #4169)

TEST CONDITION	OBSERVED VALUES				
Vol. flowrate, ℓ min^{-1}	5.5	11.0	18.0	25.0	50.0
Bed depth (total), cm	5.33	5.33	5.33	5.33	5.33
Bed diameter , cm	5.08	5.08	5.08	5.08	5.08
Bed area , cm^2	20.27	20.27	20.27	20.27	20.27
Weight , g	42.2	42.2	42.2	42.2	42.2
Bulk density, $g.cm^{-3}$	0.391	0.391	0.391	0.391	0.393
Sup. lin. vel. $cm.sec^{-1}$	4.52	9.05	14.8	20.6	41.1
Res. time, sec	1.179	0.589	0.360	0.259	0.130
Radioactive CPM on					
Bed section 1	42024	20028	23492	91145	7797
2	16921	11041	15467	65007	6142
3	7862	5754	9947	48287	5564
4	2702	4743	6316	35363	4432
5	2094	2868	4486	28985	3153
6	874	999	3222	20912	2473
7	200	732	2302	14913	2076
8	139	346	1423	11449	1355
Back-up bed	95	365	2595	28256	4464
TOTAL	72911	46876	69250	344317	37933

Charcoal #4167 was tested at varying flowrates, bed depths, and areas so that the superficial linear velocity ranged from 2.53 to 126.2 cm sec^{-1} and the residence time from 0.793 to 0.127 seconds. The data are shown in Table IV.

TABLE IV. RETENTION OF CH_3I^{131} BY IMPREGNATED CHARCOAL: VARIABLE RESIDENCE TIME AND SUPERFICIAL LINEAR VELOCITY (LOT #4167)

TEST CONDITION	OBSERVED VALUES				
Vol. flowrate, ℓ min^{-1}	2.0	5.5	11.0	18.0	50.0
Bed depth (total), cm	2.01	4.02	6.02	8.03	16.1
Bed dia. , cm	4.10	4.10	4.10	4.10	2.90
Bed area , cm^2	13.20	13.20	13.20	13.20	6.61
Weight , g	10.4	20.8	31.2	41.6	41.6
Bulk density, $g.cm^{-3}$	0.392	0.392	0.392	0.392	0.394
Sup. lin. vel. $cm.sec^{-1}$	2.53	6.94	13.88	22.72	126.2
Res. time, sec	0.793	0.578	0.434	0.353	0.127
Radioactive CPM on					
Bed section 1	92569	249967	32447	45428	58047
2	7119	80613	12294	24245	31553
3		15399	4849	13560	26503
4		2667	1779	8143	20740
5			712	4535	18991
6			247	2345	15059
7				1256	11168
8				831	10324
Back-up bed	488	328	157	848	32536
TOTAL	100176	348974	52485	101191	224921

2. Data Handling.

In order to reduce the relative error when the observed CPM retained on a bed section was of the order of magnitude of the background CPM (coupled with the reproducability limits of the instrumentation), it was decided to pair data when any one section, or the back-up section, had a CPM less than 100. This occurred in some of the observed data, associated with long residence times, in Charcoal #4167, and in these instances, therefore, the CPM of the preceding section or sections were added to the observed CPM. When this was done the necessary adjustments were made in the values for bed depth, char weight, and residence time of vapor in the bed since in effect the back-up bed increased in size by incorporating the lower sections of the original bed that had a CPM less than 100.

3. Rate Constant.

The trapping and removal of CH_3I^{131} vapor by the impregnated charcoals are considered to be primarily catalytic in behavior (5) rather than adsorptive. One necessary condition for the former is that each section, equal in volume to all other active sections in the bed, remove the same fraction of CH_3I^{131} under the same test conditions. Thus, when the fractional penetration per section was obtained from the relation

$$\text{Fractional Penetration} = 1 - \text{Fractional Retention} \qquad (17)$$

and the total bed penetration calculated from the relation,

$$\%\ \text{Bed Penetration (calculated)} = \left(\text{Fractional Penetration per section}\right)^{n} \times 100 \qquad (18)$$

where n was the number of sections, the calculated values agree very closely with the observed bed penetration percentages obtained from the relation

$$\%\ \text{Bed Penetration (observed)} = \frac{\text{CPM in back-up bed}}{\text{Total CPM Challenge}} \times 100 \qquad (19)$$

The close correspondence between these two percentages are shown for all three charcoal lots, and under all test conditions, in Table V. The first order rate constant k in sec^{-1} was calculated from equation (5) using the observed fractional bed penetration values for all charcoal lots and under all test conditions. The results are shown in Table VI.

TABLE V: OBSERVED AND CALCULATED BED PENETRATION PERCENTAGES AT VARIOUS RESIDENCE TIMES AND LINEAR VELOCITIES

Char Lot No.	Bed Depth (cm)	Res. Time (sec)	Sup. Lin. Vel. (cm sec^{-1})	Ret. Frac. per Sec.	Pene. Frac. per Sec.	% Bed Penetration* Observ.	Calc.
4171	5.33	1.27	4.2	0.492	0.508	0.42	0.44
4171	5.33	0.254	21.0	0.247	0.753	10.30	10.34
4171	8.03	0.254	31.6	0.262	0.738	8.82	8.80
4171	11.3	0.254	44.6	0.342	0.658	3.51	3.51
4171	16.1	0.254	63.1	0.367	0.633	2.56	2.58
4171	21.6	0.254	84.9	0.402	0.598	1.69	1.64
4171	30.0	0.254	118.0	0.465	0.535	0.61	0.67
4169	5.33	1.179	4.52	0.559	0.441	0.13	0.14
4169	5.33	0.589	9.05	0.452	0.548	0.78	0.81
4169	5.33	0.360	14.8	0.336	0.664	3.75	3.78
4169	5.33	0.259	20.8	0.268	0.732	8.21	8.24
4169	5.33	0.130	41.1	0.234	0.766	11.77	11.85
4167	2.01	0.793	2.53	0.930	0.070	0.49	0.49
4167	4.02	0.578	6.94	0.814	0.186	0.094	0.12
4167	6.02	0.434	13.88	0.620	0.380	0.30	0.30
4167	8.03	0.353	22.72	0.450	0.550	0.85	0.84
4167	16.1	0.127	126.2	0.215	0.785	14.47	14.42

*Observed: $\frac{\text{CPM in back-up bed}}{\text{Total CPM challenge}} \times 100$

Calculated: $(\text{Penetration fraction per section})^{n} \times 100$

where n = no. of sections in bed

TABLE VI: CH_3I^{131} REMOVAL RATE CONSTANTS OF IMPREGNATED CHARCOALS UNDER VARIOUS TEST CONDITIONS

Char Lot No.	Bed Depth (cm)	Res. Time (sec)	Sup. Lin. Vel. (cm sec^{-1})	% Bed Pene. (Observ.)	Rate Constant (sec^{-1})
4171	5.33	1.27	4.2	0.42	4.31
4171	5.33	0.254	21.0	10.30	8.95
4171	8.03	0.254	31.6	8.82	9.56
4171	11.3	0.254	44.6	3.51	13.19
4171	16.1	0.254	63.1	2.56	14.43
4171	21.6	0.254	84.9	1.69	16.06
4171	30.0	0.254	118.0	0.61	20.08
4169	5.33	1.179	4.52	0.13	5.64
4169	5.33	0.589	9.05	0.78	8.24
4169	5.33	0.360	14.8	3.75	9.12
4169	5.33	0.259	20.8	8.21	9.65
4169	5.33	0.130	41.1	11.77	16.46
4167	2.01	0.793	2.53	0.49	6.71
4167	4.02	0.578	6.94	0.094	12.06
4167	6.02	0.434	13.9	0.30	13.39
4167	8.03	0.353	22.7	0.85	13.51
4167	16.1	0.127	126.2	14.47	15.22

V. Discussion

It was shown in Section II (Theoretical) that the equation for the case of a small but finite steady gas concentration at the exit of a charcoal bed is equivalent in form and concept to the equations applying to heterogeneous catalysis. The rate constant k_v denoted adsorption and k denoted catalysis. If the rate of methyl iodide trapping is dominated by a catalytic process, the change in superficial linear velocity, reflected in a reciprocal change in the mean residence time of the gas in the bed, coupled with the observed fractional bed penetration, would be expected to result in an invariant rate constant. However, the actual rate constants for Char 4169 (Table VI) increased nonlinearly with increase of V_ℓ. This phenomenon was observed by Jonas and Rehrmann (6) in a study of the physical adsorption of benzene by activated carbon, and by May and Polson (7), Underhill (8), Ackley (9), and Lorenz and Manning (10) in studies of the trapping of radioactive vapors by impregnated charcoals. A possible explanation of this phenomenon in the case of a simple adsorption process lies in an analogy with heat flow across a stagnant air film. High velocity flow will decrease the thickness of the air film and increase nonlinearly the flow of heat across the film. If diffusional transfer across an air film is controlling in a series of sequential steps, an effect of increased flow velocity, which disturbs and decreases the film thickness, will be to increase the transfer rate until its maximum rate is realized, and then further increase in flow velocity will no longer effect the rate. In the case of an initial physical adsorption followed by chemical reaction, or by a catalytic process, no such maximum appears to exist.

A key point, therefore, in understanding the behavior of impregnated charcoals is the dependence of the fractional penetration on V_ℓ (Fig. 1). The average penetration fraction per section (Table V) was averaged for all values of V_ℓ in each impregnated charcoal with the following results:

char	mean	standard deviation	range
4171	0.632	0.094	0.508 - 0.753
4169	0.630	0.135	0.441 - 0.766
4167	0.394	0.285	0.070 - 0.785

The mean values and range of penetration fraction per section for #4171 and #4169 reflect a behavior toward methyl iodide trapping compatible with a rate constant dominated by a catalytic process. On the other hand, the mean value for #4167 showed an overall weaker dependence on V_ℓ, as evidenced by the lower mean and higher standard deviation. It is suggested that the trapping of methyl iodide by #4167 is compatible with a rate constant dominated by adsorption. This behavior can best be seen in the log - log plot of rate constant versus linear velocity (Figure 2) in which the rate constant at first increases in accord with those for #4169 and #4171 (V_ℓ range from 2.53 to 6.94 cm sec^{-1}), but as V_ℓ continues to increase the rate constant levels off. This relationship is in agreement with the concept of stagnant layer removal described above.

The effect of linear velocity on reaction rate for catalytic systems was explicity shown by Wheeler (11), in terms of the mass transfer limited rate, as

$$k \simeq 1.86\ d_p^{-3/2}\ V_\ell^{1/2} \qquad (20)$$

where d_p is the mean carbon particle diameter in cm, V_ℓ the superficial linear velocity in cm sec^{-1}, k the rate constant in sec^{-1}, and the coefficient 1.86 in consistent units. Since in this study each lot of charcoal was unique both in particle diameter and impregnation details, the $d_p^{-3/2}$ term in equation (20) was considered constant and the equation treated as

$$\log k \simeq \log A + 0.500 \log V_\ell \qquad (21)$$

where A was set equal to $1.86\ d_p^{-3/2}$. Hence, a plot of log k against log V_ℓ should result in a straight line with a slope of 0.500. Figure 2 shows a plot of log k vs log V_ℓ, and Table VII contains the data for the three impregnated charcoals tested. The slopes of the lines for char #4171 and #4169 are 0.454 and 0.447 respectively, showing excellent agreement with theory. The coefficient of correlation values for these plots are 0.994 and 0.970, indicating high confidence limits for the relationship indicated. The data for char 4171 show at constant residence time that as bed depth and linear velocity increase the rate constant increases; char 4169 at constant bed depth as residence time decreases and linear velocity increases the rate constant increases; char 4167, however, shows an initial increase in rate constant as linear velocity increases and then a leveling off as velocity continues to increase. The behavior of #4167 may be due to non-uniformities in its impregnation.

TABLE VII: RATE CONSTANT DEPENDENCE ON LINEAR VELOCITY

Lot #	Char Particle Diam. d_p, cm	Rate Constant - Velocity Eqn*	
		Calculated **	Experimental
4171	0.172	$k = 26.08\ V_\ell^{0.500}$	$k = 2.21\ V_\ell^{0.454}$
4169	0.256	$k = 14.36\ V_\ell^{0.500}$	$k = 2.85\ V_\ell^{0.447}$
4167	0.172	$k = 26.08\ V_\ell^{0.500}$	$k = 3.91\ V_\ell^{0.581}$***

*Rate constant k, sec^{-1}; Superficial lin. vel V_ℓ, cm sec^{-1}
**Calc. from eqn (20).
***For the initial increase in rate constant, based on the first 2 k vs V_ℓ values.

Differences between the calculated and experimental values of the coefficient A in Table VII are not considered significant since errors inherent in the determination of the mean spherical charcoal diameters, raised to the negative 3/2 power, could account for the variations. The close agreement between calculated and experimental values for the exponent on V_ℓ, however, which indicates the functional dependence of the rate constant on velocity, are considered very significant.

When the linear velocity, residence time, bed depth, and bed weight

are the same a higher rate constant for one impregnated char over another indicates a greater efficiency for trapping methyl radioiodide. Thus, on the basis of Table VI data, char #4167 appears superior to #4171 since even at a smaller bed depth (2.01 vs 5.33 cm) and a shorter residence time (0.793 vs 1.27 sec) the bed penetration was approximately the same (0.49 vs 0.42%) reflecting for #4167 a rate constant more than 50% greater than for #4171 (6.71 vs 4.31 sec^{-1}). However, at any linear velocity greater than 60 cm sec^{-1} the ability of #4171 to trap methyl iodide is superior to #4167, as evidenced by Figure 2. An analogous comparison can be made between #4167 and #4169, although the latter exceeds the trapping efficiency of the former at any velocity greater than 35 cm sec^{-1}.

VI. Concluding Remarks

An overview analysis of the trapping of CH_3I^{131} by the impregnated charcoals indicates two test parameters which affect its adsorption or catalytic rate constant, namely, residence time and superficial linear velocity. Although the bed residence time is used directly in equation (5) or (13) to obtain the rate constant, the data in Table VI show that for #4171 when the residence time was constant but the superficial linear velocity increased the rate constant increased. When the residence time decreased, as in the case of #4169, but the superficial linear velocity increased, the rate constant also increased. In fact, for all three charcoal lots as the linear velocity increased the rate constant increased, although the functionality depended upon whether the rate constant was dominated by a catalytic or adsorptive type process. The generalized conclusion from these data is that the superficial linear velocity plays a dominant role, whereas the residence time a more subsidiary role, in affecting the rate constant. In addition, a catalytic process appears to be more effective than simple adsorption in trapping methyl radioiodide.

Acknowledgement

The sponsorship of the Division of Nuclear Fuel Cycles and Production, Energy Research and Development Administration, and the complete cooperation of John C. Dempsey, Contract Manager, are gratefully acknowledged.

Selected References

(1) Deitz V.R., "Bibliography of Solid Adsorbents," 1900-1942.
(2) Brunauer S., "The Adsorption of Gases and Vapors", Princeton Univ. Press, 1945 (511 pp).
(3) (a) Wheeler A. and Robell A.J., J. Catal. 13, 299 (1969).
(b) Jonas L.A. and Rehrmann J.A., Carbon 10, 657 (1972).
(4) Jonas L.A. and Rehrmann J.A., Carbon 11, 59 (1973).
(5) Deitz V.R. and Blachly C.H., 14th ERDA Air Cleaning Conf. (1976).
(6) Jonas L.A. and Rehrmann J.A., Carbon 12, 95 (1974).
(7) May F.G. and Polson H.J., Methyl Iodide Penetration of Char. Beds: Variation with Relative Humidity and Face Vel, AAEC/E322 (Sep74).
(8) Underhill D.W., Mass Transfer of Krypton-85 in Charcoal Adsorbers, 9th AEC Air Cleaning Conf. (1966).
(9) Ackley R.D., Removal of Radon-220 for HTGR Fuel Reprocessing and Refabrication Off-Gas Streams by Adsorption, DRNL-TM-4883 (Apr75).
(10) Lorenz R.A. and Manning S.R., Iodine Sorption on Charcoal, Conf. on Methyl Iodide Retention by Charcoal, (25 March 76).
(11) Wheeler A., in Catalysis, Vol II, p. 150, Reinhold Publishing Co. New York, N.Y. 1955, edited by Emmett P.H.

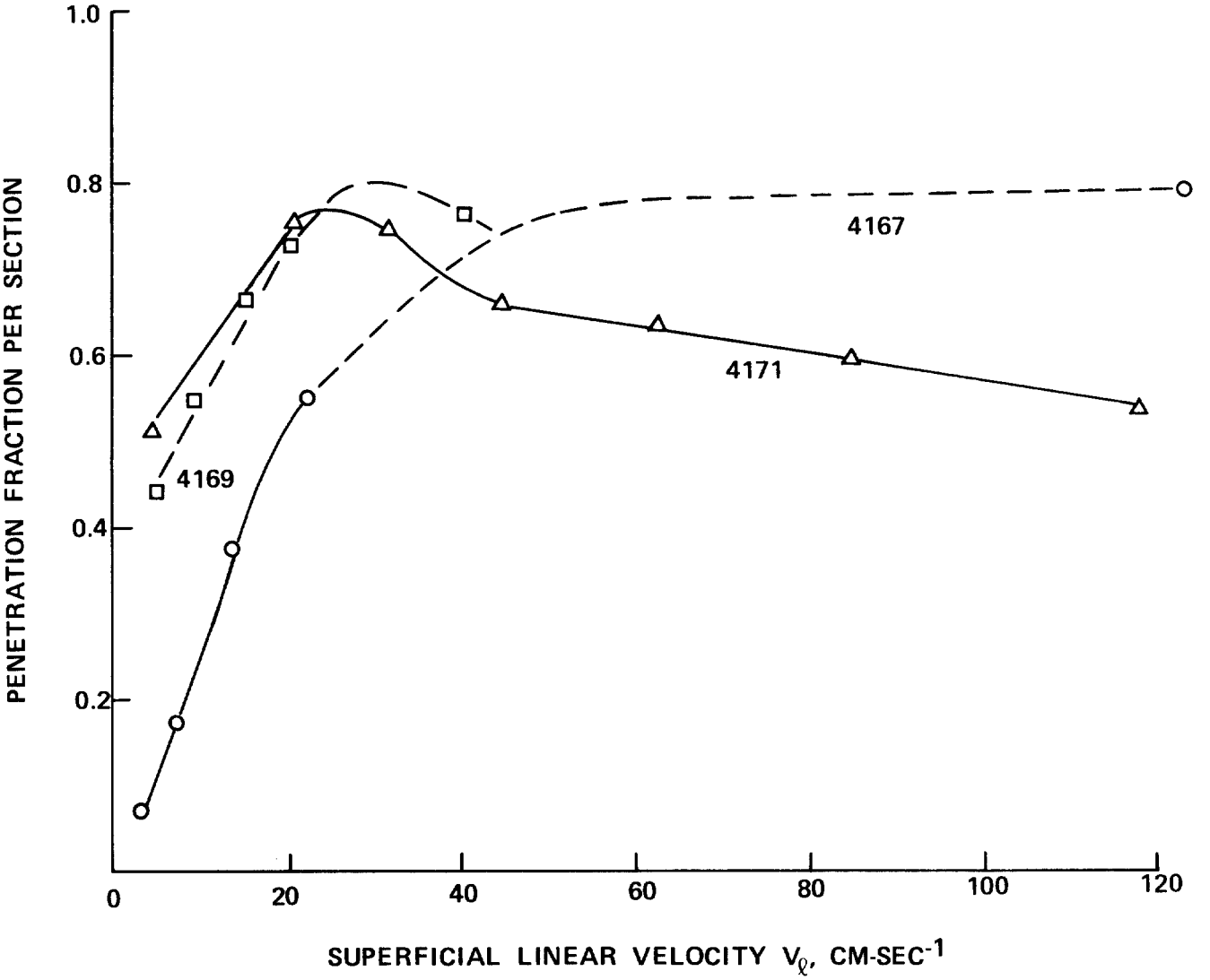

FIGURE 1. PENETRATION FRACTION OF CH_3I^{131} THROUGH IMPREGNATED CHARCOALS AS A FUNCTION OF LINEAR VELOCITY

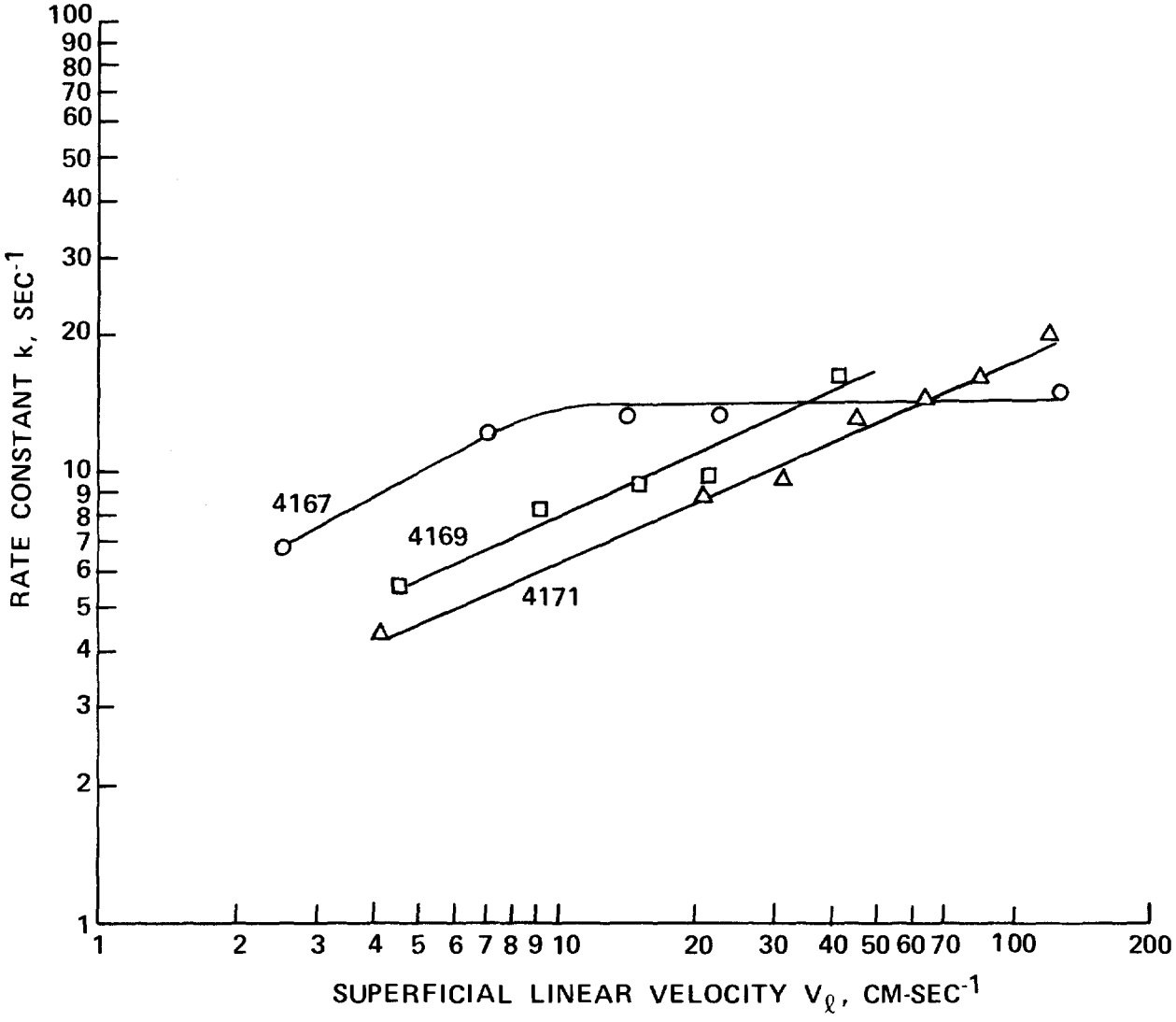

FIGURE 2. RATE CONSTANT FOR CH_3I^{131} REMOVAL BY IMPREGNATED CHARCOALS AS A FUNCTION OF LINEAR VELOCITY

DISCUSSION

LIPTON: I have a question on two equations (15 and 16) which you stated as being equivalent. Let's say there is some absorption in each of Section 1 through n-1 but then there is total penetration of Section n. That would make Equation 16 equal to one but Equation 15 less than one.

JONAS: Counts per minute were obtained on each of the eight sections. Then we calculated the penetration per section for each of the eight sections and we found them rather close to the arithmetic mean of the eight values.

LIPTON: It is just an empirical equivalent, not a mathematical equivalent?

JONAS: Yes.

KOVACH: In all of the results, you were using CPM. What assurances did you make that these actually correspond with DPM's?

JONAS: Our CPM represents 12 to 15 per cent of the total disintegrations per minute.

KOVACH: Did you have the same for all of the fractions in that range?

JONAS: Yes, in that range. We deliberately tried to have the various challenges to the total sections the same, as much as possible. They were in the order of magnitude of 10^5 counts per minute. I worried about that because when I had previously seen you in March, you mentioned this.

KOVACH: The other question that I have relates to what we have published in similar work back in 1970 over somewhat different particle size ranges. We also see a definite break in the curve that you published when it switches over from boundary layer diffusion to pore diffusion at very high velocities and at small particle sizes. The validity doesn't exist if you keep increasing a fraction and if you go to smaller particle sizes where you are more liable to be faced with pore diffusion.

JONAS: I believe that as you decrease the particle diameter, you get to the point where you no longer have the queuing-up process and that you change the rate controlling step. And I do feel there would be a change. But over our range, which was a rather wide range, it is still amazing how well the Wheeler equation holds.

KOVACH: A paper in the 11th AEC Air Cleaning Conference Proceedings showed that for beds of fine particle size the relationship between penetration and velocity shown in your work did not seem to exist. Definite breaks were observed when superficial velocity increased, causing a change from laminar to turbulent flow. Have you evaluated other particle size carbons, and do you postulate such breaks using your equations?

JONAS: The relationship I show is between catalytic rate constant and superficial linear velocity, not between penetration and velocity, per se. However, relative to your question on charcoal particle size, we have only worked on one particle size up to now. It is possible that for very small particle charcoals the effect of increased velocity on the rate constant would be minimized.

EFFECT OF SERVICE AGING ON IODINE RETENTION OF ACTIVATED CHARCOALS*

A. G. Evans
Savannah River Laboratory
E. I. du Pont de Nemours and Company
Aiken, South Carolina 29801

Abstract

The Savannah River reactor confinement systems are continuously operated off-gas cleanup systems whose components include moisture separators, HEPA filters, and halogen adsorber beds of activated charcoal. Charcoal is removed from the system periodically and subjected to a variety of physical, chemical, and iodine penetration tests to ensure that the system will perform within specification in the event of an accidental release of activity from the reactor.

Tests performed on the charcoals include pH measurement of water extracts, particle size distribution, ignition temperature, high-temperature (180°C) iodine penetration, and iodine penetration in an intense radiation field at high humidity. Charcoals used in the systems include carbon Types 416 (unimpregnated), G-615 (impregnated with 2% TEDA and 2% KI), and GX-176 (impregnated with 1% TEDA and 2% KI).

Tests at Savannah River Laboratory show that Type GX-176 carbon (currently in use) performs consistently better than the other two products. Tests performed under simulated accident conditions (the radiation test) showed that Type GX-176 carbon retains iodine better after 18 months service than does Type 416 carbon with no service exposure. The 18-month Type GX-176 carbon also showed lower iodine penetration than did Type G-615 carbon that was service-aged for only nine months. The superior performance of Type GX-176 carbon is attributed to its particle size distribution and impregnants. The high-temperature iodine retention characteristics of all three carbons is shown to be more dependent on pH of the charcoal than on service age. The rate of change of pH of the charcoals also seems to be dependent on the particle size distribution.

Separate experiments at the Naval Research Laboratory show that the methyl iodide retention of aged charcoals decreases rapidly with increasing exposure in the Savannah River Plant systems. Type GX-176 carbon performs slightly better than does Type G-615 carbon.

---

* The information contained in this article was developed during the course of work under Contract AT(07-2)-1 with the U.S. Energy Research and Development Administration.

Introduction

The airborne-activity confinement system for each of the Savannah River Plant (SRP) production reactors is a continuously online, off-gas cleanup system designed to collect halogens and particulates that could be released following a reactor accident[1]. Active components in the system include moisture separators to remove entrained moisture droplets, HEPA filters to remove particulate radioactivity, and beds of activated charcoal to remove halogens. All the air from the process areas of the reactor buildings passes through the confinement system before being exhausted to the atmosphere. A schematic diagram of the air flow through the reactors is shown in Figure 1.

Previous studies of activated charcoals at Savannah River Laboratory (SRL) showed that unimpregnated carbon (the type originally installed in the SRP systems) retains iodine less effectively than do most types of impregnated carbons[2,3]. Those studies showed that the intense radiation field that would result from the accumulation and subsequent decay of radioactive iodine causes organic iodide formation in the carbon bed[4]. The rate of formation and subsequent desorption of the organic iodides is governed by the moisture content and flow rate of the air passing through the beds[4]. The earlier studies also showed that the impregnant triethylenediamine (TEDA), either alone or in combination with iodine salts, improved iodine retention more than did other impregnants tested[4].

Subsequent studies on TEDA-impregnated carbons showed that limits must be placed on the TEDA impregnation level for high-temperature applications because of the low (~190°C) flash point of TEDA[5]. Results of these studies led to the development of Type GX-176* carbon (the type currently installed in the SRP confinement systems)[6].

Carbon in the SRP confinement system is routinely sampled and subjected to a variety of physical, chemical, and iodine penetration tests to ensure continued operation of the confinement system within performance specifications. Data on these service aging studies are presented in this paper along with observations on factors affecting the performance of several carbons exposed in the SRP confinement system.

---

* A 10 × 16 (US) mesh coconut carbon impregnated with 1% TEDA, 2% KI, and a proprietary flame retardant. Product of North American Carbon Company, Columbus, Ohio.

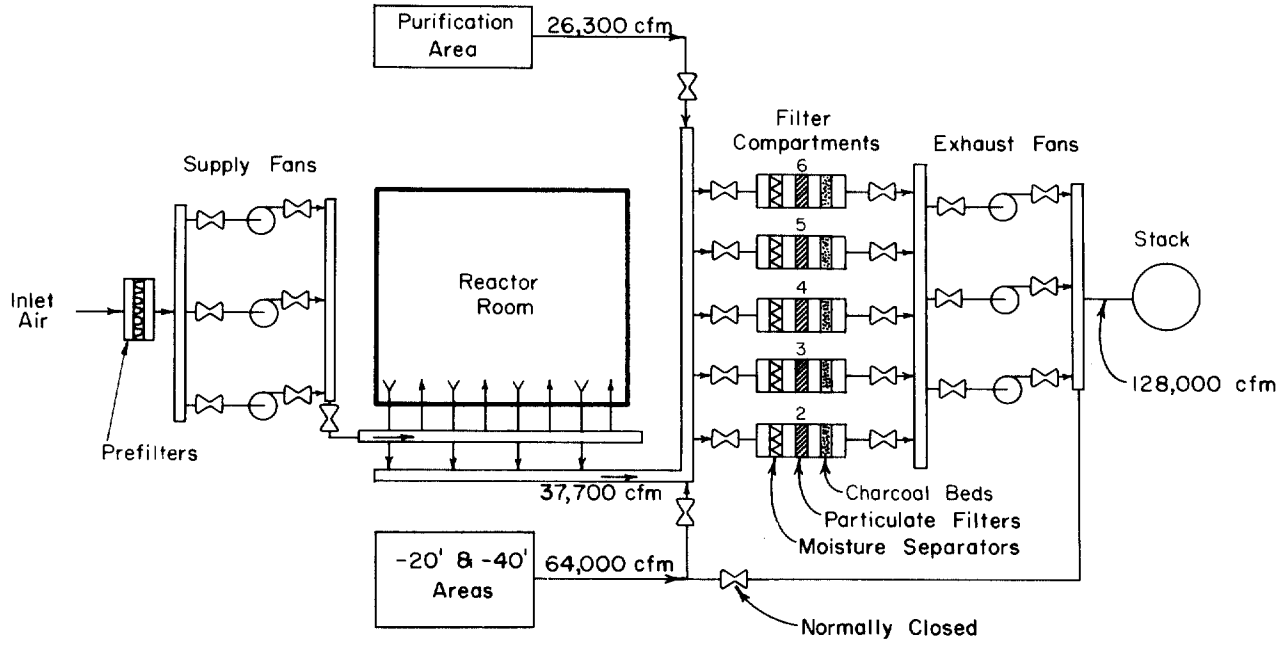

Figure 1 Flow diagram of reactor ventilation system.

Background

Unimpregnated Type 416* carbon was used as a halogen adsorber in all the SRP confinement system charcoal beds until 1975 when replacement with Type GX-176 was completed. Following the discovery of the radiation-induced iodine desorption phenomenon[2,3], a limited number of beds of Type G-615** carbon were installed in the confinement system for evaluation. Type G-615 carbon was removed from the system after nine months exposure; at that time, detailed evaluation of the ignition characteristics of TEDA carbons[5,6] along with evaluation of the performance of the confinement system HEPA filters under simulated accident conditions[7,8] indicated that Type GX-176 carbon can be used effectively in the SRP system with a lesser ignition hazard than can Type G-615 carbon.

Carbon in the SRP system is housed in stainless steel frames (beds) in the confinement compartments (32 beds per compartment, 5 compartments per reactor area)[1]. Routine, in-place leak tests are performed on the charcoal beds to ensure gasket and packing integrity[9]. Iodine retention properties of the carbon are determined by performing iodine penetration tests on samples obtained from full-sized carbon beds that have been removed from the system at periodic intervals. Two iodine tests are routinely performed on one-inch-deep beds: (1) a radiation test, a five-hour test in which I_2 is loaded on the carbon and desorbed at 80°C and 95% relative humidity in a radiation field of at least 1.5×10^7 rads/hr, and (2) a high-temperature test, a test in which I_2 is loaded on the carbon in laboratory air and then subjected to four hours of continuous air flow at 180°C[2].

Additional tests performed on the carbon samples at SRL include pH measurement of water extracts of the carbon, ignition temperature determinations, and impregnant content measurements. Selected samples of new and used confinement carbons have also been tested for methyl iodide penetration at the Naval Research Laboratory (NRL).

The three types of carbon (Types 416, G-615, and GX-176) exposed in the confinement system were all subjected to the tests described in the two preceding paragraphs.

Test Results

High-Temperature Tests

Earlier studies at SRL showed that the ability of carbon to retain iodine at elevated temperatures declines rapidly with increasing service[7]. The data in Table I show iodine penetration is less in service-aged Type GX-176 carbon than in either carbon Type G-615 or 416. A plot of the data (Figure 2) shows that observed iodine penetrations of Type GX-176 carbon are about 10% of those expected from the other two types of carbon after an 18-month exposure in the confinement system.

---

* A 10 x 14 (Tyler) mesh coconut carbon. Product of Barneby-Cheney Company, Columbus, Ohio.

** An 8 x 16 (US) mesh coconut carbon impregnated with 2% TEDA, 2% KI, and a proprietary flame retardant. Product of North American Carbon Company, Columbus, Ohio.

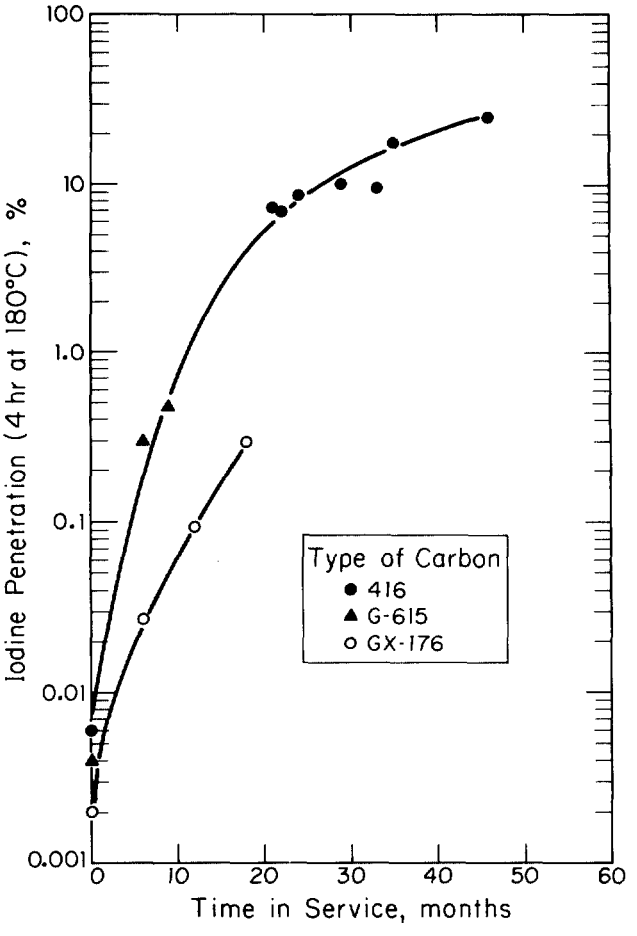

Figure 2 High-temperature tests on confinement carbons.

Figure 2 also shows that the aging rates of Types G-615 and 416 carbons in the high-temperature test are similar, despite the fact that Type G-615 is an impregnated carbon, and Type 416 carbon contains no additives. Type GX-176 carbon behaves quite differently, even though it contains the same additives as those in Type G-615 (TEDA, KI, and a flame retardant). This anomalous behavior is believed to be caused by differences in the particle size distributions of the carbons and is discussed in greater detail later.

Table I High temperature test data on confinement carbons.

Type of Carbon	Time in Service, months	Compartment Number[a]	Iodine Penetration at 180°C, %[b]
416	0	-	0.006
	21	C-2	7.22
	22	P-2	6.84
	24	L-2	8.59
	29	P-3	10.2
	33	P-2	9.48
	35	P-3	17.7
	46	K-3	25.2
G-615	0	-	0.004
	6	C-2	0.295
	9	C-2	0.474
GX-176	0	-	0.002
	6	K-2	0.027
	6	P-2	
	12	K-2	0.093
	18	K-2	0.392

a. Data presented are limited to carbon removed from compartments 2 and 3 only, since previous studies have shown more rapid carbon deterioration in these compartments[5,10]. C, K, L, and P designate production reactors.

b. See text for test conditions.

Radiation Tests

Radiation test data on carbons exposed in the confinement system compartments are presented in Table II and shown graphically in Figure 3. The data show that even after 18 months service, Type GX-176 carbon retains iodine more effectively than does new (unexposed) Type 416 carbon. The data also show that service performance of Type GX-176 carbon is better than that of Type G-615 carbon even though Type G-615 carbon has a slightly lower iodine penetration rate when new.

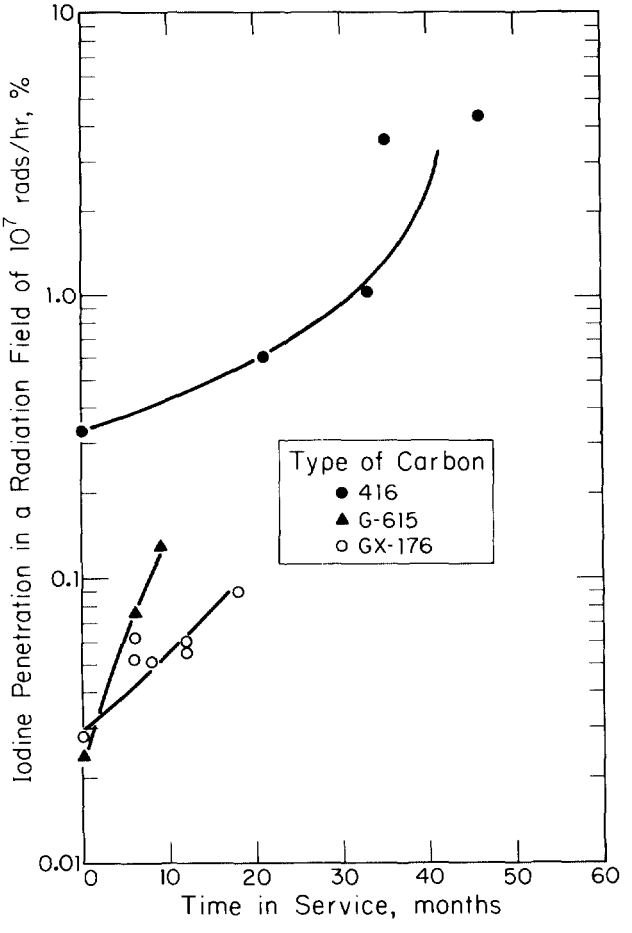

Figure 3 Radiation tests on confinement carbons.

Particle Size Distribution

Particle size distribution is determined on representative samples of all carbons installed in the SRP confinement system. The need for control of the particle size distribution was demonstrated during the early design experiments for the SRP systems[10]. Thus, the Type 416 carbon used for many years in the system had a 10 x 14 mesh (Tyler) distribution (approximately equivalent to a 10 x 16 mesh distribution using the U.S. Standard sieves). The Type G-615 carbon installed experimentally in the confinement system was an 8 x 16 mesh (U.S.) material designed for use in deep (2 inches or more) carbon beds in use in power reactor gas treatment systems. The Type GX-176 carbon now used in the SRP system has a 10 x 16 mesh (U.S.) distribution. Typical sieve analyses on the three products are shown in Table III.

Table II Radiation test data on confinement carbons.

Type of Carbon	Time in Service, months	Compartment Number	Iodine Penetration in Radiation Field, %[a]
416	0	None	0.329
	21	C-2	0.610
	33	P-2	1.04
	35	P-3	3.63
	46	K-3	4.38
G-615	0	None	0.024
	6	C-2	0.076
	9	C-2	0.129
GX-176	0	None	0.028
	6	K-2	0.052
	6	P-2	0.062
	8	P-2	0.051
	12	K-2	0.060
	12	P-6	0.055
	18	K-2	0.090

a. See text for test conditions.

Table III Typical particle size distributions for confinement carbons.

Size Range[a]	Carbon on Sieve for Three Carbon Types, wt %		
	416	G-615	GX-176
on 8	0.0	4.8	0.0
on 10	0.2	24.6	0.5
on 12	14.1	37.1	6.6
on 14	77.2	25.8	35.0
on 16	8.2	6.5	53.8
on 18	0.5	0.9	3.9
Thru 18	0.0	0.3	0.2

a. U.S. Standard ASTM E-11 Sieve Sizes using the method of ASTM D2862 for the determination.

The data in Table III shows that 66.5 wt % of Type G-615 carbon is larger than 12 mesh (greater than ~1.68 mm nominal diameter), but 92.9 wt % of the Type GX-176 carbon is smaller than 12 mesh. The only other known difference between carbon Types G-615 and GX-176 is the TEDA content shown in Table IV.

Table IV Comparison of carbon Types G-615 and GX-176.[a]

	G-615	GX-176
Base carbon	Coconut	Coconut
BET surface area[b], m^2/g	1000	1000
Mesh size (U.S.)	8 × 16	10 × 16
TEDA content, wt %	2.0	1.0
KI content, wt %	2.0	2.0
Flame retardant, wt %[c]	1.0	1.0

a. Vendor-supplied data.

b. Nominal surface area after impregnation.

c. The same proprietary compound is used on both carbons.

Earlier studies of carbon behavior in a radiation environment indicated that iodine penetration should increase with decreasing TEDA content[3,6]. However, test results on service-aged carbons show that Type GX-176 carbon performs consistently better than does Type G-615 carbon, indicating that the particle size distribution is at least as important for iodine retention as is the TEDA content. Particle size data also indicate that smaller carbon granules age more slowly in service than do larger granules.

NRL Methyl Iodide Tests

Samples of new and service-aged carbons of Types G-615 and GX-176 were sent to NRL for methyl iodide penetration testing. Type 416 carbon was not included in this test series because of the known poor methyl iodide retention efficiency of unimpregnated carbon. The NRL test conditions were 25°C temperature, 95% relative humidity, 0.25-second residence time (2-inch-deep carbon bed), 0.1-mg CH_3I/g carbon loading, and 4-hr test time (following 16 hours pre-equilibration at 25°C and 95% relative humidity). This test is intended as a carbon qualification test and is not necessarily indicative of expected carbon performance under accident conditions. Test results are shown in Table V.

Table V Methyl iodide penetration tests of confinement carbons

Type of Carbon	Time in Service, months	Methyl Iodide Penetration, %[a]
G-615[b]	0	0.79
	6	11.4
	9	22.3
GX-176[c]	0	0.45
	6	5.82
	12	28.5
	18	32.1

a. NRL test data courtesy V. R. Deitz. See text for test conditions.

b. All samples except the control exposed in the C-2 compartment.

c. All samples except the control exposed in the K-2 compartment.

Test data show that the methyl iodide retention efficiency of both carbons decreases rapidly with increasing service. The data also show that Type GX-176 carbon deteriorates more slowly than does Type G-615 carbon and confirm the earlier observations on the importance of particle size distribution.

pH Tests

pH tests are performed on the carbon by measuring the pH of water extracts of the carbon. The SRL pH test is made by placing a 5-g sample of carbon in 50 ml of cold, distilled water, heating the slurry to boiling, and then cooling to room temperature in a sealed flask. The pH measurement is made on the liquid decanted from the carbon after the sample has cooled. Data obtained by this method (Table VI) show a rapid decrease in pH with increasing service. As indicated earlier, Types G-615 and 416 carbons show similar behavior when evaluated by the high-temperature test (penetration versus service, Figure 2), but Type GX-176 carbon seemed to deteriorate more slowly. When the high-temperature penetration data are compared with the reciprocal of the pH data (1/pH instead of service age), all three carbons appear to behave similarly (Figure 4). Previous investigations of new carbons showed similar pH effect on iodine retention at elevated temperatures and indicate that one of the principal mechanisms for high-efficiency iodine retention is the conversion of elemental iodine to ionic iodine on the charcoal[8].

Table VI pH of service-aged carbons.[a]

Type of Carbon	Time in Service, months	Compartment Number	pH of Water Extract
416	0	-	9.59
	21	C-2	4.80
	22	P-2	4.75
	33	P-2	4.33
	35	P-3	3.99
	46	K-3	3.01
G-615	0	-	9.86
	6	C-2	7.20
	9	C-2	6.63
GX-176	0	-	9.70
	6	K-2	7.60
	6	P-2	7.70
	12	K-2	6.60
	12	P-6	7.15
	18	K-2	6.46

a. See text for description of method.

Other Tests

Ignition temperature tests performed on impregnated confinement carbons show an apparent increase in the ignition temperature of Type GX-176 carbon for the first few months of service followed by a decrease. The total iodine content of Type GX-176 carbon also increased during the first few months of service in the confinement system. Data are shown in Table VII.

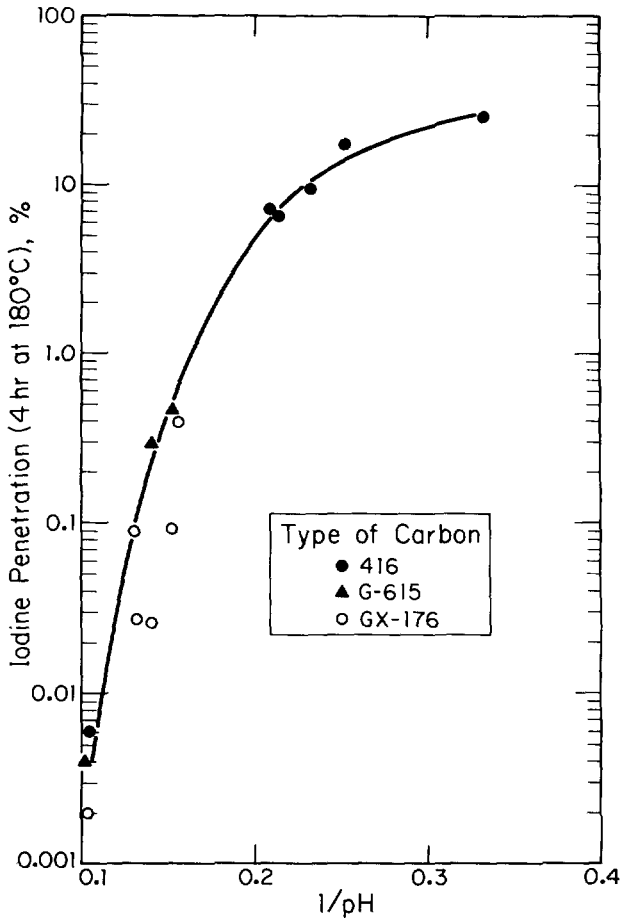

Figure 4 High-temperature iodine penetration as a function of carbon pH.

Table VII Other data on confinement carbons.

Type of Carbon	Time in Service, months	Compartment Number	Ignition Temp., °C[a]	Total Iodine Content, wt %[b]
416	0	-	340	-
	43	K-3	275	-
G-615	0	-	360	-
	6	C-2	420	-
	9	C-2	415	-
GX-176	0	-	386	1.41
	6	K-2	437	1.72
	6	P-2	420	-
	8	P-2	415	-
	12	K-2	322	1.59
	18	K-2	312	1.59

a. As measured in quartz apparatus at a heating rate of 5°C/minute and linear face velocity of 55 ft/min.

b. Determined by neutron activation analysis.

The TEDA content of Type GX-176 carbon was also determined when the carbon was purchased for installation in the confinement system. Analyses of the full-purchase lot, comprised of 16 sublots, showed variations in TEDA content from 0.86% to 1.08% with an average of 0.99% and a standard error of 0.08%. The analytical procedure consisted of TEDA extraction in carbon tetrachloride with subsequent quantitative analysis by infrared absorption spectrometry[11]. Attempts to adapt the method to used carbons were unsuccessful because of the accumulation of interfering hydrocarbons on the service-aged charcoals.

References

1. W. S. Durant, R. C. Milham, D. R. Muhlbaier, and A. H. Peters. Activity Confinement System of the Savannah River Plant Reactors. USAEC Report DP-1071, E. I. du Pont de Nemours & Co., Savannah River Laboratory, Aiken, SC (1966).

2. A. G. Evans and L. R. Jones. Confinement of Airborne Radioactivity — Progress Report: January 1971 - June 1971. USAEC Report DP-1280, E. I. du Pont de Nemours & Co., Savannah River Laboratory, Aiken, SC (1971).

3. A. G. Evans and L. R. Jones. Confinement of Airborne Radioactivity — Progress Report: July 1971 - December 1971. USAEC Report DP-1298, E. I. du Pont de Nemours & Co., Savannah River Laboratory, Aiken, SC (1972).

4. A. G. Evans. "Effect of Intense Gamma Radiation on Radioiodine Retention by Activated Carbon," Proceedings of the Twelfth Air Cleaning Conference, Oak Ridge, TN, August 28-31, 1972. USAEC Report CONF-720823, pp 401-414 (1973).

5. A. G. Evans. Confinement of Airborne Radioactivity — Progress Report: July 1972 - December 1972. USAEC Report DP-1329, E. I. du Pont de Nemours and Company, Savannah River Laboratory, Aiken, SC (1973).

6. A. G. Evans. Confinement of Airborne Radioactivity — Progress Report: January 1973 - June 1973. USAEC Report DP-1340, E. I. du Pont de Nemours & Co., Savannah River Laboratory, Aiken, SC (1973).

7. A. G. Evans and L. R. Jones. Confinement of Airborne Radioactivity — Progress Report: July 1973 - December 1973. USAEC Report DP-1355, E. I. du Pont de Nemours & Co., Savannah River Laboratory, Aiken, SC (1974).

8. A. H. Dexter, A. G. Evans, and L. R. Jones. Confinement of Airborne Radioactivity — Progress Report: January - December 1974. USERDA Report DP-1390, E. I. du Pont de Nemours & Co., Savannah River Laboratory, Aiken, SC (1975).

9. D. R. Muhlbaier. Nondestructive Test of Carbon Beds for Reactor Confinement Applications — Final Progress Report: January - June 1966. USAEC Report DP-1082, E. I. du Pont de Nemours and Co., Savannah River Laboratory, Aiken, SC (1966).

10. G. H. Prigge. Application of Activated Carbon in Reactor Containment. USAEC Report DP-778, E. I. du Pont de Nemours and Co., Savannah River Laboratory, Aiken, SC (1962).

11. A. H. Dexter and A. G. Evans. Confinement of Airborne Radioactivity — Progress Report: January - December 1975. USERDA Report DP-1430, E. I. du Pont de Nemours and Co., Savannah River Laboratory, Aiken, SC (1976).

DISCUSSION

DEMPSEY: I can't understand why particle size should affect the degradation of the charcoal. Do you have a mental picture of what might be happening?

EVANS: I don't have proof positive but one of the problems, of course, is the accumulation of acidic components from the air itself. We know in our particular system, for example, that we have oxides of nitrogen present. We also have some sulfur dioxide present. These will accumulate on the charcoal and on the larger grain size particles, particularly, but they may not penetrate into the deep sites or they may plug the surface pores. A more likely explanation has to do with the surface oxidation phenomena; that is, the trace quantities of ozone present in the atmosphere as well as atmospheric oxygen. Because of the larger surface-to-volume ratio of smaller grain sizes, the larger grain sizes simply do not allow penetration of these species or diffusion down into the internal structure of the charcoal as well as smaller grain sizes. So the smaller grains seem to weather better because they offer more surface area. There's just more surface to oxidize than there is on the larger particles. This may also suggest, if the hypothesis is correct, that there is a finite limit for any charcoal surface based, for example, on the ambient ozone level.

KOVACH: Wouldn't it be easier to determine whether it is particle size dependent or not by trying the GX-176 impregnation on a range of particle sizes? Are you speculating now that particle size is the only difference?

EVANS: Aside from some proprietary things, the only difference between the GX-176 and G-615 charcoal with respect to impregnation is the TEDA level. Two per cent TEDA is present on G-615 new charcoal. In initial tests, with 2 per cent TEDA on the new charcoal, the G-615 showed superior methyl iodide retention properties. It also showed superior properties in our radiation tests. However, it just does not weather as well, all other things being constant except the TEDA level, which very rapidly decreases with service in the case of 615 because TEDA blows off in a flowing air stream. The only other difference is the particle size distribution.

KOVACH: Do you see the identical TEDA level decrease in bulk adsorbents?

EVANS: At the lower TEDA impregnation level, we believe that the rate of depletion of TEDA is slower. We have not been able to prove this, however. Our efforts to analyze the TEDA content of used charcoal have proven, so far, somewhat less than satisfactory.

KOVACH: A word of caution; when you run ignition or high temperature stability experiments, HEMTA decomposition results in extensive HCN generation.

A METHOD FOR CORRELATING WEATHERING DATA ON ADSORBENTS USED FOR THE REMOVAL OF CH_3I

H. C. Parish and R. C. Muhlenhaupt
CVI Corporation
A Division of Pennwalt Corporation
Columbus, Ohio

Abstract

Traditionally, weathering data have been expressed in terms of removal efficiency as a function of time for a select number of bed depths. The test results are inherently a function of a multiplicity of variables, most of whose effects cannot be isolated. In addition to the exposure time and bed depth, these variables include: 1) variations in the efficiency of the adsorbent when new; 2) guard bed design (bed depth, replacement schedule); 3) air quality; and 4) air velocity. This situation has limited the usefulness of existing data to predict the performance of an adsorbent at some specific set of conditions.

This paper discusses the development of a single parameter, namely, the Effective Weathering Rate (EWR), its usefulness in correlating weathering data, and subsequent utilization during design. The effectiveness of the model was checked by analyzing several sets of data. It was found that a single value of EWR could be determined for each set of data such that the model could be used to reproduce, with reasonable accuracy, the adsorber efficiency for various bed depths as a function of time and, in one case, with and without a guard bed.

Values of EWR were determined from the limited available experimental data for air which could be described only qualitatively as ranging from relatively clean to relatively dirty air from a heavily industrialized area. As quantitative data become available, it is expected that the EWR can be correlated with the character and concentration of air contaminants such as hydrocarbons, SO_2, NO_x and O_3.

The EWR, determined from experimental data, can be used to predict adsorber efficiencies for conditions corresponding to a specific application. Thus, the analytical model can be used to extrapolate from the experimental conditions to the actual conditions for a given application. Some of the changes in conditions which can be treated by this method include: 1) bed depth of adsorbent, 2) addition of guard bed or depth of guard bed, 3) effectiveness of the carbon (new), 4) operating time, and 5) air velocity.

Some parametric studies were performed analytically to demonstrate some applications of the weathering model. These included calculating the adsorber efficiency as a function of time and bed depth, for carbons having various efficiencies when new, and for guard beds of variable bed depth and having different replacement schedules for the guard bed material.

I. Introduction

A few experimental studies on weathering have been conducted to date. Understandably, these studies have been largely independent efforts, each involving adsorbents, air quality, bed depths, air velocity and other test conditions generally selected to represent specific systems for which the tests were conducted. The result has been a collection of data that generally could not be compared in a straight-forward manner or applied to a specific application, generally characterized by another set of conditions. The published data on weathering have generally been in the form of CH_3I removal efficiencies, measured after select intervals of exposure time. Most of the experimental efforts involved nominally 2.5 cm and 5.0 cm adsorber beds with exposure times of less than 1 year. Extrapolation of these results to deeper beds and/or longer periods of exposure is difficult. Even in the one test program in which bed depths up to 15 cm were exposed for a period of up to approximately 1.75 years, extrapolation of the data to any specific application having conditions different from those of test conditions is not straight-forward. In particular, a specific application might utilize an adsorbent having different initial performance characteristics than those of the adsorbent used in the test program. In addition, if a guard bed is used, it may have a different bed depth from the one tested and periodic replacement of the guard bed would generally be expected whereas the only known guard bed data did not involve replacement. Furthermore, the guard bed data were taken over a period of only 14 months, whereas it would be expected that an adsorber, when protected by a guard bed, would have a much longer useful life.

An analytical weathering model has been developed to provide a means of calculating the CH_3I removal efficiency for a weathered adsorbent, requiring only known quantities such as bed depth, exposure time, air velocity, initial performance characteristics, etc. and one new parameter, the Effective Weathering Rate

(EWR). The EWR has been evaluated for the known weathering data and is tabulated in Table I. The EWR is expected to be primarily a function of contaminants in the air such as hydrocarbons, NO_X, SO_2 and O_3. At present, since quantitative data on the concentrations of these species were not available with the weathering data, the EWR can only be correlated loosely as being typical for clean air or dirty air, or some degree between. As more data become available, it is expected that the EWR can be correlated with the concentrations of various air contaminants.

This paper describes an analytical tool that could provide the following benefits:

1) a means for describing available weathering data in terms of a single correlating parameter, considered to be primarily a function of the quality of the air.
2) a means for simplifying the application of weathering data to specific applications and to maximize the utility of experimental weathering data.
3) a means for simplifying future experiments on weathering by minimizing the number of conditions that need be investigated.
4) a basis for an analysis of the effectiveness of guard beds and economic evaluation of guard beds.

Two versions of the analytical model were investigated. The more simplified one is referred to as the zero transition model, and the more refined version is described as the finite transition model. Both are discussed in this paper. The two versions of the weathering model provide consistent results when applied to the same set of data, and hence reinforce and support each other. More importantly, since both can be used to evaluate the EWR, the confidence level of the results is enhanced.

The recommended procedure for applying the weathering model includes the use of both the zero transition and the finite transition models to analyze the appropriate data and to determine the combined best estimate of the EWR. This value of EWR would then be used with the finite transition model to calculate the adsorber efficiency for design conditions including bed depth, exposure time, performance of the new adsorbent and guard bed design factors.

The weathering model, the key concepts and the principle equations are given in the Analysis section of this paper. The efficiencies calculated from the weathering model and a comparison of the calculated and experimental efficiencies are presented in the Results section. The calculations were performed for the complete range of both bed depth and exposure time for which there is experimental data.

The EWR used in the analyses were obtained from the experimental data using both the zero and the finite transition models. The consistency of the EWR, determined by the two versions of the weathering model is also illustrated.

II. Analysis

Description of Weathering Model

The conceptual weathering model used in this analysis is an intuitively obvious one. It was assumed that the weathering phenomenon could be represented as a progressively advancing zone of ineffective adsorbent. This assumption was indicated by data from the literature and further justified, post priori, by the results of the subsequent analysis.

Two versions of this model were investigated, and each was found to have certain useful properties. The first model was the simplest in which the transition from weathered to unweathered carbon had zero thickness. The second model considered a finite transition. The general equation as applied to both of these concepts and the associated analytical procedures are described below.

General Performance Equation

A few observations can be made with respect to the removal of CH_3I by the commonly used adsorbents that apply to either of the two weathering models.

In a homogeneous material, CH_3I performance can generally be described by relating the fractional penetration to bed depth by the equation:

$$P = e^{-Bx} \tag{1}$$

where

P = fractional penetration
B = characteristic constant of a given adsorbent under a standard set of test conditions [cm^{-1}]
x = bed depth [cm]

By definition, the fractional penetration at any moment in time for N beds or bed segments in series is given by:

$$P = P_1 \cdot P_2 \ldots\ldots P_N = e^{-\sum_{i=1}^{N} B_i \Delta x_i} \quad (2)$$

where B_i is considered to be constant over each segment Δx_i. In the limit as $\Delta x \rightarrow 0$, this can be written as:

$$P = e^{-\int B'(x)dx} \quad (3)$$

where $B'(x)$ is a function of x for any moment in time. From Equation 3, the penetration at any moment is given by the exponential of the area under the curve in which $B'(x)$ is plotted as the instantaneous function of x.

Weathering Model with Zero Transition Zone

The initial analyses were performed using the simplest possible model in which it was assumed that the adsorbent in the weathered zone, represented by the cross hatched area in Figure 1-A, was rendered totally ineffective in the removal of CH_3I while the remainder of the adsorbent maintained 100% of its original effectiveness. It is recognized that this is a simplified model since it is unrealistic to expect the demarcation between the weathered and unweathered zone to be a sharp line. Rather, a "gray" area of transition would be expected as illustrated conceptually in Figure 1-B. Nevertheless, the data calculated from this model does provide physically meaningful information.

Based on this weathering model, an equivalent depth of the weathered zone can be calculated from Equation 4, given the new carbon performance (to determine B_o) and a measured penetration, P. See Figure 1-A for physical representation of variables.

$$X_1 - X_2 = \frac{\ln P}{B_o} \quad (4)$$

where

P = ratio of the outlet to inlet concentrations
B_o = the adsorbent characteristic constant
X_1 = the weathered zone length
X_2 = the total bed length.

This approach was tried initially. The results were reasonably consistent for adsorbent weathering penetrations up to approximately 45%.

The unweathered zone length, shown in Figure 1-A, can be expressed in terms of the integral of $B'(x)$ by combining Equations 1 and 3. Thus

$$(X_2 - X_1) = \frac{1}{B_o}\int B'(x)dx \quad (5)$$

From Equation 5, the area under the $B'(x)$ vs x curve is equal to the product $B_o\,(X_2 - X_1)$ as illustrated in Figure 2-A.

It can be demonstrated that this model provides consistent results independent of the bed length from which the data are taken, provided the leading edge of the transition zone has not "broken through" the bed, that is, if $X_b \leqslant X_c$ (See Figure 1-B).

For example, consider the variation of $B'(x)$ with x as illustrated in Figure 1-B in which this condition is met. The integral of Equation 5 can be evaluated in two steps, from zero to X_b and from X_b to X_c using the notation shown in the figure. Rearranging the equation then gives

$$B_o(X_2 - X_1) = \int_o^{X_b} B'(x)dx + \int_{X_b}^{X_c} B_o dx$$

or

$$B_o(X_2 - X_1) = \int_o^{X_b} B'(x)dx + B_o(X_c - X_b). \quad (6)$$

The length of weathered carbon, X_1 in Figure 1-A, is determined from

$$X_1 = X_2 - (X_2 - X_1) \tag{7}$$

where $(X_2 - X_1)$ is calculated from Equation 6.

Thus, for any increment $\triangle L$ added to the total length, X_2, a corresponding $\triangle L$ is added to $(X_2 - X_1)$ from Equation 6 and X_1 is unaffected by Equation 7. The same reasoning can also be used to show that the calculated length X_1 will vary with the total length chosen if the transition zone has broken through the section from which the data were taken. Therefore, the calculated value of X_1 will be in error under this condition.

Therefore, one of the principle guidelines to be observed in the application of the simplified model is that the data be taken on a bed of sufficient length and at a time such that the weathering effect has not progressed to the end of the bed. A quantitative criterion was analytically developed requiring that the calculated weathered zone should not exceed 43.8% of the total bed length. If this criterion is met, it can be shown by analysis that the error will be less than 5%. This, of course, does not consider experimental error or "real world" deviations from the analytical model.

Weathering Model with Finite Transition Zone

The simplified model described above was refined to include a transition zone of finite length as illustrated in Figure 1-B. The application of the new model differs somewhat from that of the previous one, in that the simplified model can be used to calculate the weathered zone length directly in the form of a closed solution, whereas the new model utilizes a trial and error process to determine the adsorbent weathering rate.

The analysis was performed in the following manner. The transition zone was divided into 100 equal increments of x, and a function B(x,t) was defined such that an average value of B for each increment at a given time could be determined. The total penetration was then calculated using Equation 2.

The major effort was in determining the correct expression for the function B(x,t) in equation form. The experience with the simplified model suggested defining the effective length of weathered zone (L_W) as the distance into the adsorber bed at which the characteristic constant B is one half its value for the new adsorbent. That is B equals $B_O/2$ at x equals L_W as illustrated in Figure 2-A. Values for B(x,t) were calculated from data obtained in Table 1 of Reference 1.

The function (B(x,t) can be expressed in equation form as:

$$B(x,t) = B''(x,L_W) \tag{8}$$

where

$$L_W = B'''(t) \tag{8A}$$

The function $B''(x,L_W)$ was determined empirically from the data in Table 1 of Reference 1, and is expressed in Equation II.

The function $B''(x,L_W)$ was not changed after it had been established for that one set of data. It was felt that the usefulness of the correlation procedure would be limited if more than one variable had to be determined for each application. Fortunately, the results of this effort indicated the function $B''(x,L_W)$ to be sufficiently universal.

The function $B'''(t)$, was determined from

$$B'''(t) = L_W = EWR \cdot t. \tag{9}$$

As noted earlier, the EWR is considered to be a constant for a given air velocity and quality of air.

The calculations were then performed in the following manner. Using Figure 2-A as a guide, the position corresponding to B equals $B_O/2$, shown as L_W, was determined from Equation 9. For correlation of experimental data the EWR was determined by trial and error. Also, the zero transition model was initially used to provide a good first estimate of the results. This technique is developed below. If the calculations are for design purposes, the EWR is based on experimental data or obtained from the data reported herein. The location of Q, the trailing edge of the transition region, was determined from:

$$Q = L_W(1 - 0.3565 \cdot L_W^{0.25}) \tag{10}$$

where the units for L_W and Q are cm.

B(x,t) was calculated using Equation 11.

$$B(x,t) = B''(x,L_W) = \frac{B_O}{2}\left(\frac{x-Q}{L_W-Q}\right)^{0.3} \quad (11)$$

The constants for Equations 10 and 11 were determined from the data given in Table 1 of Reference 1. These constants were then used for all subsequent analyses described in this paper. Experimental values for B(x,t) were calculated from the data in Table 1 of Reference 1 and are shown in Figure 2-B as the solid lines. Figure 2-B also shows curves representing B(x,t) calculated from Equations 10 and 11. The calculated data fit the experimental data reasonably well, particularly since the integral of the curve is used in calculating penetration (see Equation 3).

Relationship Between dX_1/dt and EWR

The rate at which the weathered zone progresses through the adsorbent in the zero transition model is described by the derivative dX_1/dt, which has the same units (i.e., cm/yr) as the EWR of the finite transition model. It is interesting and useful to note the relationship between the two quantities.

From the definition of the two models and Figures 1-A, 1-B, and 2-A, it would be expected that a functional relationship should exist between dX_1/dt and the EWR. This was confirmed by calculations, the results of which are presented in Figure 3.

III. Results

The calculated data, illustrated in Figure 4 thru Figure 18, were based on actual experimental conditions and were obtained by essentially the same procedures that would be used in performing design calculations. The experimental data points are plotted along with the calculated data (lines).

Two values of EWR were initially determined for each set of experimental data shown in Figures 4 through 11. One value was calculated using the zero transition model while the other was determined using the finite transition model. The final EWR for each set of data was then established considering the results from both models.

The EWR for the experimental data in Figure 12 was determined entirely from the zero transition model (dX_1/dt) and Figure 3. The resultant EWR was used with the finite transition model to obtain the analytical results illustrated in the figure.

In all cases, the zero transition model was used to calculate dX_1/dt only for data meeting the requirement that X_1 (calculated) did not exceed 43.8% of the test bed depth.

Having determined the EWR from one or both versions of the weathering model, that value was used in the finite transition model to calculate the adsorber efficiency as a function of bed depth and exposure time for the test conditions.

One of the significant results is the degree to which the calculated data fit the experimental data. In some cases, a wide range of bed depths and exposure times were represented by a single set of experimental data. Nevertheless, the data for each set were generally reproduced well by the model using the EWR characteristic for that set of data. In addition, consistency in the results obtained using the zero and finite transition models is apparent from Figures 13 through 18, considering that the EWR (represented by the lines) used with the finite transition model reproduced the experimental data while the EWR from the zero transition model was calculated directly from the data.

Figures 4 thru 12 show the experimental data from the various references plotted as discrete points and the corresponding analytical data plotted in curvilinear form.

The results shown in Figure 4 are based on the data in Table 2.10 of Reference 2. As with all of the data reported to date, no measurements of air contaminants were provided. However, it is expected that the quality of the air would typically be good for the part of the country (Oak Ridge, Tennessee) in which the test was conducted. It is recognized that air from any closed space could be highly contaminated; however, no indication of any unusual contaminants were reported. The air velocity during the exposure period was 10.2 cm/s (20 fpm) compared to the more common velocity of 20.3 cm/s (40 fpm). The velocities are indicated in the graphs using the symbol V.

As may be noted in the figure, the calculated values for both the 2.5 cm and 5.0 cm bed depths agreed well at an EWR of 1.75 cm/yr, for up to 300 days. Consistency of the two models is illustrated in Figure 13. The zero transition zone results at 300 days did not meet the less than 43.8% weathered criterion and hence were not included. However, as noted, the X_1 values calculated directly from the experimental data

from the 2.5 cm and 5.0 cm beds fall very close to the finite transition zone curve (EWR that reproduced the data in Figure 4).

Figure 5 represents the data in Figure 4 (LITR-BSR data) of Reference 3. For this set of data, the best overall (considering both the 2.9 cm and the 5.8 cm beds) fit of calculated efficiencies to the experimental results would be achieved with a slightly lower EWR than the value used. A smaller EWR would tend to raise the calculated efficiencies for both the 2.9 cm and 5.8 cm beds, but the efficiency of the smaller bed would increase more rapidly. However, the 5.33 cm/yr EWR was chosen partially on the basis that this value produced results that correspond favorably to those calculated using the zero transition model (see Figure 14). In addition, since 5 cm beds are much more commonly used for the removal of CH_3I than 2.5 cm beds, it was considered desirable to preferentially fit the 5.8 cm bed depth data.

The experimental data in Figure 6 are also from Figure 4 of Reference 3, but represent the HFIR data. Again, the calculated efficiencies would fit the experimental data a little better using a slightly lower EWR than that shown. However, factoring in the data from the zero transition model, a rate of 4.04 cm/yr was selected for the EWR. Thus, both the zero and finite transition models were used to determine a consistent EWR from the experimental data. The resultant EWR was used with the finite transition model to calculate efficiencies as indicated by the curves in Figure 6.

Figure 7 presents the results of the calculations based on the KI-impregnated carbon data listed in Table 1 of Reference 1. In this case an EWR of 10.8 cm/yr provided the best overall fit (also see Figure 16).

The results shown in Figure 8 are based on data obtained from Figure 3 of Reference 1. An EWR of 7.62 cm/yr provided the best overall fit of calculated efficiencies to experimental data. The calculated efficiencies compare well with the measured efficiencies for bed depths of 2.5, 5.0, 12.5, and 15.0 cm. Although the comparison is not as good for bed depths of 7.5 and 10.0 cm at 387 days, the overall correlation between calculated and experimental data is considered to be very acceptable. Consistency of the two analytical models is illustrated in Figure 17. Only two data points were applicable for the zero transition model, since the others exceeded the X_1/L value of 0.438.

The experimental data in Figure 9 are from Figure No. 5 of Reference 1. In this case an EWR of 10.16 cm/yr provided the best overall fit of analytical and experimental data. The calculated and experimental data compared reasonably well for bed depths of 2.5, 5.0, and 7.5 cm. Even though the comparisons were not as good at 10 and 12.5 cm, the overall correlation between calculated and experimental data is considered to be acceptable. There were no data meeting the X_1/L less than 0.438 requirement; therefore, the zero transition zone model was not used in evaluating the EWR.

Figure 10 shows the results obtained using the experimental data from Figure 2 of Reference 1. These test data were taken using comparable air with the same type of impregnated carbon as that in Figure 7 of this paper, but this time preceded by a guard bed material of the same base carbon but without the impregnant. Therefore, it seemed reasonable to assume that the same function B(x,t) would apply as before, starting at the inlet to the guard bed at time t = 0. The penetration through the adsorber can be calculated from Equation 3 at any time "t", where the integral is evaluated from the inlet to the outlet of the adsorber. If the model is valid, the EWR should be the same as that used for Figure 7 of this paper. Accordingly, an EWR of 10.80 cm/yr was assumed with no effort being made to determine a best fit value. Fortunately, as seen in Figure 10, the same value of EWR fit the data with guard bed fairly well.

The results shown in Figure 11 are based on the limited test data shown in Table II of Reference 1. Again, none of the data was suitable for the application of the zero transition model. In addition to the usual test data for the first bed and for two beds in series, the data from Reference 1 included an efficiency for the second bed alone (the first bed in effect being a guard bed). The analysis included a calculation for the same bed. Both the experimental and calculated values for the second bed are shown in Figure 11. The calculated efficiencies are in good agreement with the measured.

The experimental data in Figure 12 are from Figure 4 (TEDA data) of Reference 3. This analysis was performed somewhat differently from the previous ones in that the zero transition model alone was used to calculate the EWR from the experimental data. The EWR thus determined was then used as usual in an analysis by employing the finite transition model to calculate efficiencies for various bed depths and exposure times. It can be seen from Figure 12 that the EWR, as determined solely by the zero transition model, provides a good fit of the data when used in the finite transition model.

It should be mentioned that experimental data shown in Figure 4 and Table III of Reference 1 were not used in this effort. The data from Figure 4 were from a test consisting of a sodium zeolite/silver zeolite,

guard bed/adsorber bed combination and the current weathering model is not suited to a system in which the guard bed would have significantly different removal characteristics for the weathering agents than that of the adsorbent. However, it is anticipated that this restriction can be removed with some additional development. For now though, the data of Figure 4 is not compatible with the model since, as Wilhelm concluded, the sodium zeolite apparently did not adequately remove the weathering agents that attacked the AgX because the weathering did not seem to be significantly retarded by the addition of the guard bed[1].

Data from Table III of Reference 1 were not included because there was some uncertainty over one of the data points. That is, there appeared to be an inconsistency between the reported CH_3I removal efficiencies at 5 months and 6 months for filter bank No. 1.

Ranges of EWR for Data Evaluated

The values of EWR determined for each set of experimental data are summarized in Table 1. Based on the assumption that the EWR is proportional to the air velocity for a given adsorbent and quality of air, the indicated EWR is adjusted for velocity. The results for EWR, adjusted to a velocity of 20.3 cm/s are listed in the Table. These data are tabulated in ascending order of adjusted EWR.

Table I. Summary of EWR data

Reference Figure No.	Indicated EWR (cm/yr)	Superficial Velocity (cm/s)	EWR Adjusted to 20.32 cm/s (cm/yr.)	Air Quality* Code No.	Adsorbent
4	1.75	10.16	3.51	1	Carbon, KI_3
6	4.04	20.32	4.04	2	Carbon, KI_3
12	4.24	20.32	4.24	3	Carbon, TEDA
5	5.33	20.32	5.33	3	Carbon, KI_3
8	7.62	25.0	6.20	4	Silver Zeolite
9	10.16	25.0	8.26	5	Silver Zeolite
7	10.80	25.0	8.79	4	Carbon, KI
10	10.80**	25.0	8.79	4	Carbon, KI**
11	20.32	30.0	13.74	5	Carbon

*Air Quality Code No. Descriptions –

1. Ambient Air from the Oak Ridge Research Reactor
2. Air from the Oak Ridge High Flux Isotopes Reactor; reasonably steady relative humidity and temperature
3. Air from the Oak Ridge Bulk Shielding Facility – a swimming pool type. Unsteady relative humidity and temperature
4. Industrial Environment – "very near to several chemical factories, oil fired power plants, etc."
5. Air from a reactor building

**EWR taken from inlet to guard bed

The data are also coded by numbers "1" thru "5", incorporating the available information with respect to the quality of the air. Although quantitative data on this parameter are not available, the trend appears to be towards increasing EWR with poorer quality air, as would be expected. Relatively little is known about the quality of the air coded as No. 1 from the Oak Ridge Research Reactor Building. However, these data and data coded as No. 2 and 3 were obtained in tests conducted using air from comparatively unindustrialized areas of Tennessee where the air is presumed to be relatively clean. This, of course, is not necessarily true for closed spaces which could be contaminated, for example, by cleaning agents or paints.

The air coded as No. 3 was considered by Davis and Ackley to present a somewhat more severe weathering condition than that coded as No. 2 because of relatively large swings in temperature and relative humidity[3]. For the two sets of data using air identified as code No. 3, the EWR for KI_3 impregnated carbon was 5.33 cm/yr compared to 4.24 cm/yr for TEDA impregnated carbon.

The air coded as No. 4 is described in Reference 1 as industrial air "very near to several chemical factories, oil fired power plants, etc." As seen in Table 1, the EWR values for data using air coded No. 4 were higher than those for the adsorbents exposed to the Tennessee air. The EWR for KI impregnated carbon was also somewhat higher than that for Silver Zeolite with the same air.

The air coded as No. 5 is from a reactor building. The quality of that air is not indicated; however, Table 1 shows that the EWR is consistently high for both the carbon and the silver zeolite adsorbents.

Example Applications of the Weathering Model

In addition to serving either as the basis for the analysis and correlation of data as described above or as a useful tool in estimating adsorbent life in a specific application, the weathering model can be used in various parametric studies. Two examples are described below to demonstrate some of the possible applications of the model. An EWR of 5.08 cm/yr was used in both examples as a representative value based on the range of EWR indicated in Table 1. It should be emphasized that these results are presented on the basis of actual operating time, not calender time.

Note: It is recommended that the weathering model be proven by additional comparison to experimental data, especially guard bed data, prior to placing extensive reliance on these or other results from the weathering model.

Calculated Effect of Initial Adsorbent Efficiency on Service Life

An analysis was performed to estimate the effect of the efficiency of the adsorbent (when new) on its predicted life under weathering conditions. These calculations were made for a 5.0 cm bed and a 10.0 cm bed, using the finite transition zone model. As noted earlier, an EWR of 5.08 cm/yr was used in the calculations. The results of this analysis are illustrated in Figure 19. For purposes of discussion, an arbitrary limit of 90% removal efficiency was used as the criterion to define the bed life. Three adsorbents (A, B, and C) having initial efficiencies of 99.99%, 99.9%, and 99.0%, respectively for a bed depth of 5.0 cm were analyzed. Based on the 5 cm bed depths, adsorbent "C" would last 130 days whereas adsorbent "B" would last 223 days (a 72% increase), and adsorbent "A" would last 301 days (a 132% increase). Similar relative increases were determined for a 10 cm bed.

Also, the analytical results indicate a disproportionate increase in bed life with increased bed depth. For example, doubling the bed depth results in an adsorbent life of approximately 5.5 times as long. Wilhelm made a similar observation from his experimental data [1].

Guard Bed Calculations

The weathering model can be applied readily to calculate the effectiveness of guard beds of various bed depths, within the present limitation that the guard bed and adsorber have approximately the same removal characteristics for the weathering agents. It is believed that this restriction can be removed with a further refinement of the model. The results of a sample guard bed analysis are presented in Figure 20. Although it is beyond the scope of this paper, this type of analysis has been combined with estimated replacement and capital costs to provide economic evaluations for the use of guard beds.

The results in Figure 20 indicate the efficiency of the adsorber as a function of time for two combinations of guard bed thickness and replacement schedule. Both analyses were performed for a 5 cm deep adsorber bed. One analysis was based on a guard bed thickness of 5 cm and a replacement schedule of every six months while the other was based on a guard bed thickness of 10 cm and a replacement schedule of every 12 months. All calculations were based on an EWR of 5.08 cm/yr as discussed earlier and an initial adsorbent efficiency of 99.9%.

IV. Summary

The weathering model was tested by analyzing several sets of experimental weathering data, using the data to determine an EWR and subsequently calculating adsorber efficiency as a function of bed depth and time. The results of all the analyses were considered to be satisfactory, especially in view of the range of bed depths and exposure times covered in many of the experiments. The results of one test, conducted without a guard bed, were even extrapolated to successfully predict the results of another test in which a guard bed was used.

The recommended procedure for applying the weathering model in a design situation is summarized as follows:

If weathering data from the literature is to be used, either refer to Table I of this paper for the appropriate value of EWR or use any other available data to select or calculate an EWR which is associated with the air quality that would be considered to represent a weathering condition at least as severe as the expected operating situation.

If a weathering test is to be performed, the air used in the test should be as representative of the operating air as practicable. Certainly, the more data that are taken, will result in a higher degree of confidence in the results. However, the weathering model has shown sufficient promise that at least interim

design information could be obtained by a relatively modest weathering test program. For example, data taken at 60 days and 120 days on a 5 cm and 10 cm bed (four data points) could be extrapolated to substantially longer operating periods, different bed lengths and various guard bed design configurations, provided the guard bed material meets the conditions described earlier.

Whether the data is taken from the literature or from a weathering test conducted especially for the specific design effort, it is recommended that both the zero transition model and the finite transition model be used to evaluate the EWR, with the selected value being that which provides the best overall fit for the two versions of the weathering model.

Having determined the EWR that characterizes the design conditions, that value should be used with the finite transition model to calculate the adsorber efficiency corresponding to whatever design bed depth and operating time may be required and for the appropriate guard bed parameters, if a guard bed is to be used.

One condition for application of the weathering model should be noted; it is important that the adsorber efficiency test conditions be consistent throughout. That is, the tracer test used to measure the removal efficiency of the adsorber must use the same relative humidity, temperature, air velocity, etc., for testing the new adsorbent and all subsequent tests as the adsorbent is aged.

In addition to its use as a design tool in the sense indicated above, the EWR, used with the weathering model, could be used as a correlating parameter.

If future weathering data are used to calculate an EWR from this weathering model and if quantitative data are taken on the concentration of trace contaminants as well as relative humidity, then it may be possible to correlate the EWR with SO_2, NO_X, O_3 and hydrocarbon concentrations. If sufficient data become available, it may also be possible to define and correlate a function $B''(x,L_W)$ for each of the contaminants and combine the functions to obtain an overall $B''(x,L_W)$ based on the concentrations of each contaminant. In this event, given a set of air quality measurements, the life of an adsorber could be predicted with relative confidence for various adsorber thicknesses, adsorbents, air velocities, and with or without guard beds, without requiring further weathering tests. Even now, since the range of EWR is not as large as might be expected for the data reported, a value for the EWR or a range of values could be assumed.

The weathering model could also be potentially useful in performing parametric studies including the optimization of adsorber bed depth, adsorber quality (initial performance) and, for guard beds, the optimization of guard bed depth, and replacement schedule for the guard bed material.

Although the results reported herein are encouraging, some refinement of the weathering model may be indicated as additional data become available.

References

1. Wilhelm, J. G., Dillman, H. G., Gerlach, K., "Testing of Iodine Filter Systems Under Normal and Post – Accident Conditions", Proceedings of 12th AEC Air Cleaning Conference 1972, pp. 434-444.
2. Cottrell, Wm. B., "ORNL Nuclear Safety Research and Development Program Bimonthly Report for November-December 1967", ORNL-TM-2095, February 5, 1968, p. 42.
3. Davis, R.G. and Ackley, R. D., "Long-Term Effects on Radioiodine Trapping by Charcoal", Proceedings of 12th ACE Air Cleaning Conference 1972, pp. 469-483.

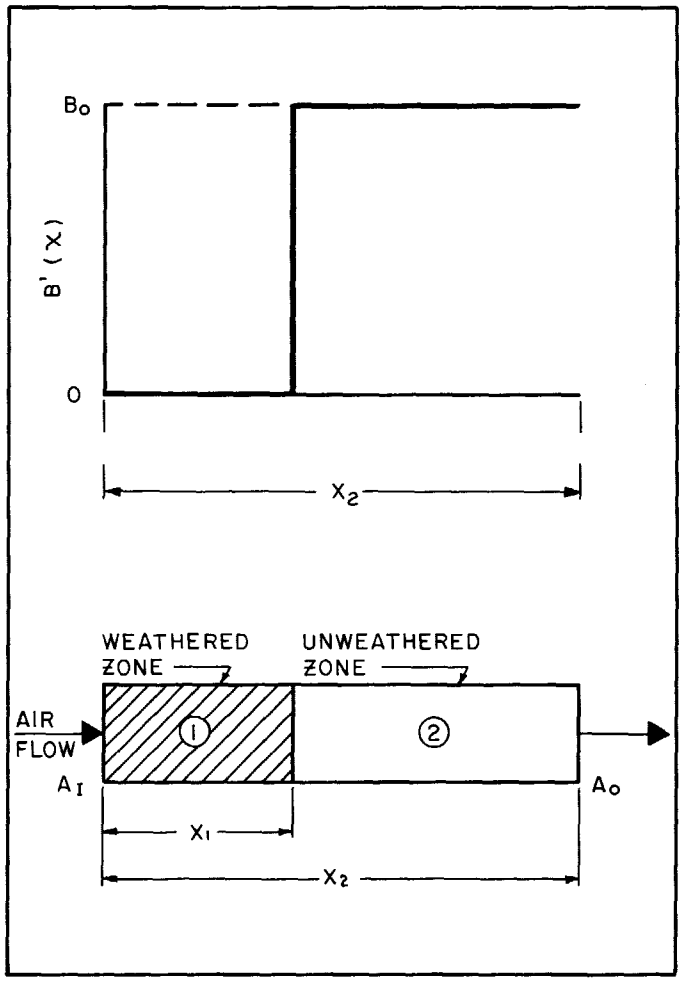

Figure 1-A. Schematic drawing illustrating concepts of simplified weathering model with a transition zone of zero length.

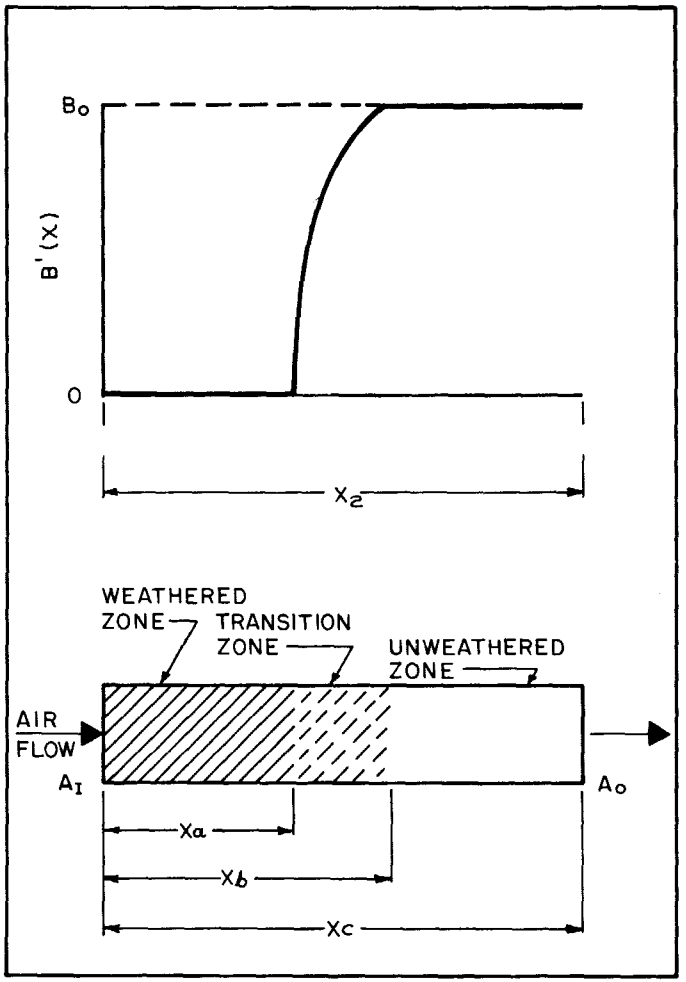

Figure 1-B. Schematic drawing illustrating concepts of weathering model with a transition zone of finite length.

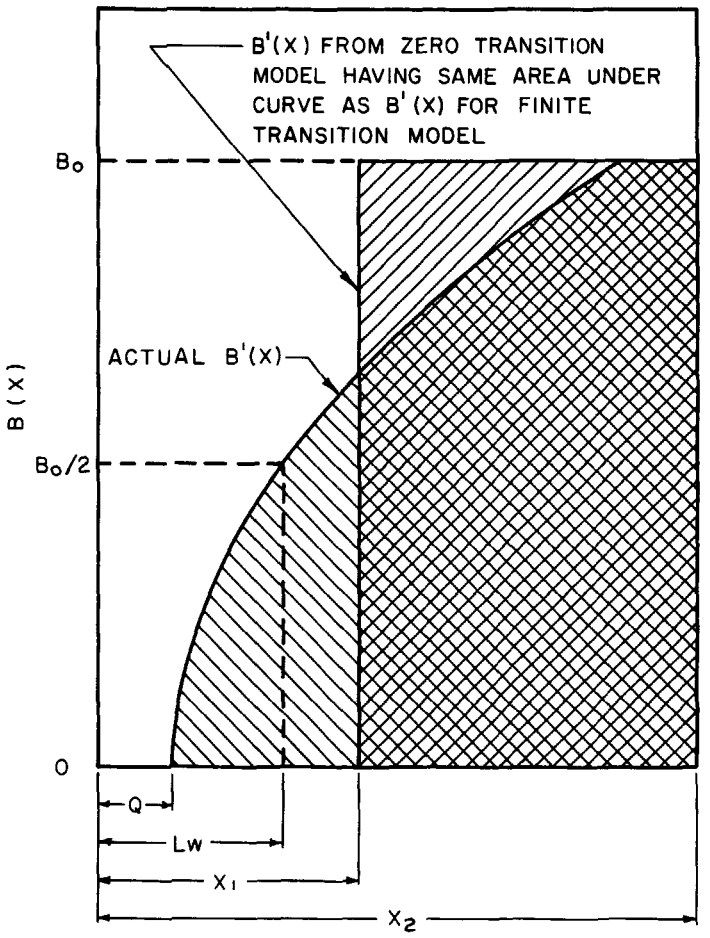

Figure 2-A. Typical curves representing actual B'(x) and step function form of B(x) from simplified model.

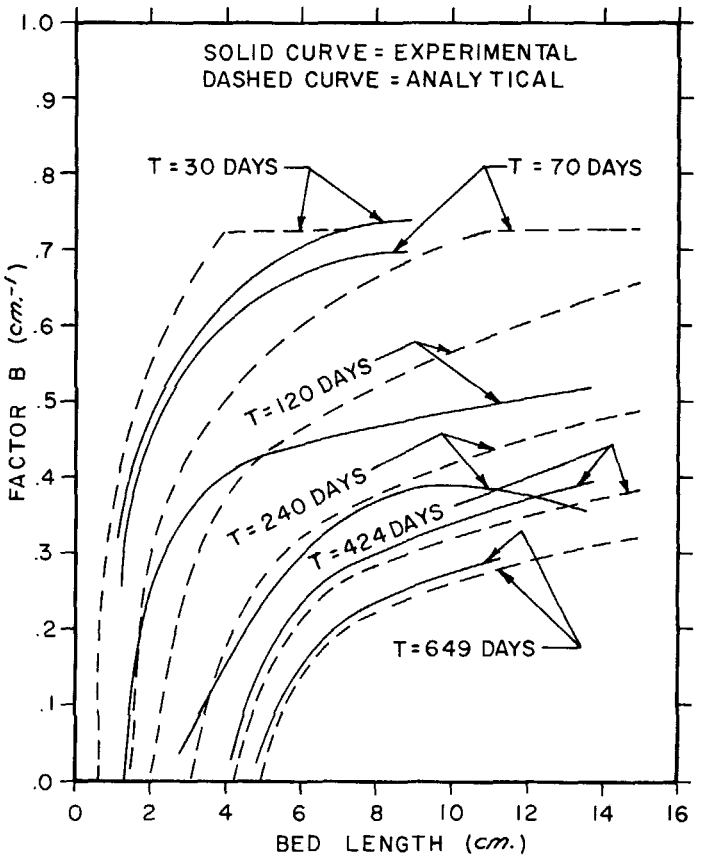

Figure 2-B. Comparison of experimental and curve fit values for performance exponential "B" factor.

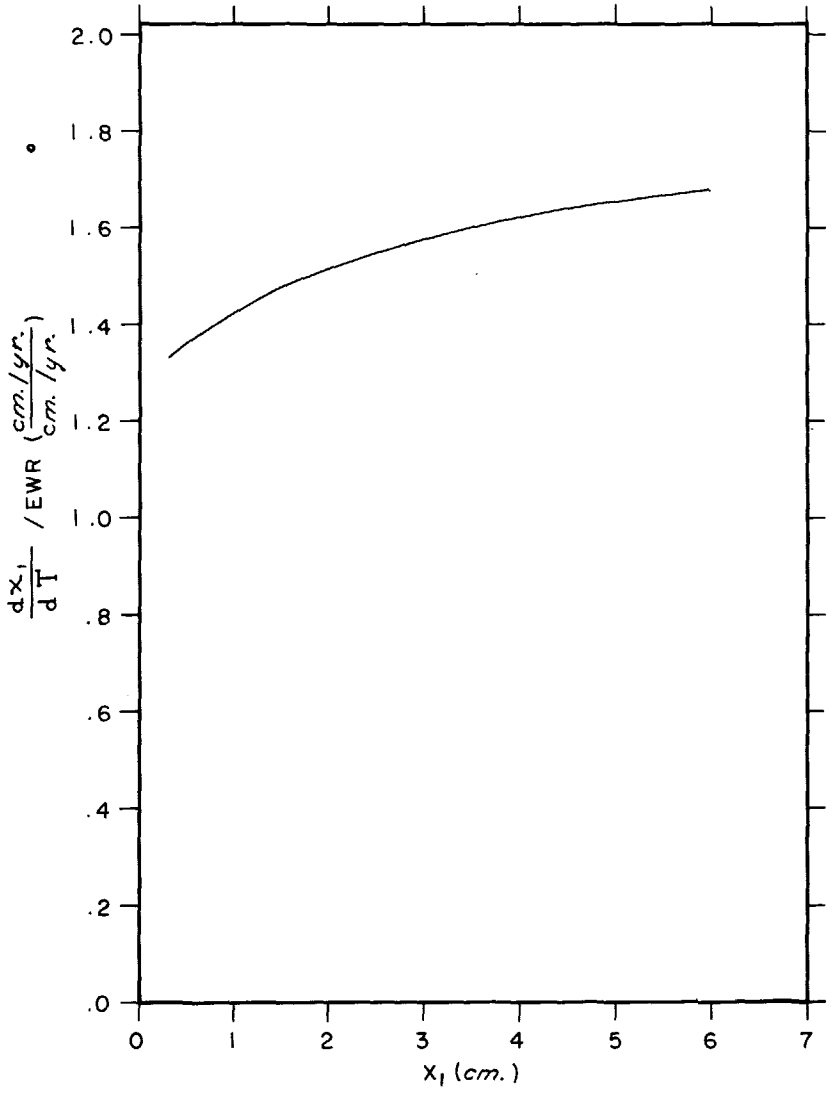

Figure 3. Relationship between rate of weathering calculated using two different weathering models.

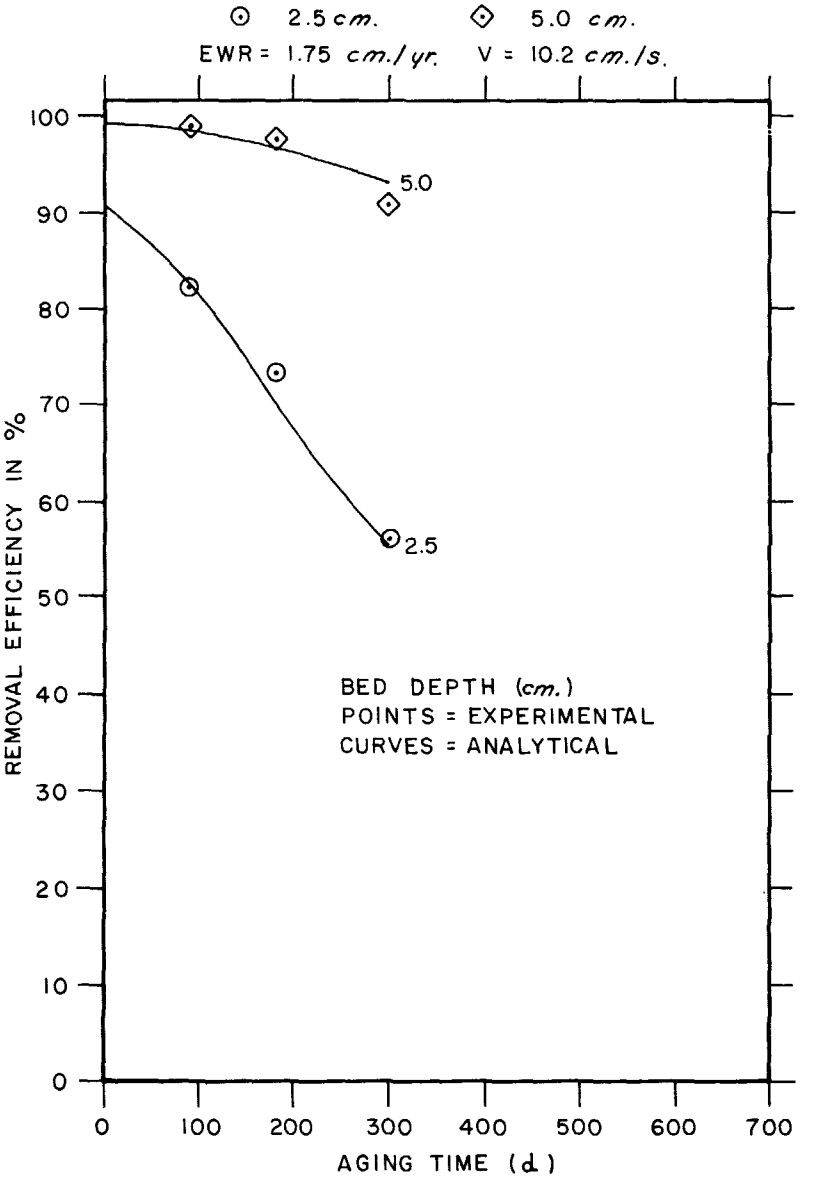

Figure 4. Experimental data from Table 2.10 of Reference 2 and corresponding analytical results.

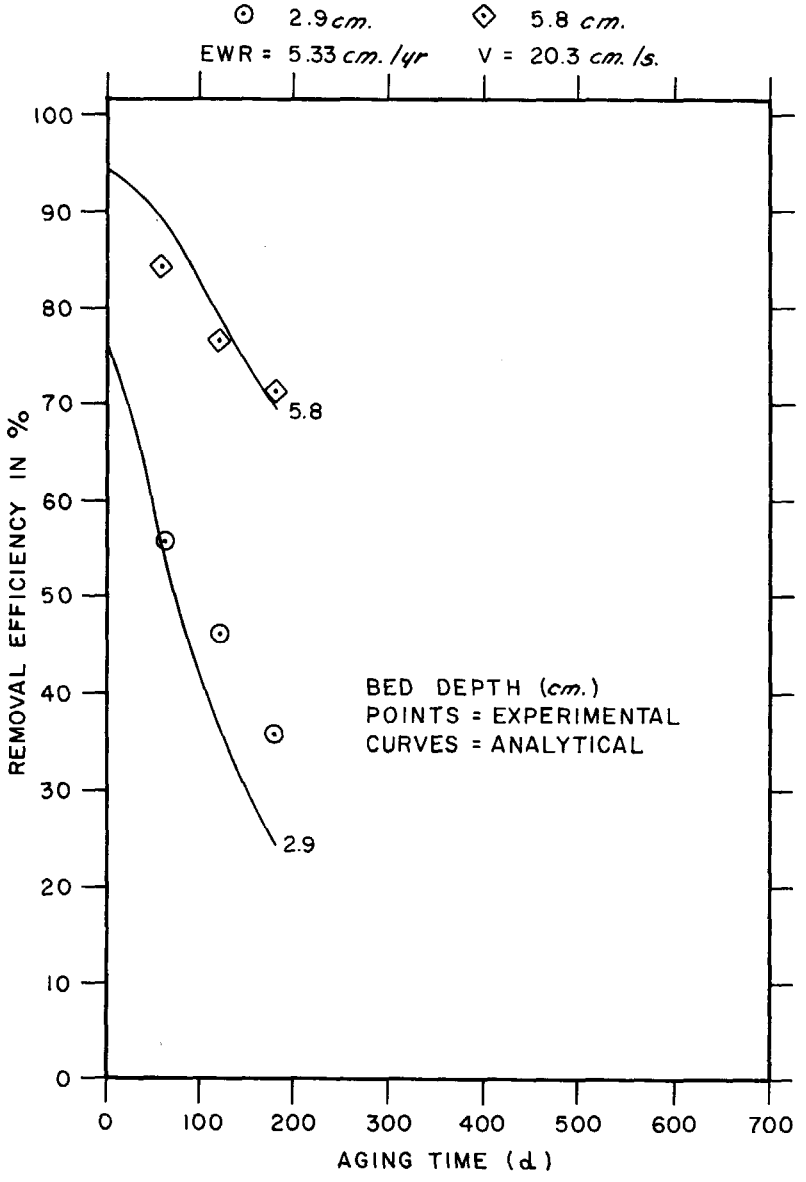

Figure 5. Experimental data from Figure 4 of Reference 3 (G617-BSR) and corresponding analytical results.

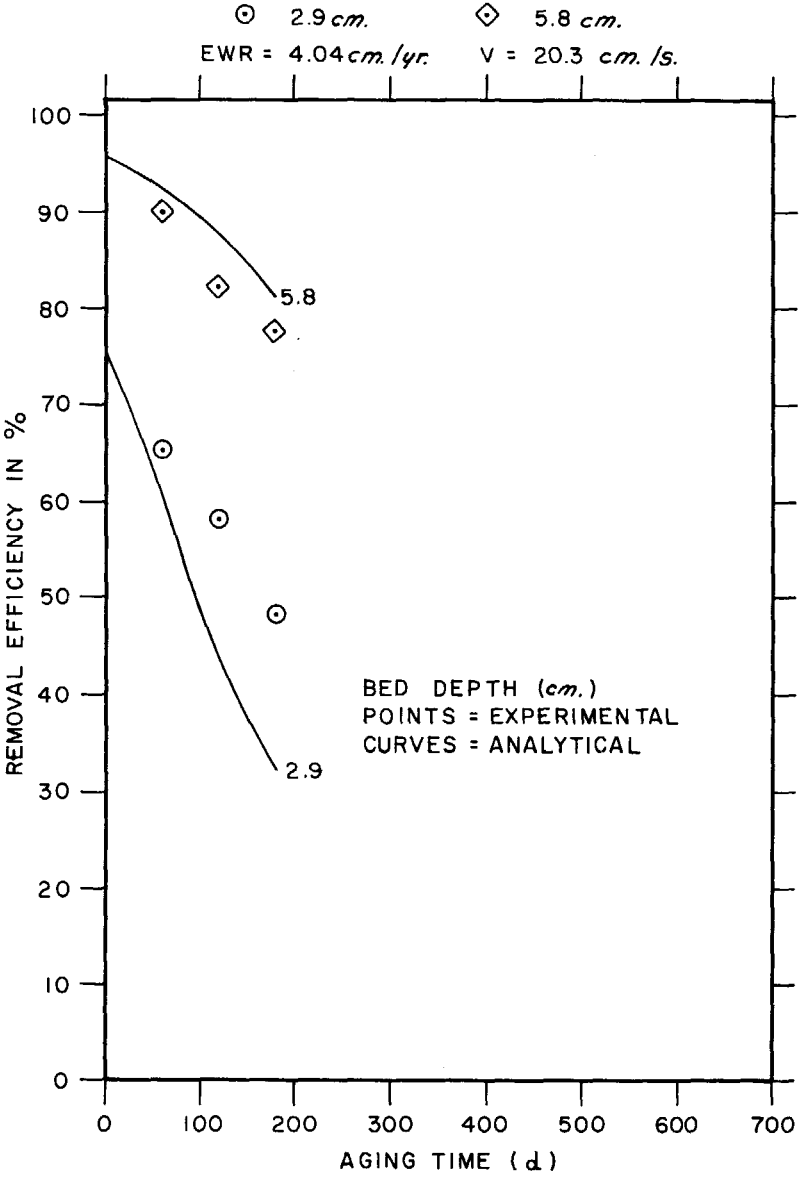

Figure 6. Experimental data from Figure 4 of Reference 3 (G617-HFIR) and corresponding analytical results.

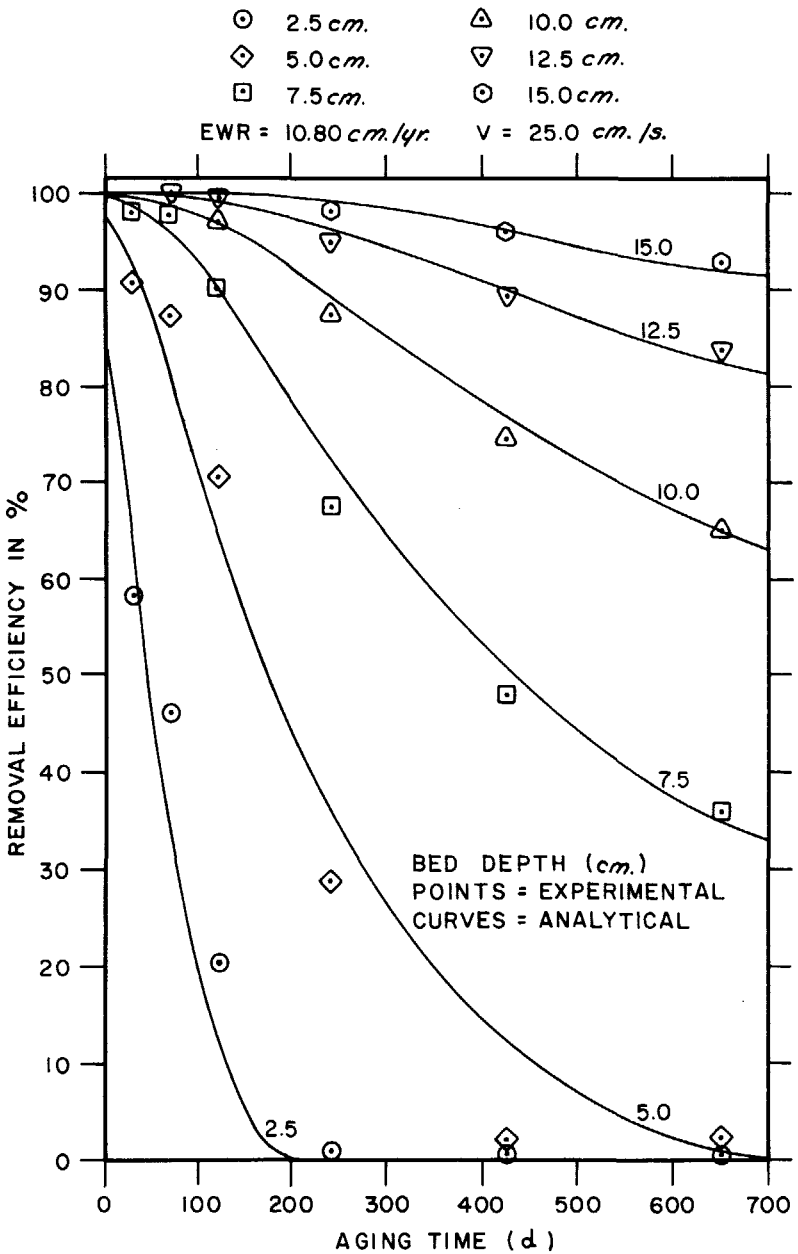

Figure 7. Experimental data from Figure 1 of Reference 1 and corresponding analytical results.

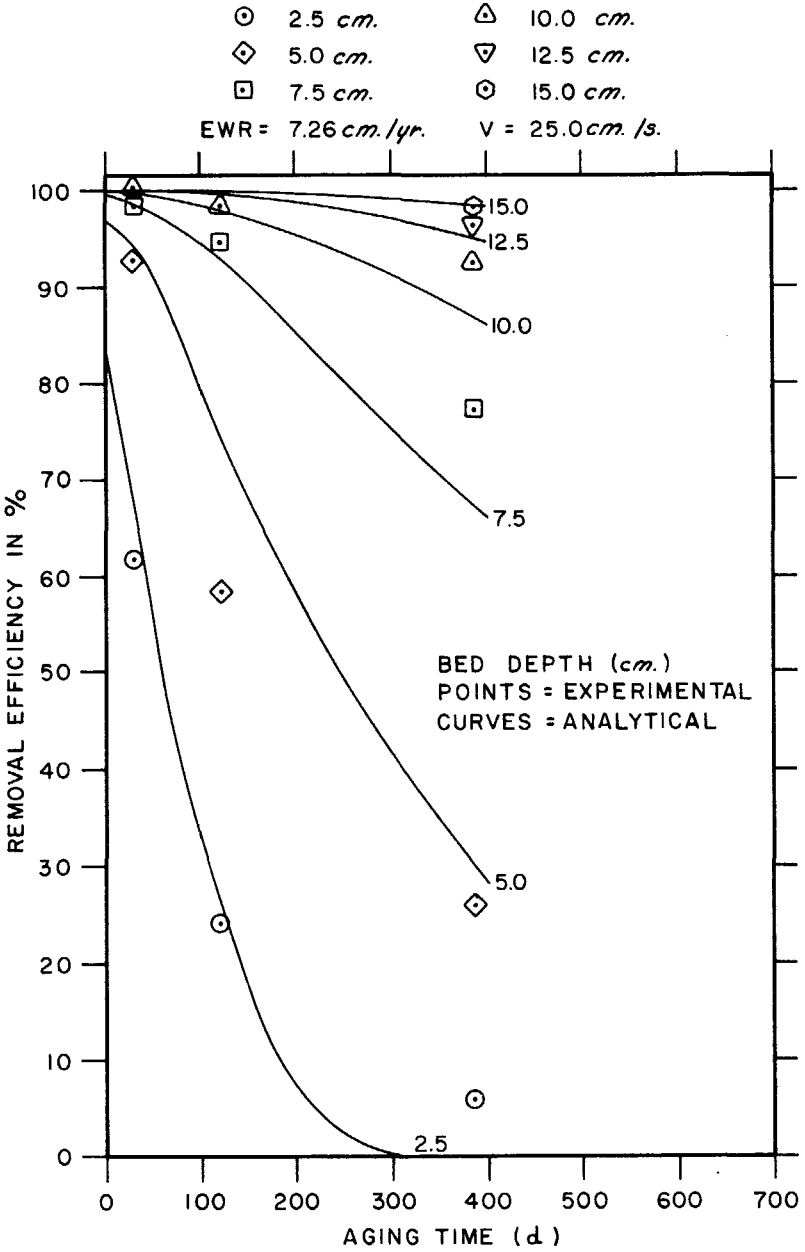

Figure 8. Experimental data from Figure 3 of Reference 1 and corresponding analytical results.

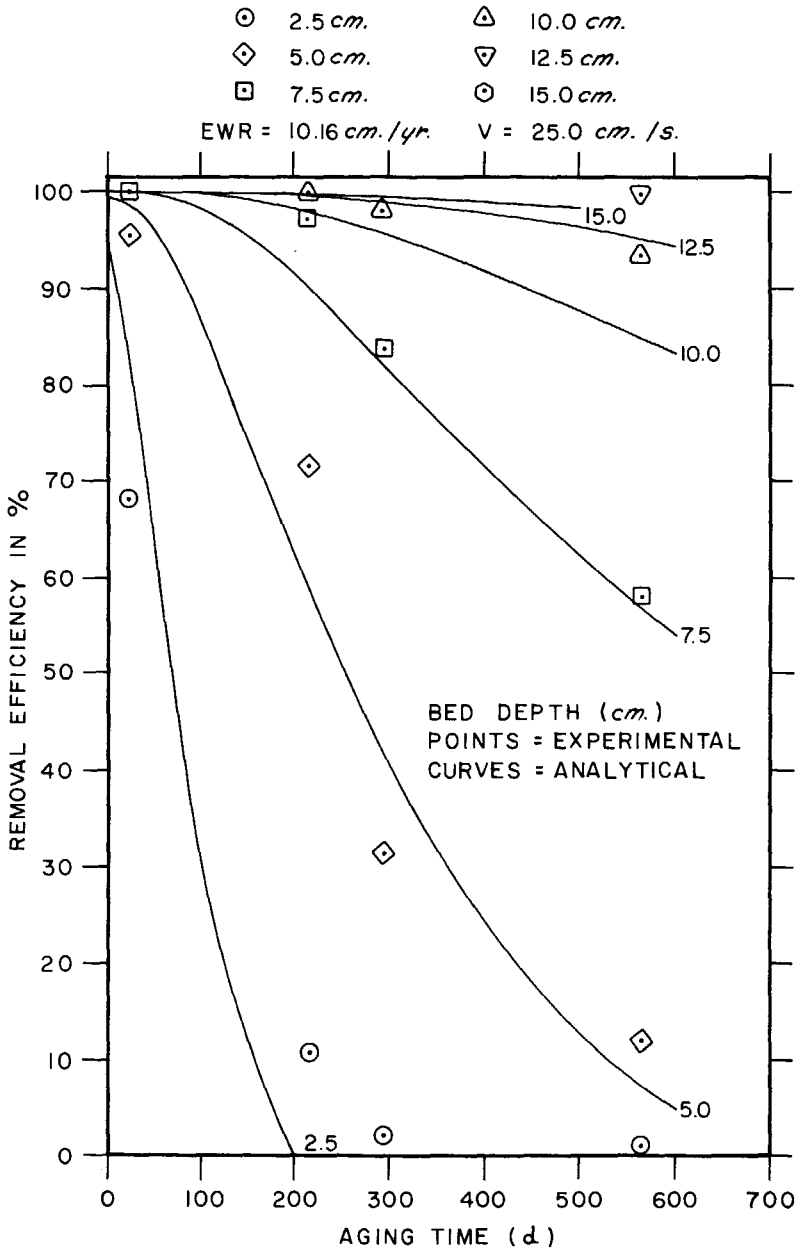

Figure 9. Experimental data from Figure 5 of Reference 1 and corresponding analytical results.

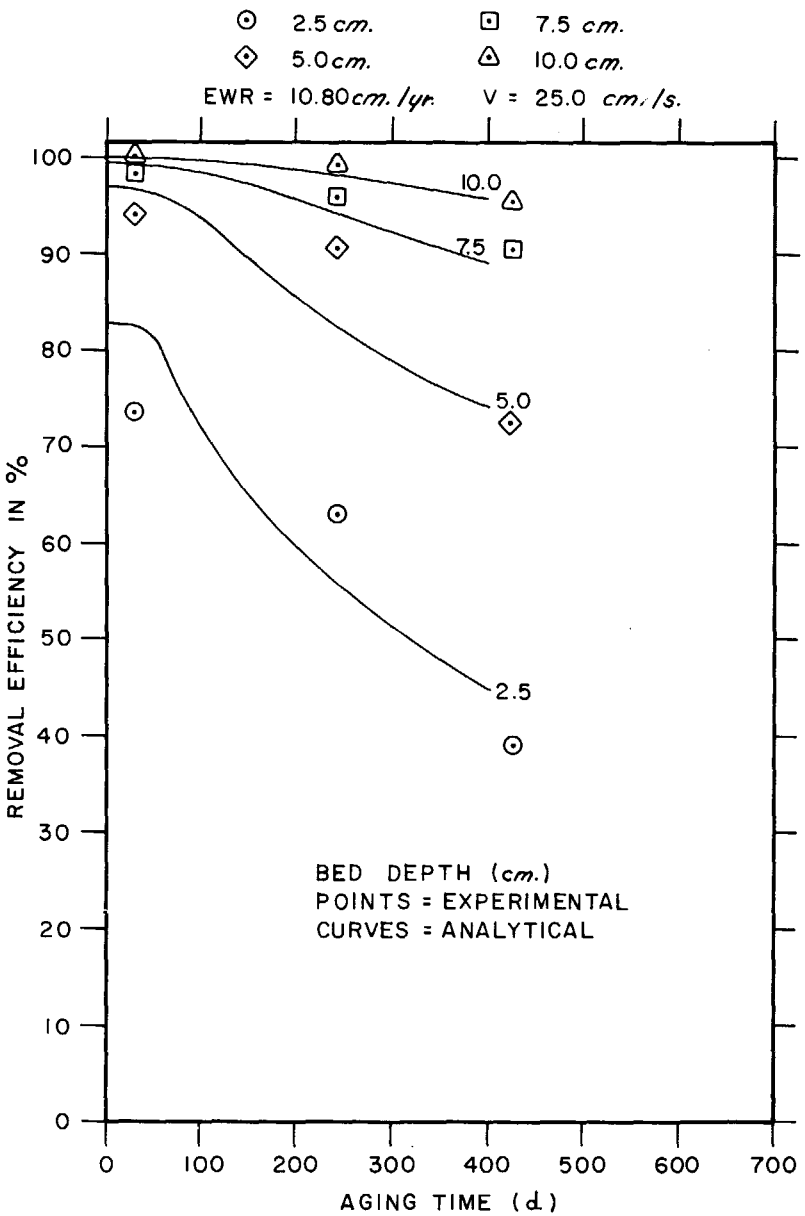

Figure 10. Experimental data from Figure 2 of Reference 1 and corresponding analytical results.

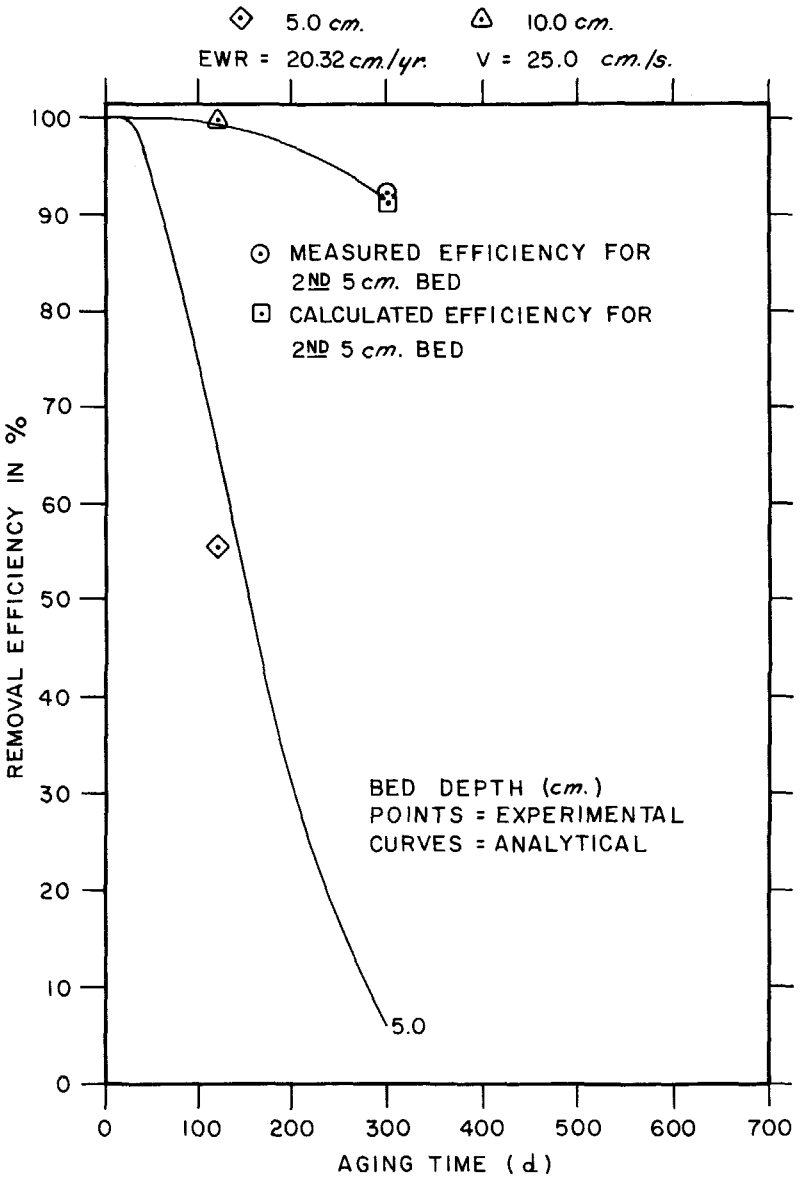

Figure 11. Experimental data from Table II of Reference 1 and corresponding analytical results.

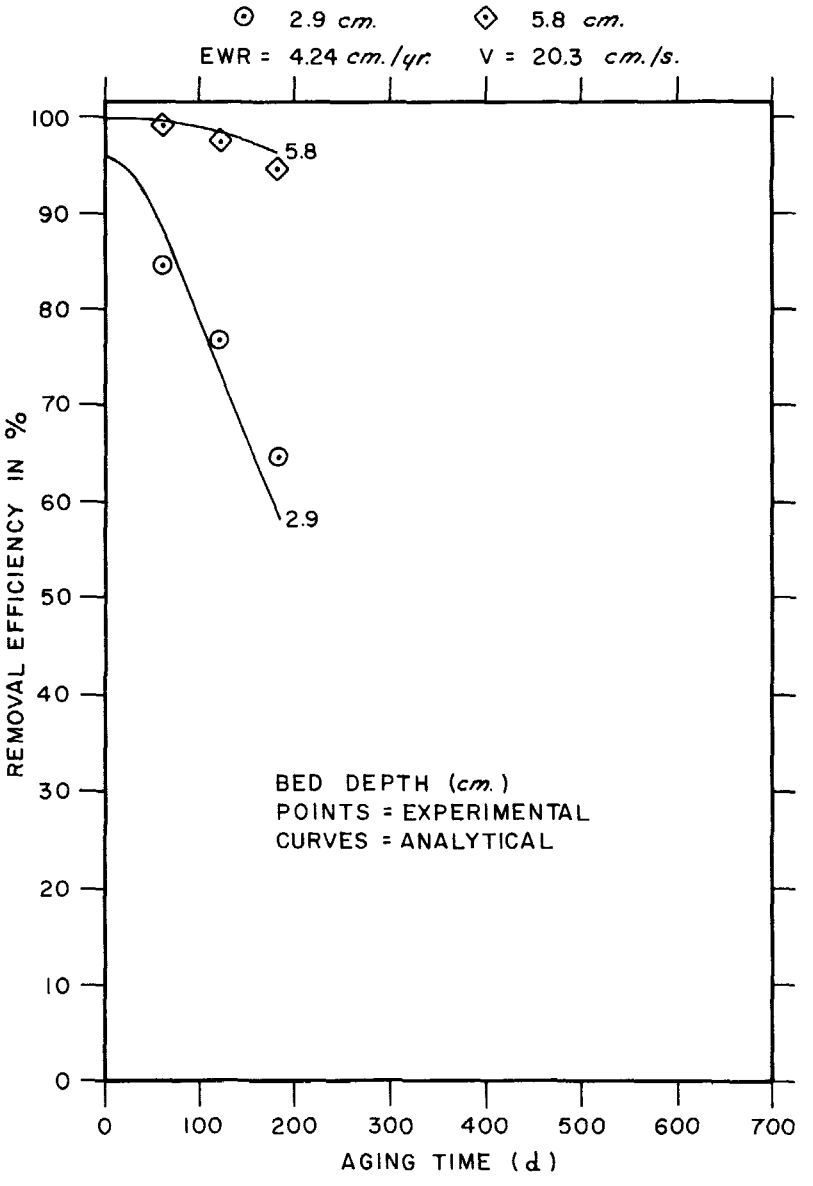

Figure 12. Experimental data from Figure 4 of Reference 3 (G618-E) and corresponding analytical results.

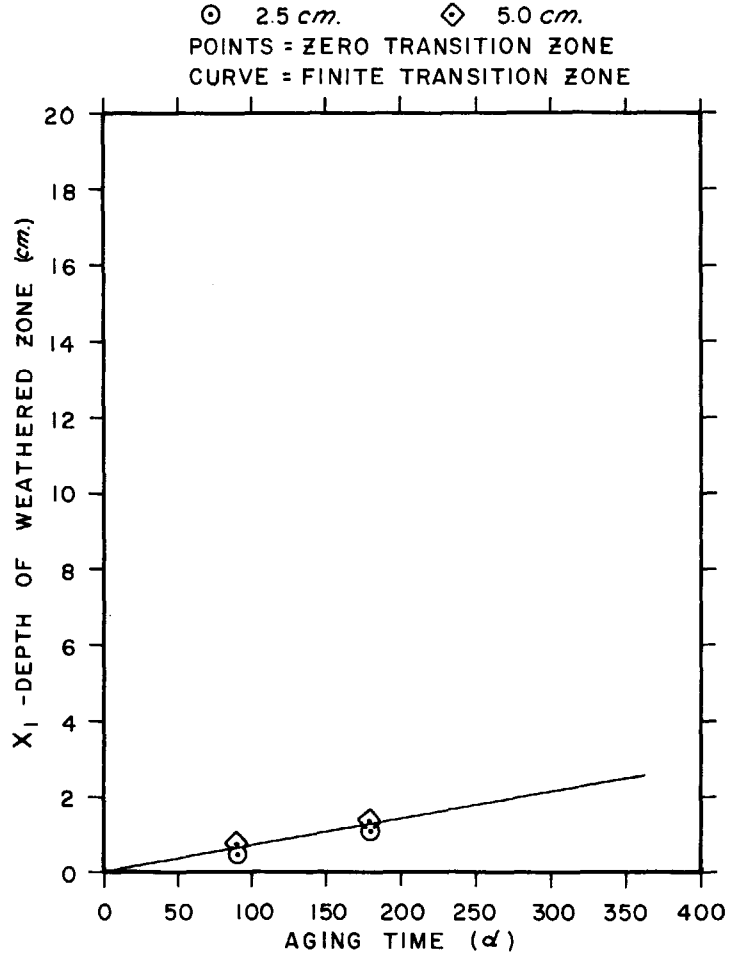

Figure 13. Comparison of results from two analytical models using data in Table 2.10 of Reference 2.

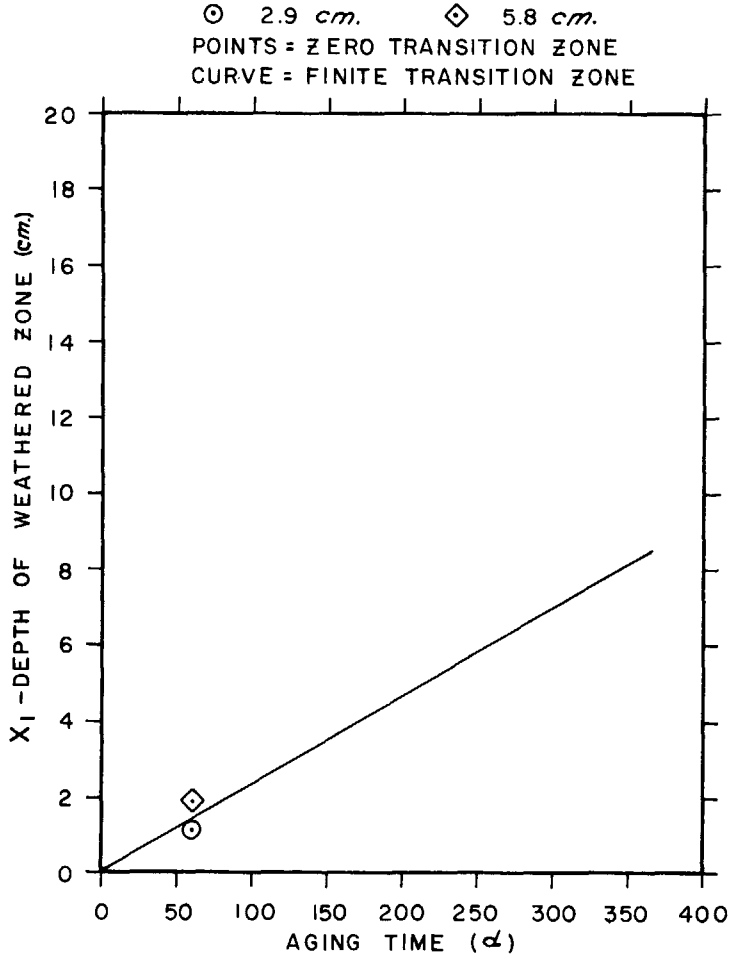

Figure 14. Comparison of results from two analytical models using data in Figure 4 of Reference 3 (G617-BSR).

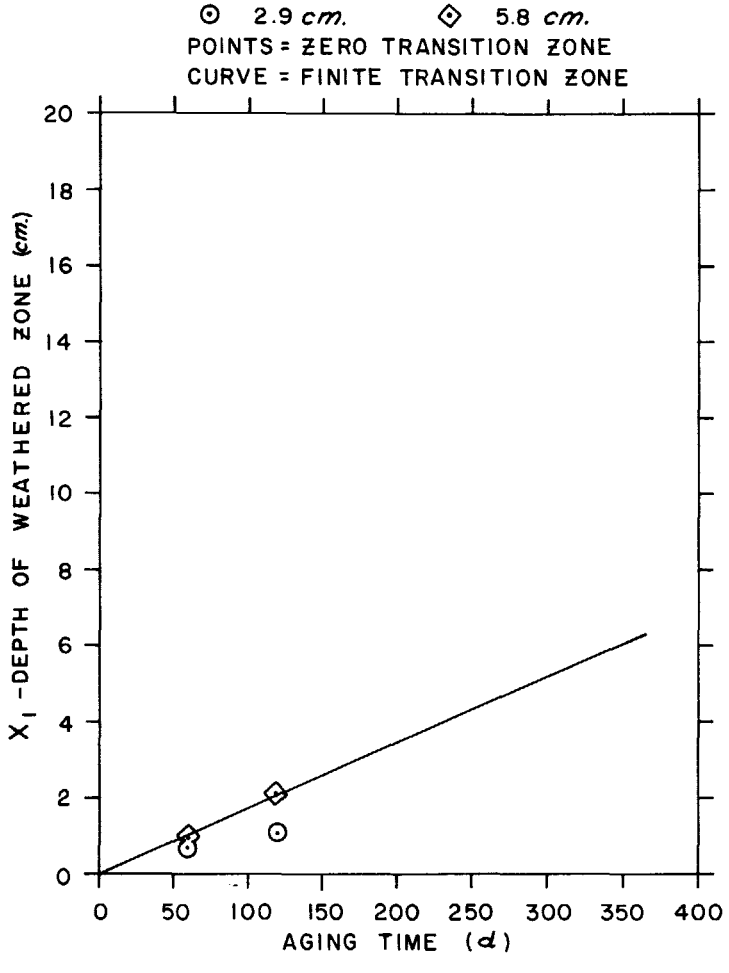

Figure 15. Comparison of results from two analytical models using data in Figure 4 of Reference 3 (G617-HFIR).

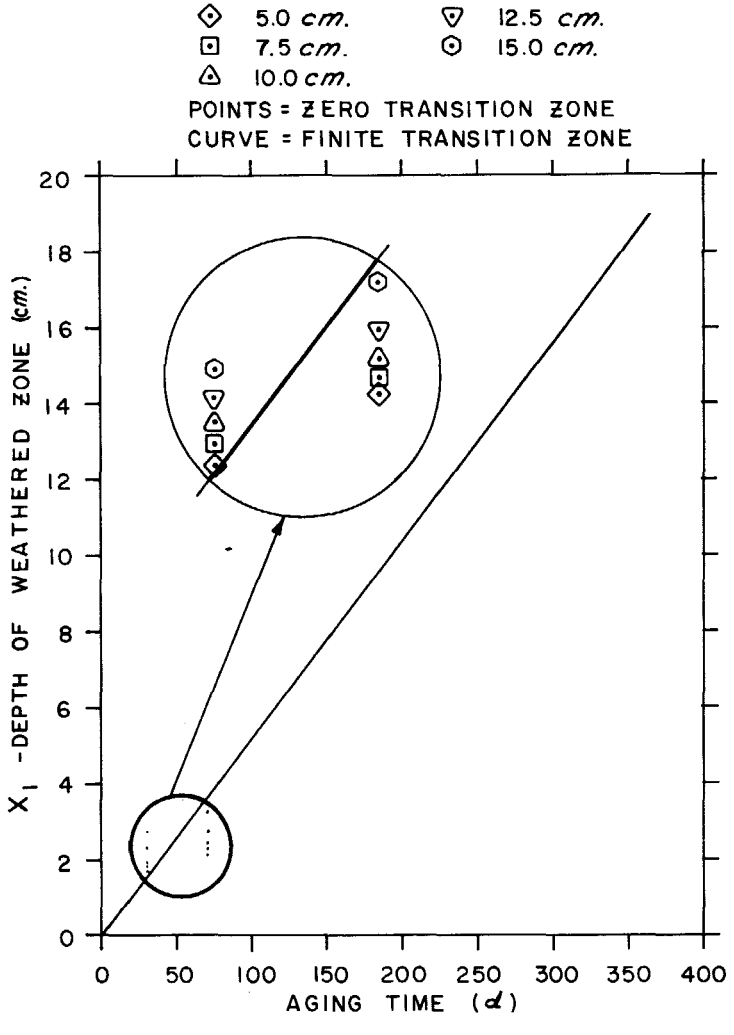

Figure 16. Comparison of results from two analytical models using data in Table I of Reference 1.

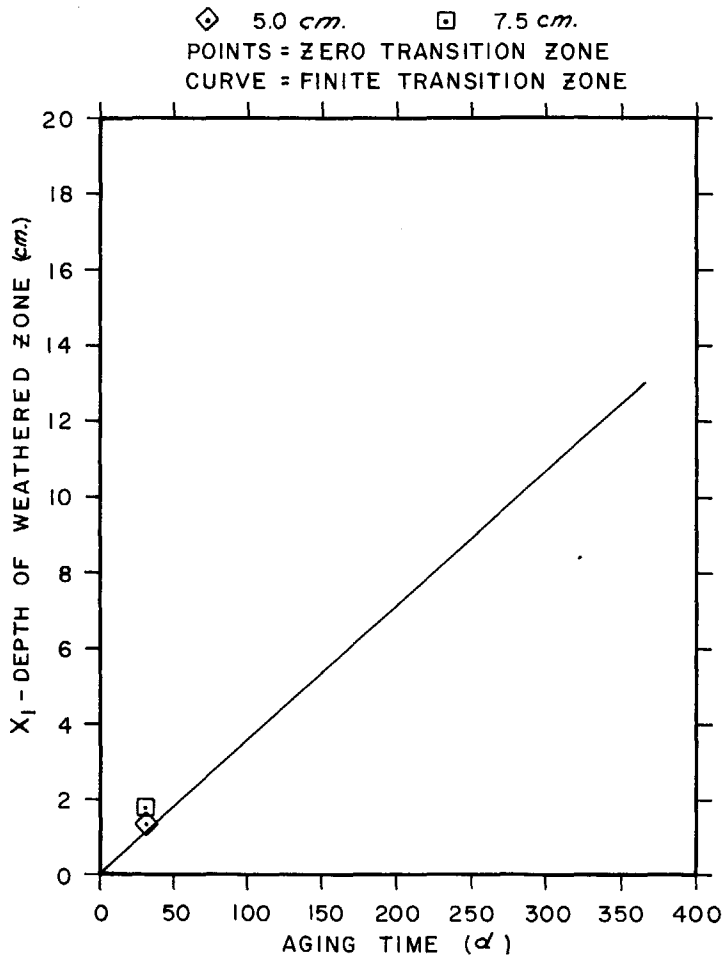

Figure 17. Comparison of results from two analytical models using data in Figure 3 of Reference 1.

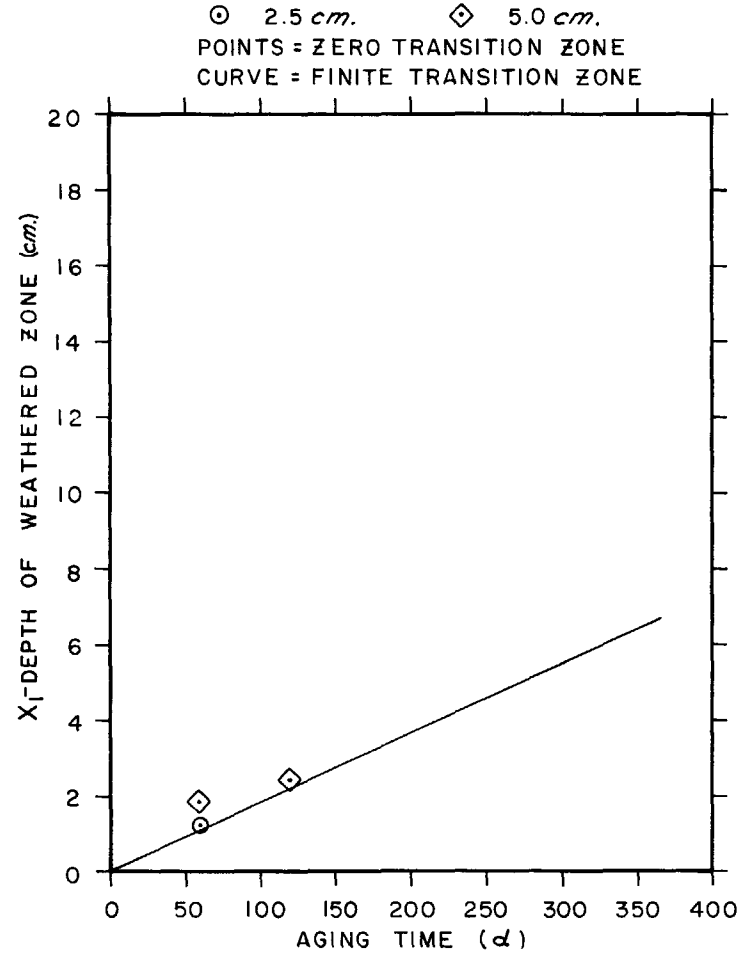

Figure 18. Comparison of results from two analytical models using data in Figure 4 of Reference 3 (G618-BSR).

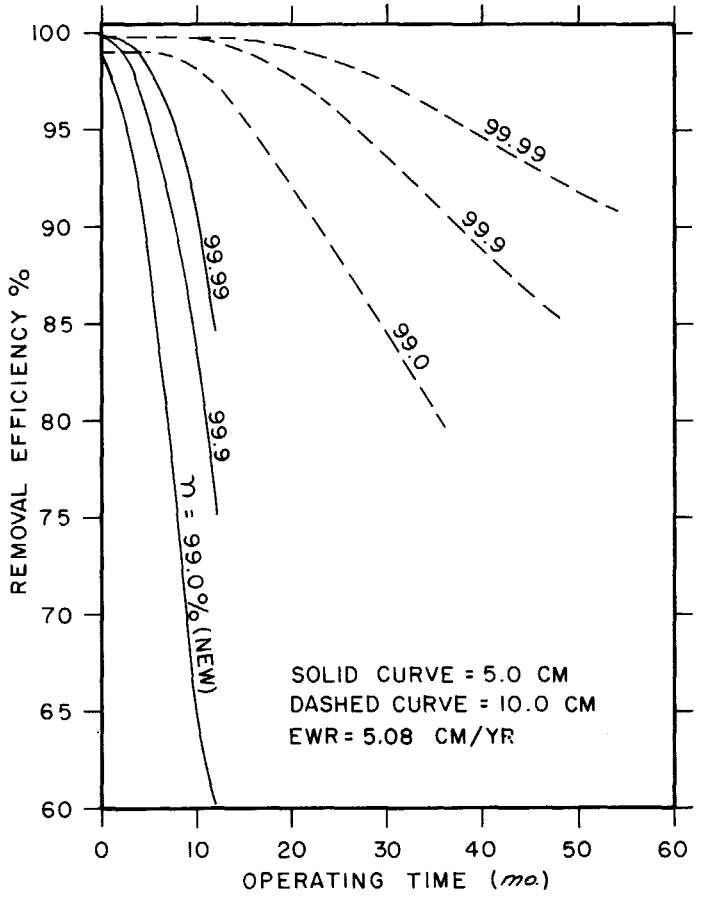

Figure 19. Predicted adsorber efficiency change with time as a function of performance in new condition.

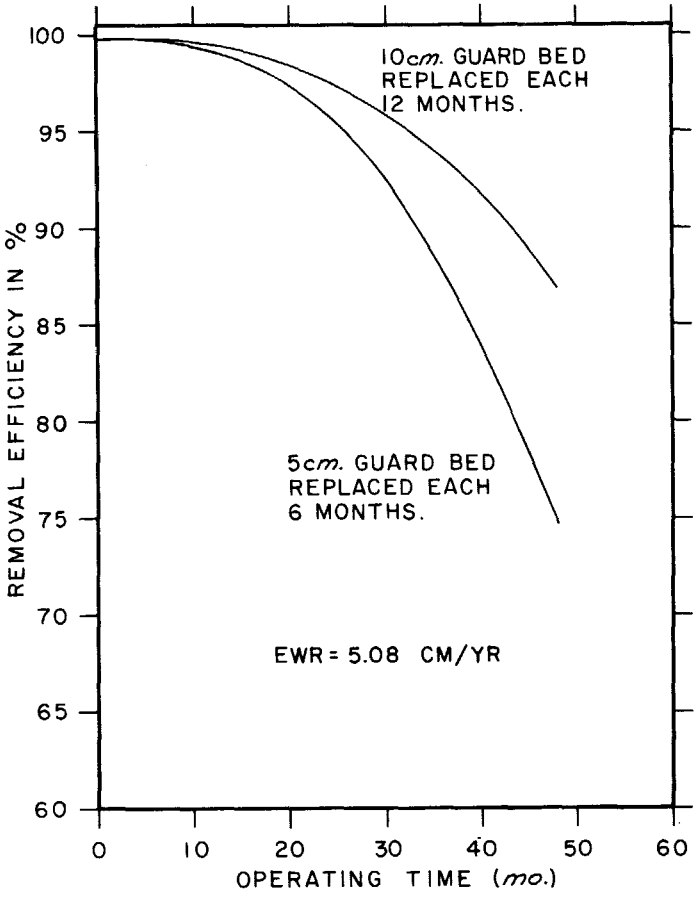

Figure 20. Predicted change in adsorber efficiency with sample guard bed depths and replacement schedules.

DISCUSSION

WILHELM: The reason for very quick loss of removal efficiency is a large amount of solvents and plastics being adsorbed by charocal. We found that there is no homogeneous function to describe the real effect of the degradation of the charcoal. We found from our early experience in some reactor stations that were erected four years ago that charcoal with a given thickness should last two years. The data didn't fit all the new stations because solvents from recent painting were responsible for rapid degradation. I am a little hesitant to develop functions and correlations for the useful operation time of charcoal.

PARISH: I think we developed these ideas in the paper although I did not have time to elaborate here. It is our contention that the effective weathering rate (EWR) parameter is a function of the air quality. We are anticipating that it is quite possible that, based on analyses from data like this, we could correlate the variation in effective weathering rates with the concentration of hydrocarbons, sulfur dioxide, or other suspected weathering agents. By allowing the EWR parameter to vary, we have been able to fit all of the data that we have examined so far, which included quite a spectrum of data with respect to air quality. Remember that this is an empirical model, requiring experimental data in order to evaluate the EWR parameter. As far as we know, the data in our references were subject to the same limitation, in that they did not reflect performance after painting. Therefore, the analytical model is no more or no less applicable than the published data. As data on adsorbent efficiencies after painting activity become available, we would like to evaluate an EWR for that also. It should also be noted that the weathering model does not inherently require a constant EWR. It could very readily be adapted to a time variant EWR, so that it may be possible to handle transient behavior, also. To retain a proper perspective on this paper, I would emphasize that it is not suggested that this analytical model is a substitute for periodic testing of an adsorbent system. It is intended primarily as a design tool and a means for extending the utility of experimental data.

IODINE REMOVAL ADSORBENT HISTORIES, AGING AND REGENERATION

J.R.Hunt, L.Rankovic, R.Lubbers, J.L. Kovach
Nuclear Consulting Services Inc.
Columbus, Ohio

Abstract

The experience of efficiency changes with life under various test conditions is described. The adsorbents were periodically removed from both standby and continuously operating systems and tested under various test methods for residual iodine adsorption efficiency.

Adsorbent from several conventional "sampler" cartridges versus the bulk adsorbent was also tested showing deficiency in the use of cartridge type sampling.

Currently required test conditions were found inadequate to follow the aging of the adsorbent because pre-equilibration of the sample acts as a regenerant and the sample is not tested in the "as is" condition.

The most stringent test was found to be the ambient temperature, high humidity test to follow the aging of the adsorbent.

Several methods were evaluated to regenerate used adsorbents; of these high temperature steaming and partial reimpregnation were found to produce adsorbents with near identical properties of freshly prepared adsorbents.

I Introduction

Test conditions currently required by the NRC (1) (2) to follow adsorbent aging have been found inadequate because pre-equilibration of the sample can act as a regenerant and the sample is therefore not tested in the "as is" condition.

The CH_3I removal efficiency evaluation of new activated carbon is a well established technique, however evaluation of impregnated carbon exposed in stand-by or continuous service under a variety of environmental hazards is not as well known. Activated carbon, if exposed to an atmosphere containing organic vapors (paint, plastic outgassing, degreasing solvents, oil vapor, etc.), will adsorb and retain these vapors and such "aging" will decrease its efficiency for isotope exchange type removal of $CH_3\ ^{131}I$. Most procedures specified for adsorbent evaluation (1) (2) require extensive pre-equilibration under the test conditions to assure the establishment of moisture and temperature equilibrium between the test vapor and the test carbon. If the test conditions are near ambient (25°C) this "precaution" is acceptable even for "aged" carbons which may contain adsorbed organics. However if the postulated use condition is at elevated temperature, the impurities which "poison" the carbon are removed during the "pre-equilibration" period and the carbon regenerated before the introduction of the $CH_3\ ^{131}I$ test charge.

Therefore the test will show a higher residual efficiency than the system, particularly if the system is normally at ambient and heaters would be activated only in case of humidity control. It is difficult to postulate initiation of heaters and "regeneration" of the adsorbent bed 4-16 hours prior to an accident.

II Procedure & Apparatus

During routine radioiodine testing of adsorbent samples sent to NUCON for analysis by various nuclear power plants, samples are occasionally tested which contain organic "poisons".

In one instance, adsorbed organics were suspected due to an extremely low $CH_3\ ^{131}I$ efficiency. Subsequent steam stripping (100°C saturated steam) of the adsorbent revealed a 10-15% loading of organic material with a turpentine-like odor.

In another case, "poisoning" was suspected by a turpentine-like odor of the condensate after pre-equilibration during a steam-air test, not because of a low $CH_3\ ^{131}I$ efficiency. Steam stripping of a fresh sample of this adsorbent indicated an organic loading of $< 1\%$.

In this experiment, the two adsorbent samples described above (both BC727 KI_3 impregnated coconut shell) and a sample of new BC727 were evaluated under various conditions of temperature, relative humidity and pre-equilibration time for $CH_3\ ^{131}I$ removal.

Apparatus

The test apparatus consisted of stainless-steel and glass test bed assemblies fully enclosed in an environmental chamber. Temperature, relative humidity, pressure and flow were monitored continuously. Methyl iodide was supplied at a constant rate from a pressurized stainless steel generator.

Counting was performed in a 4.0 inch NaI well crystal. The counting efficiency of the system for ^{131}I is approximately 63%.

III Results

Table 1 Methyl iodide removal efficiency for new carbon (BC 727)

Temperature	Efficiency
20°C	89.20
40°C	90.80
60°C	94.72
80°C	98.75

Bed Diameter:	2.0 inch
Bed Depth:	2.0 inch
Face Velocity:	40 FPM
Relative Humidity:	95%
Pre-equilibration:	4 hours
Loading:	1 hour
Post Sweep:	2 hours
CH_3 I Loading:	0.5 mg/m^3

Table 2 Decontamination factors for used carbon
(BC 727, 2 years, 10-15% organic contamination)

	Pre-equilibration time, hours					
Temperature	0		4		16	
Bed depth	1"	2"	1"	2"	1"	2"
20°C	---	1.46	1.23	1.42	1.17	1.37
40°C	1.40	2.00	----	----	----	----
60°C	1.89	3.54	----	----	2.3	4.4
80°C	2.19	5.18	----	----	2.2	35.97

Bed Diameter: 2.0 inch
Bed Depth: as indicated
Face Velocity: 40 FPM
Relative Humidity: 70%
CH_3I Loading: 0.5 mg/m^3

Table 3 Methyl iodide removal efficiency for used carbon
(BC 727, 2 years, 10-15% organic contamination)

	Pre-equilibration time, hours					
Temperature	0		4		16	
Bed depth	1"	2"	1"	2"	1"	2"
20°C	----	31.75	18.36	29.76	14.39	26.86
40°C	28.71	49.92	-----	-----	-----	-----
60°C	47.02	71.74	-----	-----	56.53	77.31
80°C	54.41	80.93	-----	------	54.62	97.21

Bed Diameter: 2.0 inch
Bed Depth: as indicated
Face Velocity: 40 FPM
Relative Humidity: 70%
CH_3I Loading: 0.5 mg/m^3

Table 4 Decontamination factors for used carbon
(BC 727, $<$1% organic contamination)

	Pre-equilibration time, hours			
Temperature	0	1	2	16
25°C	6.37	3.03	2.24	2.17
88°C	357.0	83.3		

Bed Diameter: 2 inches
Bed Depth: 2 inches
Face Velocity: 40 FPM
Relative Humidity: 95%
CH_3I Loading: $\sim 0.5 mg/m^3$

Table 5 Methyl iodide removal efficiency for used carbon (BC 727, <1% organic contamination)

Temperature	Pre-equilibration time, hours			
	0	1	2	16
25°C	84.30%	67.02%	54.44%	53.82%
88°C	99.72%	98.80%		

Bed Diameter: 2 inches
Bed Depth: 2 inches
Face Velocity: 40 FPM
Relative Humidity: 95%
CH_3I Loading: $\sim 0.5 mg/m^3$

IV Evaluation of Methyl Iodide Test Results

Table 1 reflects the well-known effect of decreasing $CH_3{}^{131}I$ efficiency with decreasing temperature on a new BC727 type carbon.

Although data is incomplete at 40° C (Tables 2, 3), at 60° C the lowering of the decontamination factor due to higher carbon moisture content is masked by the improvement obtained by desorption of the organic. At 80° C the effect is pronounced.

Tables 4 and 5 indicate results similar to those obtained with new BC727 except that due to "aging", the efficiencies are lower. Decreasing efficiency with increasing pre-equilibration time even at 88° C indicates the improvement is not as significant as the decrease in efficiency due to the increased moisture content of the carbon. Although it is not clear from the data available here, it is possible that the change in efficiency @ 88° C between 0 and 1 hour pre-equilibration due to increased carbon water content would have been much greater and in fact significant organic desorption did occur.

From Tables 2 and 3, it is evident that under certain conditions dramatic "improvement" of adsorbent samples may occur due to test methods which do not account for contaminant removal during pre-equilibration.

The degree to which efficiencies are "improved" and the ease with which such "improvements" are identified in the test data depends on a number of factors.

The results obtained in Tables 2 and 3 make identification of the problem in this particular case more simplified than in others.

More data is needed concerning water adsorption of nuclear grade activated carbons at various relative humidities over time and associated effects on $CH_3{}^{131}I$ efficiencies.

Identification of contaminants and their sources should be performed.

Additional test methods should be devised to assure that reported efficiencies represent the condition of the adsorbent as it will be used.

Although adsorbent regeneration may offer economic promise on a large scale, in the test rig it is often responsible for inaccurate results for systems which can least afford errors in the measurement of their efficiencies.

V Regeneration of Poisoned Carbons

One batch of chemically poisoned iodine impregnated carbon, which was in use at a PWR for four years and had insufficient methyl iodide removal efficiency was treated in various manners to improve or regenerate its efficiency.

The following treatment - CH_3I efficiency values were obtained:

Treatment	pH	$CH_3{}^{131}I$ Efficiency %	
None	5.2	42.60	130° C (RDT)
None	5.2	16.11	25° C (RDT)
16 Hours oven drying at 150° C	6.8	56.70	130° C (RDT)
3 Minutes at 400° C	7.5	78.50	130° C (RDT)
6 Minutes at 400° C	8.2	77.65	130° C (RDT)
Reimpregnate with KOH (1% Wt.)	9.5	86.70	130° C (RDT)
6 Minutes at 400°C and reimpregnate with KOH (1% Wt.) and KI (0.5% Wt.)	10.4	92.50	130° C (RDT)
6 Minutes at 400° C and reimpregnate with KOH (1% Wt.) and TEDA (0.5% Wt.)	10.8	96.82	130° C (RDT)

The residual total iodine both after the 3 and the 6 minutes exposure at 400° C was 1.2%.

Based on the results it appears that some grades of chemically contaminated carbons can be regenerated successfully by flashing-off the impurities and reimpregnating the carbons.

The hardness and ignition temperature of the carbon after regeneration, reimpregnation and rescreening are in the RDT and Regulatory Guide 1.52 specified acceptable region.

Based on evaluation of carbons to date, there appears to be two distinct types of poisoning. One results in acidification of the carbon; the other is solvent contamination, however often both methods of poisoning exist and it is difficult to state generalized treatment for regeneration of all carbons.

VI Random Observations Regarding Testing of Systems and Adsorbents

Several observations were made which may contribute to the improvement of components and systems.

(1) Adsorber cells, where the rough side of the perforated cell is turned toward the carbon, generate more fines and result in faster loading of downstream HEPA filters.

(2) Adsorber cells which inadvertently got wet if not emptied and washed immediately completely disintegrate due to iodide corrosion.

(3) The mechanical integrity of many cells is inadequate to withstand repeated handling. Cells shipped to NUCON for refilling show missing handles, missing slide plates and broken studbolts.

(4) Many currently installed "sampling" cartridges are totally inadequate. Tests performed on cartridges and on bulk carbon were found to be different by 2-25% in $CH_3{}^{131}I$ removal efficiency--in all cases the cartridges showing higher remaining efficiency. Additionally, the cartridges often contain loose carbon, indicative of faulty filling methods.

(5) Radiation exposure of test personnel during in-containment tests results in 75-500 mR dose primarily from neutron radiation. Such systems should be converted to permit remote leak testing where personnel are in shielded area.

Non-containment systems testing results in average of 5-15 mR dose per test series of 2-4 days' duration.

References

1. "Design, testing and maintenance criteria for atmospheric cleanup system air filtration and adsorption units of light-water-cooled nuclear power plants." Regulatory Guide 1.52 (June 1973)

2. "Gas-phase adsorbents for trapping radioactive iodine compounds." RDT M 16-T (October 1973)

DISCUSSION

RIVERS: In your Table 5, at 25°C the penetration increased steadily as pre-equilibration time was increased; which is rather the reverse of the high temperature situation.

HUNT: In this case, the decrease in efficiency was due directly to the varying pre-equilibration time. In other words, as the pre-equilibration time increased, the adsorption of water on the carbon also increased. Adsorbed water on the carbon decreases methyl iodide efficiency.

EVANS: The regeneration technique that seemed to be most effective was raising the temperature to 400°C. The effect of this was to burn off organic vapor and surface oxides, was it not?

KOVACH: Yes, you are correct.

WILHELM: We agree that if you test aged charcoal in the laboratory, you will find all you have just told us. The question is, really, how meaningful is the test in the laboratory, leaving apart the dependence on the preconditioning time and other conditions. We found that, in most filter systems, the test charcoal in a bypass of the installed filter doesn't have the same air changes as the main unit. Therefore, it doesn't compare well enough to the main unit. One reason may be that the bulk density of the charcoal in a small scale sampler is often lower than the bulk density in big charcoal beds. Thus, laboratory results may not relate directly to full scale performance.

HUNT: I would like to make another comment. The second carbon was run originally in a steam-air test at 130°C and the removal efficiency was really quite good. However, the man that was running the test noticed a distinct odor, and the odor on both of these carbons was something like kerosene. In the condensate after equilibration, this odor was noticed on the sample, which had 1 per cent organic contamination. That is how we discovered there was organic contamination on the carbon; not because we got a poor test result. In fact, probably the reason we got such a good test result was because we steamed off the organic contaminant during pre-equilibration.

NEW CHARCOAL IMPREGNANTS FOR TRAPPING METHYL IODIDE I. SALTS OF THE IODINE OXYACIDS WITH IODIDE OR IODINE AND HEXAMETHYLENETETRAAMINE

Victor R. Deitz and Charles H. Blachly
Naval Research Laboratory
Washington, D. C. 20375

Abstract

Iodine in its various chemical compounds can have the oxidation states I^-, I^o, I^{+1}, I^{+5} and I^{+7}. When alkali salts of the iodine oxyacids (KIO, KIO_3 and KIO_4) are mixed with iodides (I^-) and/or elementary iodine in basic solution, the mixtures containing the extremes in valence states are converted into compounds of intermediate charge. A number of charcoals were impregnated with selected mixtures and these proved to be excellent trappers for methylradioiodide. Hexamethylenetetraamine (HMTA), a tertiary amine having a high flash point and low volatility, was also included in the impregnations investigated as a second impregnate. About two hundred samples were impregnated with the iodine mixtures and HMTA using the 2-stage process on a variety of base charcoals and these were evaluated for methyliodide trapping and ignition behavior. Some of the promising impregnated charcoals were also evaluated in other laboratories. The results are presented and a fundamental interpretation proposed for the trapping mechanism based upon a dissociation-controlled exchange (the exchange controlled by dissociation of one of the species) via a simple effective chain reaction.

I. Introduction

Previous charcoals for trapping methyl iodide have been impregnated with potassium iodide plus iodine (KI_x) and/or with triethylenediamine (TEDA). The impregnation process has been chiefly proprietary information. A detailed study of a trapping process must, however, start with known systems: well-characterized base charcoals, known impregnating solutions, and a well defined test procedure for contacting the charcoals with methyl iodide. Thus, the chemical problems fall within two groups:

(1) adsorption of the impregnant chemicals from solution including the surface changes that take place upon subsequent drying of the impregnated charcoal, and

(2) the surface reactions at the gas-solid interface during the trapping process.

The latter have been described in general terms as either an isotope exchange, when a large amount of normal iodine is present as e.g. KI_x, or as the formation of the adsorbed quartenary iodide by dissociative addition when TEDA was present.

The many publications and reports of the Oak Ridge National Laboratory in this country (1a, 1b, 1c) and those of the U.K. Atomic Energy Authority (2) have been very helpful in the present investigations and these are gratefully acknowledged.

II. Adsorption from the Impregnating Solutions

Iodine in its various chemical compounds includes the oxidation states I^-, I^0, I^{+1}, I^{+5} and I^{+7}. Noteworthy features (3) are the instability of the compounds with respect to disproportionation in alkaline solution, the comparative stability of IO_3^-, and the instability of the +3 oxidation state (i.e. no chemical evidence for its presence has been found). It is apparent, therefore, that the alkali salts of the iodine oxyacids (KIO, KIO_3 and KIO_4) can have a complex solution chemistry when mixed with the iodides (KI) and/or elementary iodine (I_2).

When the salts of the iodine oxyacids are present in basic aqueous solutions, there are several equilibria that convert the initial species to intermediate oxidation state. In general, one of the iodine species is oxidized and the second reduced. Some of the combinations reported in this paper as impregnating solutions on charcoal are: KIO_4+KI, KIO_4+I_2, KIO_3+I_2, KIO_3+KI, and KOH+I_2. In many cases the calculated heats of formation were favorable for certain postulated reaction products of intermediate oxidation states.

A systematic study of the adsorption from solution of oxyiodine salts by charcoals has not been reported. Although limited solubility is in general accompanied by high adsorption, the oxyiodine salts of interest have a high solubility. Since the adsorption from solution increases with concentration, the impregnating solutions were dispersed by a sprayer into fine droplets which were contacted with a quantity of dry charcoal contained in a slowly rotating cylinder having inclined lifts. Some water in the solution could thus migrate into the microstructure of the charcoal leaving the solute at high concentration to be adsorbed in the outer structure. The conditions were selected so that charcoal always had a dry appearance after impregnation.

Subsequent to the impregnation of the oxyiodine salts, a very effective measure was to impregnate the charcoal with a high flash-point amine such as hexamethylenetetraamine (HMTA)*. As will be shown, such a two-step process was found to yield the minimum penetration of methylradioiodide for most base charcoals. Furthermore, the use of a high flash-point amine after the introduction of the oxyiodine salts was found to raise the ignition temperature of the charcoal. With the concentrations carefully adjusted, the charcoal retained a dry appearance after the 2-stage impregnation.

---

* Synonyms for hexamethylenetetraamine $(CH_2)_6N_4$ are methenamine, formamine, hexamine and urotropin. The rhombic crystals melt with charing at 270°C and the flash point is 233°C.

The drying of the charcoal after impregnation is an important operation. Times longer than 5 hours and temperatures in the range 95 to 105°C are preferred.

Base charcoals from different sources yield individual trapping efficiencies when the same impregnation formulation is used. The behavior may be due to the extent to which the reactants on the various charcoals yield the necessary intermediate species for trapping methyl iodide.

III. Methyl Iodide Trapping: Procedure and Results

The test procedure outlined in the RDT Standard M-16[4] was followed. The results given in this paper used the parameters listed below:

Diameter	5.08 cm	2 in
Length	5.08 cm	2 in
Air Flow	25 L/min.	0.88 CFM
Linear Velocity	21 cm/sec.	41.5 ft/min.
Contact time	0.254 sec.	
Relative humidity %	95-97	
Prehumidification time	16 hours	
Time of dose	2 hours	
Time for purge	2 hours	
Temperature	22°C	

The dose of methyl iodide was 55 microliters or 125 micrograms of the liquid per g. charcoal. The total air flow for 2 hours is equivalent to 3 cubic meters. With sample weights of 40, 50, and 60 grams, the total doses were 5.0, 6.25, and 7.5 mg or 1.67, 2.10 and 2.5 mg/m^3. The methyl iodide was purchased from ICN Life Sciences, Irvine, California at 5000 μCi per ml liquid. The liquid was injected with a Gilmont digital micrometer syringe of 0.25 ml capacity directly into the air stream at equal increments over the 2-hour dosing period.

Figure 1 is a diagrammatic sketch of the charcoal test container and the back-up beds. Each component was fabricated from a pair of Pyrex O-ring (Viton) connectors, size 50mm I.D. (Kontes Glass Co., Type M). The Viton did not become radioactive after exposure to methylradioiodide. The connectors were held together with "Pinch Type" clamps. The humidified air stream enters at the top: A is the humidity sensing element, b thermometer, C septum closure, D test sample of charcoal, E backup beds, F location of an O-ring, G exit to flowmeter. The charcoal is supported on discs of perforated stainless steel screen.

The counting was done with a Nuclear-Chicago Model 470 gas-flow detector with the Model 8712 Decade Scaler. The percent penetration of the bed was determined from the relation

$$\% \text{ Penetration} = \frac{\text{CPM in back-up beds}}{\text{Total CPM in sample and back-up beds}}$$

The reproducibility for several samples may be seen from Table 1. The volume of each charcoal, 106 cm^3, was divided after mixing into 8 aliquots and each (5.6 mm average depth) was counted. The variance was found to be less than 5%. The efficiency was estimated in the counting of the charcoals with the above facility (Table 1) and the value appears to depend on the charcoal, the impregnation and possibly to the extent on prehumidification. The following tests were made keeping the three parameters constant. Preparation 4144 was prehumidified in duplicate (34% weight gain). The top section was counted after methyl iodide dosing and then the section was progressively diluted with equal volumes of non-dosed prehumidified charcoal. A linear dependence (Figure 2) was observed between the count and the dilution factor indicating a constant counting efficiency for the sample.

Table I

Reproducibility in the Counting of Impregnated Charcoals After Exposure to Methyl Iodide - 131

	4017 17 June	4184 19 June	4185 19 June	4186 20 June
	13820	5243	2989	79232
	12431	5273	2947	77278
	14079	5273	3023	76003
	13910	5001	2956	81000
	14162	5222	3002	79804
	13278	5357	3026	77178
	13013	5503	3124	75369
	12928	5284	3019	76020
Mean	13452	5269.5	3011	77736
Std. dev.	630.5	140	54.6	2044
Variance	4.7%	2.7%	1.8%	2.6%
Efficiency	12.6%	7.9%	4.6%	2.6%

The results (Table II) are for independent impregnations using a coal-base charcoal (Union Carbide MBV 6/14). The reproducibility of the procedure includes the uncertainties in withdrawing the sample from the supply of base charcoal, the preparation of the solution, the impregnations, and the drying. In addition, the introduction of the impregnants via a 1-step or 2-step process indicates that the latter yields a product of about half the penetration, everything else being kept the same.

Table II

Penetration of Methylradioiodide Through a Coal-Base Charcoal: 1-step vs 2-step Process of Impregnation

Sample	Impregnant for 100g Charcoal		Methyl Iodide Penetration %
4203	5g HMTA, 1g I_2, 1.5g KOH		0.41
4206	5g HMTA, 1g I_2, 0.375g KOH		0.58
4208	5g HMTA, 1g I_2, 0.375g KOH		0.85
4212	5g HMTA, 1g I_2, 0.44g KOH		0.72
4212R	5g HMTA, 1g I_2, 0.44g KOH		0.93
			0.70 av.
	Step 1	Step 2	
4215	I_2, KI, KOH	HMTA, 5g	0.51
4221	I_2, KI, KOH	HMTA, 5g	0.30
4222	I_2, KI, KOH	HMTA, 5g	0.43
4225	I_2, KI, KOH	HMTA, 5g	0.30
4226	I_2, KI, KOH	HMTA, 5g	0.29
4227	I_2, KI, KOH	HMTA, 5g	0.29
			0.35 av.

Test conditions: Bed diameter 2-inch; height 2-inch; contact time 0.25 second; prehumidification 16 hrs. at 96 RH %

Two series of impregnations were made with a coal-base charcoal (Union Carbide MBV 6/14) in which the total iodine was maintained at 1 wt. % of the charcoal. The common aspect of these impregnations is the disproportionation to form the hyperiodite group, which is more favorable in alkaline than in neutral media. It is rapid at room temperature

$$I_2 + 2\ KOH \longrightarrow KOI + KI + H_2O \qquad (1)$$

The disproportionation of KOI to form the iodate and the iodide is also rapid at room temperature

$$3\ KOI \longrightarrow KIO_3 + 2\ KI \qquad (2)$$

There are no substantiated accounts of the isolation of solid hypoiodites. However, in solution the presence of excess base stabilizes

the OI^- to some extent and it is reasonable that this may be carried over to the adsorbed species on charcoal. The presence of KIO_3 and KI on a charcoal may be viewed as a potential source of KOI in small but finite quantities. The use of KOH plus KI as reactants in the impregnating solutions was likewise found effective. The results (Table III) include variations in the proportion of I_2 and KI, all with KOH present at a solution pH of 10 to 11. The observed penetrations of methyl iodide were quite low, all being in the range 0.1 to 0.4% and an average of 0.25%.

Table III

Impregnation of Coal-Base Charcoal (Total Iodine 1 wt.% of Charcoal)

Sample	Impregnation in 2 Steps 1st	2nd	Methyl Iodide Penetration (%)
4236	I_2, KI, KOH	1% HMTA	0.44
4246	I_2, KOH	2% HMTA	0.13
4248	I_2, KOH, Na_2HPO_4	2% HMTA	0.06
4243	I_2, KI, KOH	1% HMTA	0.17
4242	I_2, KI, KOH	3% HMTA	0.29
4238	KI, KOH	None	0.29
4229	KI, KOH	None	0.38
4244	I_2, KOH	None	0.15
4231	I_2, KI, KOH, Na_2HPO_4	5% HMTA	0.26
4227	I_2, KI, KOH	5% HMTA	0.29
4225	I_2, KI, KOH	5% HMTA	0.30

Test Conditions: 2-inch diameter, 2-inch height, contact time 0.25 second; prehumidification 16 hrs. at 96 RH%

The sources of the iodine in one series of impregnations were from the following binary solutions: KIO_3 and KI, KIO_3 and I_2, KIO_4 and KI, and KIO_4 and I_2. The total iodine has been varied from 1 to 4 wt.%; about 2 wt.% appears to be optimum. However, it was shown in other preparations that the base charcoal itself is also a strong factor. The quantity of HMTA has been varied from 1 to 5 wt.% and again the base charcoal dictates the particular amount to use for the minimum penetration of methyl iodide. The results in Table 4 were obtained for a 2-step impregnation on the coal-base charcoal (Union Carbide MBV 6/14) and the total iodine in these preparations was 1 wt.%. It will be noted that a second series was repeated without HMTA and for this particular charcoal the presence of HMTA appears to contribute a second order effect insofar as methyl iodide penetration is concerned.

Table IV

Impregnation with Binary Mixtures of Iodate or Periodate with Iodide or Iodine Using the Coal-Base Charcoal

Sample	Impregnations		% Penetration
	Step 1	Step 2	
4250	KIO_3 and KI	1% HMTA	0.26
4251	KIO_3 and I_2	1% HMTA	0.47
4252	KIO_4 and KI	1% HMTA	0.18
4253	KIO_4 and I_2	1% HMTA	0.60
4254	KIO_3 and KI	None	0.54
4255	KIO_3 and I_2	None	0.56
4256	KIO_4 and KI	None	0.44
4257	KIO_4 and I_2	None	0.51

Test Conditions: 2-inch diameter, 2-inch height, contact time 0.25 second; prehumidification 16 hrs at 96 RH %

A total of 45 preparations were made with one particular base charcoal. A frequency plot (Figure 3) indicated that the results might be better presented by a bimodal distribution. For a normal distribution for n=45 and the mean penetration = 0.33, the standard deviation was 0.13. For a bimodal distribution the corresponding values were n=26, mean=0.239, std deviation=.07 and n=19, mean=0.46, standard deviation=.06. The explanation is considered to be in the evaluation procedure for penetration rather than in the uncertainties of the impregnation procedure.

Several parameters were also evaluated for methyl iodide penetration by the American Air Filter Company**. The results (Table V) at ambient temperature are compared from both laboratories and demonstrate the effectiveness of the new impregnation and the good reproducibility.

** The authors are indebted to J. F. Fish, R. D. Rivers and M. Pasha for complete cooperation in these tests.

Table V

Determination of the Penetration of Methyl Iodide by American Air Filter Co. and NRL

	AAF Co.		NRL	
Preparation	Temp. °C	% Penetration	Temp. °C	% Penetration
4264	132	0.117	22	0.36
4266	131	1.07	22	0.50
4267	129	1.19	22	0.43
4230	32	0.15	22	0.28
4231	30	0.005	22	0.26
4225	28	0.58	22	0.30
4227	27	0.28	22	0.29

IV. Thermal Stability

The thermal stability of impregnated charcoals has been reported [5,6] under a number of conditions pertinent to an unlikely ignition of an adsorbent by the heat of fission-product decay. The new impregnations have, therefore, been examined by determinations of the spontaneous ignition temperature (SIT) upon programmed external heating and by the composition of the effluent gases during heating. Only the SIT behavior is reported in this paper.

The pertinent observation is that a high flash point amine (HMTA) added to the impregnation formulation generally elevates the ignition temperature of the charcoal relative to the case when the amine was omitted. Table VI is a brief summary of the spontaneous ignition temperatures for the original base charcoal and the impregnated products. The desirable behavior of HMTA is evident when the comparison is made with other impregnations.

The evolved gases during the above ignition measurements have been analyzed for elementary iodine, alkyl iodides, carbon monoxide and carbon dioxide. These are decomposition products of the impregnated charcoals in the flow of air and as such are probably not directly responsible for the primary ignition process of the charcoal. The ignition is quite rapid once the critical temperature range is reached as shown by either the rapid rise in effluent gas temperature or by the visual incandescent appearance. Johnson and Woods [7] showed that adsorbed vapors of low flash points determine the SIT of a charcoal in service. For example, n-decane (13 to 30 wt.%) on a coconut charcoal or on a coal-based charcoal showed values of SIT near those of liquid n-decane, i.e. 216°C. There appeared to be no catalytic effect by the charcoals to promote the spontaneous ignition of hydrocarbons; air passing continuously through charcoal beds need not result in any significant temperature rise due to hydrocarbon oxidation. The observations of Johnson and Woods are pertinent to

charcoals in service. In the nuclear reactor application there is an urgent need to study impregnated charcoals after typical service exposures. In this case there is a potential heat source and good heat transfer to the air stream is essential. While quite satisfactory new materials are available, more information is needed to determine the expectant life of the various impregnated charcoals.

Table VI

Comparison of Spontaneous Ignition Temperatures of the Base and the Impregnated Charcoals

Prepn.	Charcoal	Impregnation	SIT(°C)
4008	Nuchar 6x16, Coal	None	510
4146	" " "	I_2 + HMTA	460
G212	Coconut	None	338
4097	"	TEDA	208
4045	"	TEDA	186
4065	"	TEDA	207
4014	JXC 6/14	None	500
4127	"	I_2, HMTA	470
4128	"	I_2, HMTA	455
4015	MBV 6/14	None	492
4227	"	I_2, KI, HMTA	409
4258	"	KIO_4, KI, HMTA	445
4244	"	I_2, KOH, HMTA	465
4238	"	KI, KOH	334
4229	"	KI, KOH	332
4020	207B 8/12	None	447
4220	"	I_2, KI, HMTA	375
GX202	Wood	None	436
4218	"	I_2, KI, HMTA	440
4280	"	KI, KIO_3, HMTA	395
4239	"	KI, KOH	337

V. Role of the Base Charcoal

The selection of base charcoals for the nuclear industry application of iodine removal must take into account a number of properties:

(1) After impregnation, the product must, of course, be a satisfactory trapper for organic iodides at high relative humidity.

(2) The charcoal must be available in the desired particle size range and possess particle integrity against excessive dust formation.

(3) The charcoal must possess a large surface area in order to adsorb the impregnants and to yield a large final gas-solid interface.

(4) There must be a suitable open porosity within granules to accommodate the adsorbed impregnants and to permit the transport of the gaseous reactants and products.

(5) The charcoal must be compatible with a high pH of the impregnating solution which also serves to protect the impregnant in service.

(6) An adequate adsorption capacity must exist after impregnation to handle the pollutants present in the carrier air.

The study in progress at NRL seeks to evaluate these aspects of behavior for many of the available commercial adsorbents [8].

VI. Mechanism for Trapping Methyl Iodide

A reaction mechanism for CH_3I retention is desirable as a guide to an investigator in the conduct of further research and development. Collins, Taylor and Taylor [2] discussed the particular examples of KI_x and the amine impregnants, the latter forming a quaternary iodide.

The many combinations of the salts of iodine oxyacids used as impregnating solutions in the present study have one thing in common. Although starting with various combinations of iodine species, it is possible in basic solutions to form the hyperiodite species. The formation is thermodynamically possible as shown by calculated heats of formation. Postulating a small but finite concentration of OI^- in the boundary surface of a charcoal, the following trapping mechanism may occur:

$$CH_3I^{131}(g) + K^+ OI^- (c) \longrightarrow CH_3OI(g) + KI^{131}(c) \qquad (3)$$

$$CH_3OI(g) + K^+OH^-(c) \longrightarrow CH_3OH(g) + K^+ OI^-(c) \qquad (4)$$

The calculated total free energy change for the sum of these two reactions is -17.45 Kcal. A CH_3I (131) molecule in approaching a OI^- species on the surface (Figure 4) is oriented with the CH_3 towards the ion and the I(131) directed away. By means of a Waldon Inversion [9] the transition state I is formed which readily is transformed into products II as indicated in Figure 4. A neighboring mobile OH surface group then rapidly forms the transition state II which results in the formation of products III, CH_3OH and the original reactive OI^- species. A chain reaction is thus established with the following overall features:

1. The chain reaction involves the regeneration of the active species OI^- and furnishes a stable sink for radioiodine, namely KI^{131}.

2. The free energy change is quite favorable.

3. The charcoal support could serve as a sink for the CH_3OH molecules produced.

4. The mechanism accounts for high trapping efficiency when the pH is high and for a low efficiency observed when the pH is reduced.

5. Economical quantities of impregnants are employed.

6. The observed I(131) concentrations in the charcoal bed in the direction of air flow follows catalytic kinetics [10].

One test for the reaction mechanism is the detection of methyl alcohol as a reaction product. Obviously, excess methyl alcohol will serve as a "poison" in the proposed mechanism.

The complete reaction mechanism is doubtlessly very complex. In some cases the adsorption process appears to dominate the trapping kinetics. However, in most cases, efficient trapping appears to occur via the catalytic process.

VII. Concluding Remarks

The base charcoal is not an inert carrier for the impregnant. For example, the pH of the water extract of the impregnated charcoal is normally lower by 3 to 4 pH units than that of the impregnating solution, a behavior compatible with surface interaction.

The advantages of the oxyiodine salts as impregnation agents may be summarized as follows:

1. When paired with suitable base charcoals, excellent trapping agents are obtained for methyl iodide that are efficient in air flows at 95-97 RH, contact times of 0.25 second, and in 2-inch bed depths of charcoal.

2. The cost of the impregnants is nominal and the shelf life under dry conditions appears to be indefinite.

3. A number of domestic charcoals, mainly those prepared from coal, are available as satisfactory base charcoals.

4. A high ignition temperature can be realized, in the range 350 to 450°C, using impregnated coal-based charcoals.

A number of unsolved problems and complications arise in the practical applications, but an optimistic view may be justified based on the current laboratory work in progress.

Acknowledgements

The sponsorship of the Division of Nuclear Fuel Cycles and Production, ERDA, and the complete cooperation of John C. Dempsey, Contract Manager, are gratefully acknowledged. Many thanks are due

to A. G. Evans, Savannah River Laboratory, for his close cooperation in several aspects of the investigation.

References

1a. Adams, R. E., Ackley, R. D., and Browning, W. E., Jr., ORNL-4040 UC-80-Reactor Technology, January 1967.

1b. Adams, R. E., Ackley, R. D. and Combs, Zell., Nuclear Safety Program Annual Report, ORNL-4374, 93-105, Dec. 31, 1968.

1c. Ackley, R. D. and Adams, R. E., ORNL-TM-2728, December 1969.

2. Collins, D. A., Taylor, L. R. and Taylor, R., Proc. 9th AEC Air Cleaning Conference 1, 159-198 (1966); TRG Report 789(W) 1964, U.K.A.E.A., Windscale.

3. Downs, A. J. and Adams, C. J., "The Chemistry of Chlorine, Bromine, Iodine and ASTATINE", Pergamon Texts in Inorganic Chemistry, Vol. 7, Pergamon Press (1975).

4. RDT Standard M16-1T, October, 1973. Division of Reactor Research and Development Technical Information Center, Oak Ridge, Tennessee.

5. Evans, A. G. and L. R. Jones, DP-1355, Savannah River Laboratory, Aiken, S. C. 29801.

6. Evans, A. G., Proc. 13th AEC Air Cleaning Conference, 743-755 (1974).

7. Johnson, J. E. and Woods, F. J., J. Fire & Flammability 2, 141-156 (1971).

8. Deitz, V. R. and Burchsted, C. A., "Survey of Domestic Charcoals for Iodine Retention", NRL Memo Report 2960, January 1975.

9. Fieser, L. F. and Fieser, M., "Advanced Organic Chemistry", pp. 320-321 (1961 Edition), Reinhold Publ. Corp., New York.

10. Deitz, V. R., Blachly, C. H. and Jonas, L. A., Proc. 14th ERDA Air Cleaning Conference (1976).

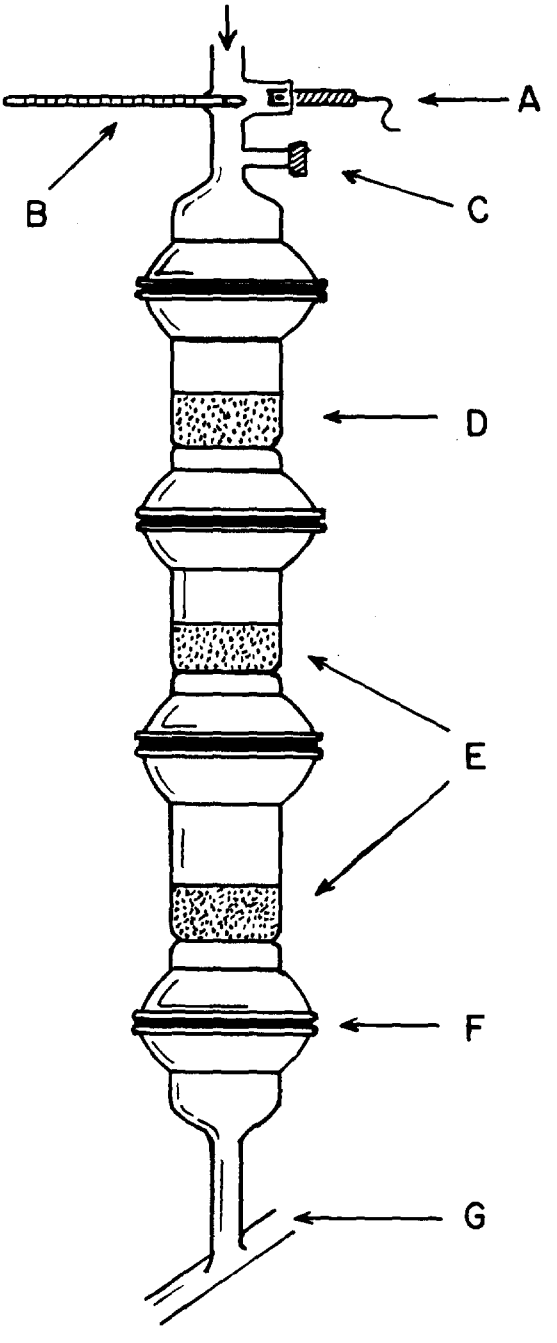

Figure 1: Diagrammatic Sketch of the Charcoal Test Chamber

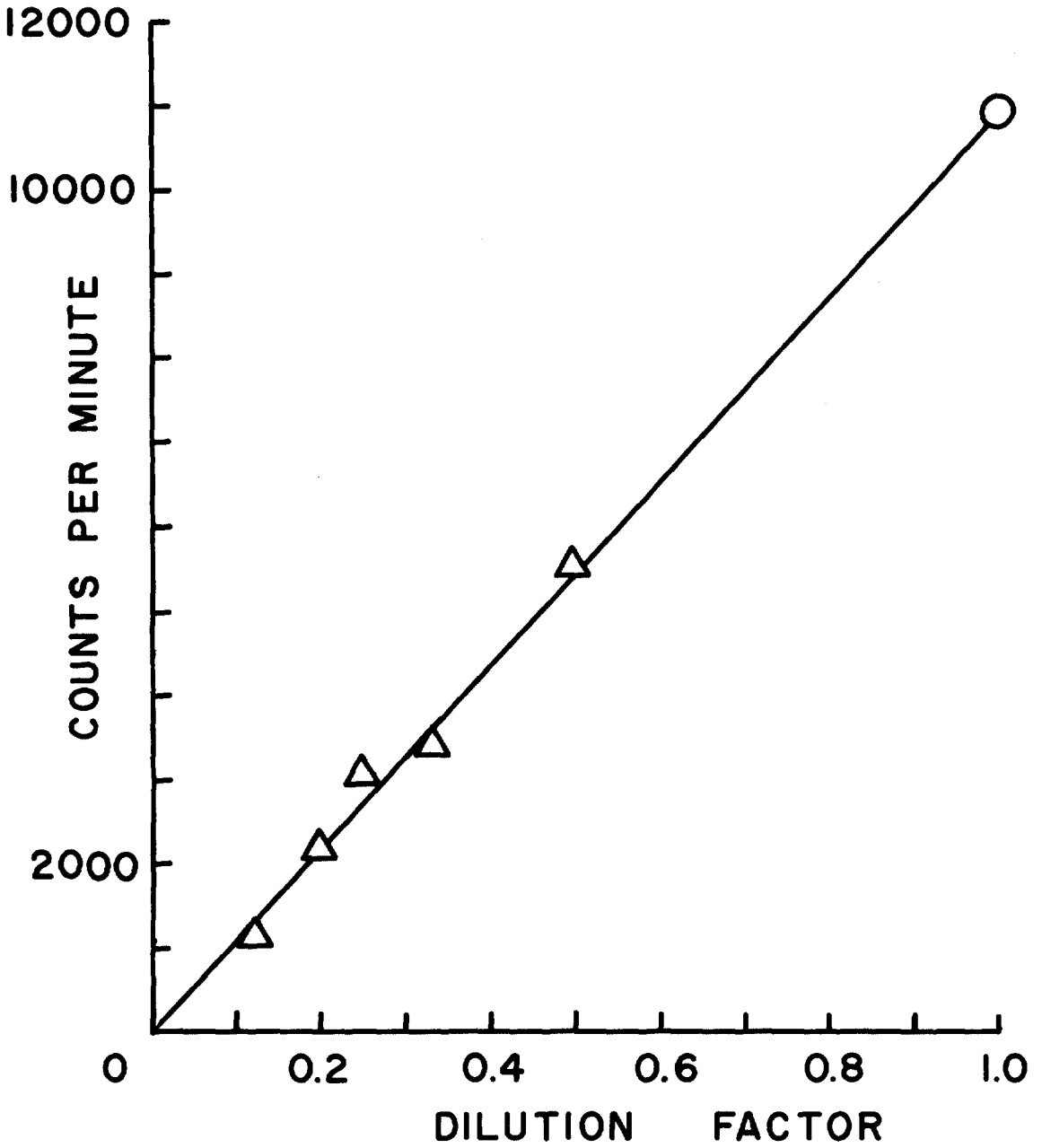

Figure 2: The Counting of Adsorbed CH_3I(131) on Impregnated Charcoal (4144) Diluted with Humidified Original Sample

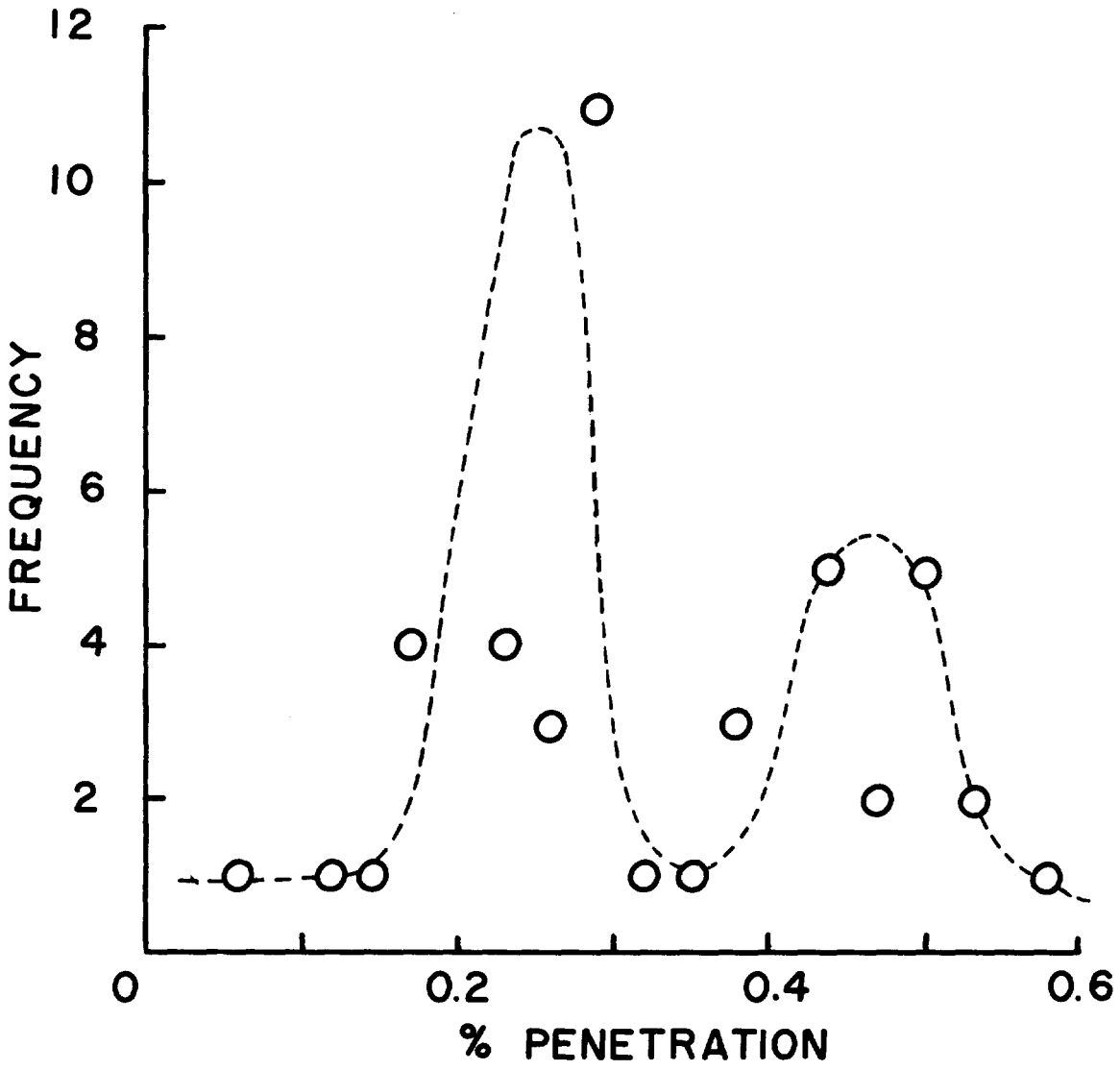

DISTRIBUTION	n	MEAN	STD. DEV.
Normal	45	0.33	0.13
Bimodal	26	0.239	0.07
	19	0.46	0.06

Figure 3: Frequency Plot of the Penetration Values using MBV Impregnated Charcoals

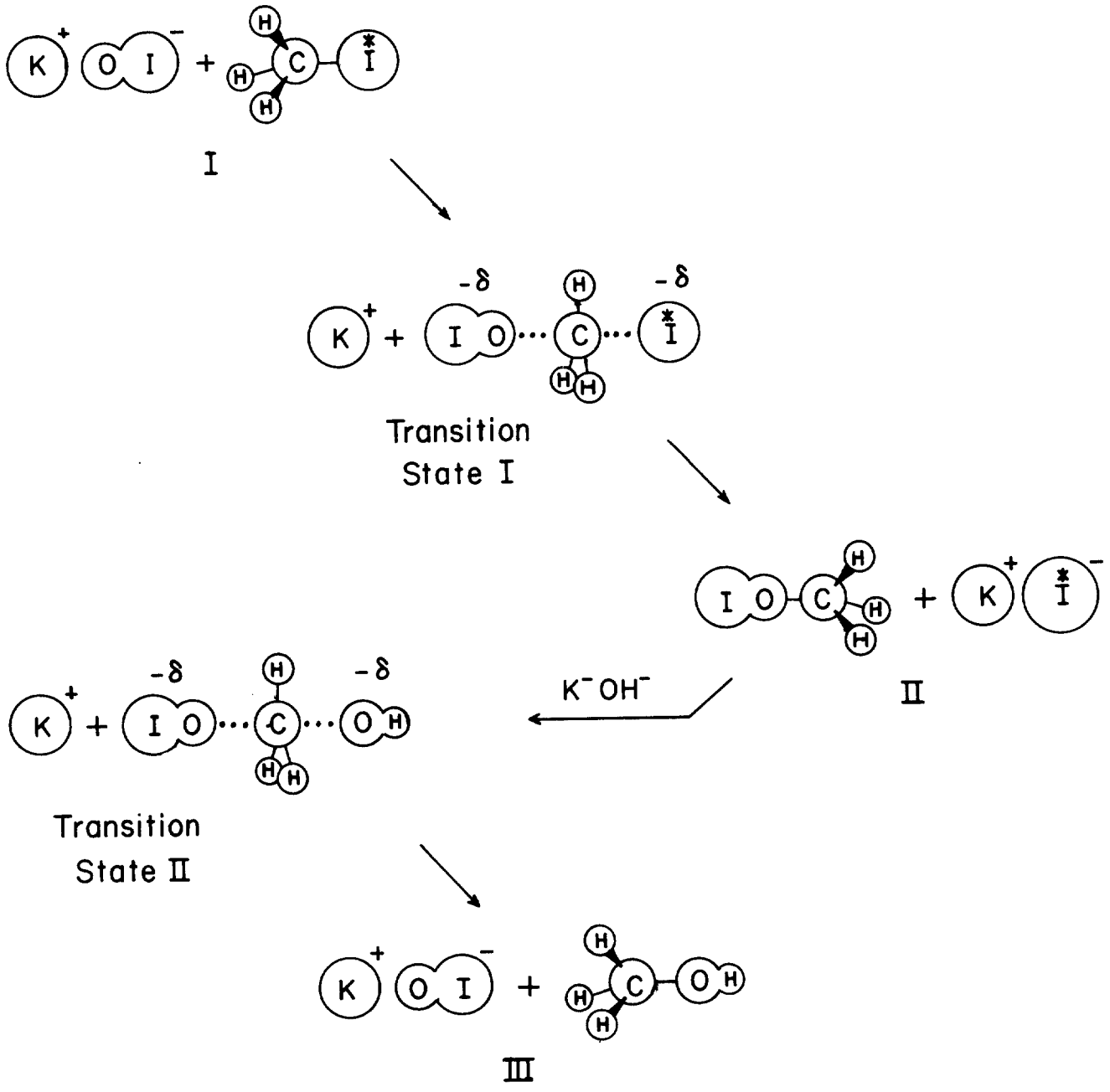

Figure 4: A Catalytic Mechanism for the Trapping of Methyl Iodide on Oxyiodine-Impregnated Charcoals

NEW CHARCOAL IMPREGNANTS FOR TRAPPING METHYL IODIDE PART II. APPLICATIONS TO A VARIETY OF BASE CHARCOALS*

A. G. Evans
Savannah River Laboratory
E. I. du Pont de Nemours and Company
Aiken, South Carolina 29801

Abstract

The most common impregnated charcoals in use at nuclear power reactors in the United States are coconut carbons containing iodine salts or a combination of iodine salts and TEDA (triethylenediamine). Although carbons impregnated with TEDA have proven to be quite effective for trapping methyl iodide, enough undesirable characteristics of TEDA have been observed (e.g., high cost, high vapor pressure, and low flash point) to stimulate a search for other effective impregnants.

Cooperative efforts between the Naval Research Laboratory (NRL) and Savannah River Laboratory (SRL) have led to the development of several promising new impregnation formulations containing HMTA (hexamethylenetetramine) and iodine salts. SRL has applied the new formulations to base carbons derived from coconut shells, coal, petroleum, and wood. The newly developed impregnated carbons, according to tests at NRL, perform as well as, or better than, commercial charcoals containing TEDA. The most successful combinations consist of coal carbon impregnated with 2% HMTA, 2% iodine (as KI and KIO_3), KOH, and $NaH_2PO_4 \cdot H_2O$.

Performance data are reported for the complete series of tests performed on the charcoals. Tests include methyl iodide retention tests, high-temperature I_2 penetration tests, ignition temperature tests, measurement of the carbon pH (water extracts), and confirmation of impregnation levels by neutron activation analysis. Specific impregnation techniques are also discussed.

*The information contained in this article was developed during the course of work under Contract No. AT(07-2)-1 with the U. S. Energy Research and Development Administration.

Introduction

In the United States, the most commonly used impregnated charcoals for trapping radioiodine and methyl iodide are prepared by treating coconut shell-base carbons with iodine salts or with combinations of iodine salts and TEDA (triethylenediamine). Several studies have shown that TEDA-KI formulations are more effective than those containing KI or KI_x[1-3]. However, the use of TEDA in some gas treatment systems is limited by some of its physical and chemical characteristics, and by its high cost.

On carbon, TEDA has a flash point of ~190°C[4,5]. In some accident situations, the combination of radioiodine decay heat and TEDA combustion heat may exceed the heat removal capacity of the system and cause carbon ignition at temperatures as low as 190°C[5,6,7].

TEDA has a finite vapor pressure over much of the operating temperature range of gas treatment systems. Consequently, some TEDA is lost from the system when air flows through the carbon beds. The manufacture of TEDA carbons therefore requires careful drying to minimize TEDA losses and impregnation costs. At a TEDA cost of eight dollars per pound, impregnation costs are about ten cents per pound for each weight percent TEDA in the final product.

Efforts began at SRL and NRL in 1974 to find an effective impregnant to replace TEDA. Desired characteristics of the new impregnant included: (1) methyl iodide removal efficiency equal to or better than that of TEDA, (2) low enough vapor pressure at 100°C to prevent significant loss of impregnant in service or during manufacture, (3) thermal stability to withstand temperatures up to at least 300°C without ignition and 200°C without decomposition, and (4) a lower cost than TEDA.

NRL studies showed that HMTA (hexamethylenetetramine) had the characteristics stated above when used in combination with iodine or iodine salts[8]. SRL and NRL have collaborated in efforts to adapt the HMTA formulations to a variety of base carbons.

Base carbons from coconut, petroleum, coal, and wood have been impregnated at SRL with several combinations of HMTA, iodine, and iodine salts. Tests that were run on all the carbons include methyl iodide penetration measurements, elemental iodine penetration measurements at 180°C, ignition temperature measurements, pH determinations (on water extracts), and specific analyses for sodium, potassium, and iodine by neutron activation analysis. Samples of six of the experimental carbons were also installed in the SRP Carbon Test Facility (CTF) for service aging studies.

Discussion

The basic techniques for HMTA impregnations were developed at NRL. SRL modifications to the formulations included adjusting iodine and potassium contents to achieve more favorable [(I/K)/pH] ratios[9,10] and the addition of flame retardants to the formulations to obtain more favorable ignition characteristics.

The initial SRL samples were impregnated by a one-step technique, i.e., all the impregnants were dissolved in a single solution. A two-step impregnation technique (two solutions applied serially), developed later, simplified preparation of the impregnation solution. Both techniques are discussed below.

One-Step Impregnation

The first step in the preparation of impregnating solution is grinding HMTA and I_2 crystals together (with a mortar and pestle, or a laboratory ball mill for larger samples). NRL tests showed that intimate mixing of HMTA and I_2 is necessary. Water, KOH, and other ingredients are added to the iodine-HMTA mixture in a flask, and the slurry is stirred until a solids-free solution is obtained. Complete dissolution of the ingredients frequently requires several hours of stirring. Application to the carbon by drip or spray addition techniques was most effective for uniform carbon impregnations when solution volume was carefully adjusted to saturate (but not flood) the carbon sample. Experience showed that the solution should be prepared with slightly less than two-thirds of the volume of water necessary to saturate the carbon.

The first SRL series of HMTA samples were prepared with the one-step technique and consisted of systematic variations of the iodine and HMTA contents to determine optimum impregnation level for each component. Samples were prepared with and without flame retardants to determine the most effective additive to improve the ignition characteristics of the final product. Type G-210* carbon was chosen as the base material for this series of samples so comparisons could be made with Type G-615* carbon containing TEDA. Impregnation levels and test results are shown in Tables I (constant HMTA) and II (constant iodine). The constant HMTA samples were prepared and tested first to select the optimum combination of iodine and iodine salts. The data show that methyl iodide retention is best, i.e., penetration is lowest, when contents of iodine as I_2 and I^- are each 1 wt % (Sample 2). Although addition of KI to the sample increased the ignition temperature (compare Sample 2 with Sample 3), the ignition temperature was still lower than the desired 350°C. Addition of 1% monobasic sodium phosphate ($NaH_2PO_4 \cdot H_2O$) to the formulations brought the ignition temperatures into the desired range, but the methyl iodide penetration values increased also (compare paired Samples 3 and 6 and 2 and 7). Addition of the dibasic sodium salt ($Na_2H_2PO_4 \cdot 2H_2O$) also increased the ignition temperature, but caused an even greater increase in methyl iodide penetration (Samples 2, 7, and 8). Thermal desorption data (I_2 desorption at 180°C) are all quite low because of the low [(I/K)/pH] values.

---

* An 8 x 16 mesh coconut carbon having surface area of ~1100 m^2/g (before impregnation). Product of North American Carbon Company, Columbus, Ohio.

After the optimum combination of I_2, I^-, and KOH was determined, a group of samples was prepared in which iodine contents were constant and HMTA content was varied from 1 to 6%. The data (Table II) show that the lowest methyl iodide penetration was obtained at the 2% impregnation level (Sample 10). Note that the methyl iodide penetration for Sample 10 compares favorably with that of the commercial TEDA carbon (G-615). Sample 10 exhibits a slightly higher I_2 penetration at 180°C than do other SRL formulations, but its I_2 penetration remains lower than that of the commercial product.

Table I One-step impregnations of coconut carbon[a] with constant HMTA (5%)

Sample No.	Impregnation Level, wt %				Ratio (I/K)/pH[c]	Ignition Temp., °C	Iodine Penetration, %	
	I_2	I^-[b]	KOH	Other			I_2[d]	CH_3I[e]
1	1.0	-	0.7	-	0.024	275	0.00061	9.32
2	1.0	1.0	0.7	-	0.041	325	0.00031	1.33
3	2.0	-	1.4	-	0.037	265	0.00041	2.53
4	3.0	-	2.1	-	0.043	265	0.00045	2.61
5	1.0	2.0	0.7	-	0.050	315	0.00060	2.39
6	2.0	-	1.4	1.0[f]	0.036	355	0.00060	3.05
7	1.0	1.0	0.7	1.0[f]	0.038	390	0.00052	1.86
8	1.0	1.0	0.7	1.0[g]	0.045	355	0.00057	3.18

a. Type G-210 base carbon, see text for description.

b. KI used. Addition calculated on the basis of weight percent iodine added.

c. Determined from analyses of carbons after impregnation (see Reference 9).

d. SRL thermal desorption test at 180°C.

e. NRL methyl iodide test data. Test run at 25°C, 95% relative humidity, 0.1 mg CH_3I/g C loading, and 0.25-second residence time in 2-in.-deep carbon bed.

f. $NaH_2PO_4 \cdot H_2O$ (monobasic sodium phosphate) flame retardant added.

g. $Na_2HPO_4 \cdot 2H_2O$ (dibasic sodium phosphate) flame retardant added.

Table II One-step impregnations of coconut carbon[a] with constant iodine (1% I_2, 1% I^-

Sample No.	Impregnation Levels, wt % HMTA	KOH	Other	Ratio (I/K)/pH[b]	Ignition Temp., °C	Iodine Penetration, % I_2[b]	CH_3I[b]
9	1.0	0.7	1.0[c]	0.034	350	0.00067	0.99
10	2.0	0.7	1.0[c]	0.038	370	0.00141	0.65
11	3.0	0.7	1.0[c]	0.029	415	0.00105	1.19
12	4.0	0.7	1.0[c]	0.036	422	0.00092	1.37
7	5.0	0.7	1.0[c]	0.038	390	0.00052	1.86
13	6.0	0.7	1.0[c]	0.037	435	0.00076	1.76
G-615[d]	TEDA	-	1.0[e]	0.039	360	0.0060	0.79

a. Type G-210 base carbon, see text for description.

b. See Table I for details.

c. $NaH_2PO_4 \cdot H_2O$.

d. A commercial carbon containing 2% TEDA and 2% KI.

e. Proprietary flame retardant.

Two-Step Impregnation

Additional NRL studies on impregnation techniques revealed that addition of the iodine salts and HMTA in separate impregnation steps saved substantial time in the solution preparation step and resulted in improved methyl iodide retention by the impregnated product[8]. In this technique, the inorganic ingredients (I_2, KI, KOH, $NaH_2PO_4 \cdot H_2O$, etc.) are dissolved in one solution that is added to the carbon in a volume of water equal to approximately half that required to saturate the carbon. A second solution containing the HMTA (with enough KOH added to adjust solution pH) is added to the carbon (without drying the partially wetted charcoal) in an equal volume of water. The total volume of water required to prepare the two solutions is only slightly less (~95%) than the volume of distilled water required to saturate the carbon.

The initial SRL samples impregnated by the two-step technique were prepared with 5% HMTA and the I_2-KI-KOH formulation found best in the first one-step sample series (test results on samples of varied HMTA content were not yet available). Additional samples were prepared using 2% HMTA with KI, KIO_3, and KOH instead of the I_2-KI-KOH combination used in earlier formulations. The chemistry of specific formulations will be discussed in greater detail later. A third set of samples was prepared with KI, KIO_3, KOH, and $NaH_2PO_4 \cdot H_2O$ to show the effect of HMTA on iodine retention. Base carbons used for these three sets of samples included charcoals derived from coconut shells, coal, petroleum, and wood. Test data are shown in Tables III (coconut and wood carbons) and IV (coal and petroleum carbons).

The data in Tables III and IV show that two types of carbon (Type G-212, a high surface area coconut carbon, and Type GX-202, a wood base carbon) do not retain

Table III Two-step HMTA impregnations on coconut and wood carbons.

Type of Carbon	Impregnation Levels, wt % HMTA	Iodine Salts	KOH	Other[a]	(I/K)/pH[b]	Ignition Temp., °C	Iodine Penetration, % I_2[b]	CH_3I[b]
G-210	5.0	2.0 (I_2,I^-)	0.7	PO_4^{3-}	0.030	398	0.00289	1.74
	2.0	2.0 (I^-,IO_3^-)[c]	0.8	PO_4^{3-}	0.028	320	0.00104	0.46
	2.0	2.0 (I^-, IO_3^-)	0.8	BO_3^{3-}[d]	0.034	275	0.00084	4.45
	0.0	2.0 (I^-,IO_3^-)	0.4	PO_4^{3-}	0.040	377	0.00079	4.10
G-212[e]	5.0	2.0 (I_2,I^-)	0.7	PO_4^{3-}	0.027	335	0.00231	2.47
	2.0	2.0 (I^-,IO_3^-)	0.4	PO_4^{3-}	0.026	335	0.00120	0.91
GX-202[e]	5.0	2.0 (I_2,I^-)	0.7	PO_4^{3-}	0.048	436	0.00450	0.90
	2.0	2.0 (I^-,IO_3^-)	0.4	PO_4^{3-}	0.042	412	0.00115	1.49
	0.0	2.0 (I^-,IO_3^-)	0.4	PO_4^{3-}	0.044	403	0.00153	1.42

a. Flame retardant, 1.0% $NaH_2PO_4 \cdot H_2O$ unless otherwise indicated.

b. See Table I for details.

c. 2.2% KI, 0.6% KIO_3.

d. 0.8% H_3BO_3.

e. Products of North American Carbon Company, Columbus, Ohio.

Table IV Two-step HMTA impregnations on coal and petroleum carbons.

Type of Carbon	Impregnation Levels, wt % HMTA	Iodine Salts	KOH	Other[a]	Ratio (I/K)/pH[b]	Ignition Temp., °C	Iodine Penetration, % I_2[b]	CH_2I[b]
G-352[c]	5.0	2.0 (I_2,I^-)	0.7	PO_3^{3-}	0.045	450	0.00141	0.50
	2.0	2.0 (I^-,IO_3^-)[d]	0.7	PO_3^{3-}	0.065	435	0.00121	0.36
	2.0	2.0 (I^-,IO_3^-)	0.8	BO_3^{3-}[e]	0.062	395	0.00160	1.17
	0.0	2.0 (I^-,IO_3^-)	0.8	PO_3^{3-}	0.060	420	0.00325	0.21
BPL[f]	5.0	2.0 (I_2,I^-)	0.7	PO_3^{3-}	0.087	433	0.00337	0.53
	2.0	2.0 (I^-,IO_3^-)	0.6	PO_3^{3-}	0.065	420	0.00184	0.69
	0.0	2.0 (I^-,IO_3^-)	0.8	PO_3^{3-}	0.057	392	0.00079	1.30
W-965[f]	5.0	2.0 (I_2,I^-)	0.7	PO_3^{3-}	0.095	425	0.00721	0.73
	2.0	2.0 (I^-,IO_3^-)	0.8	PO_3^{3-}	0.055	415	0.00057	0.44
	0.0	2.0 (I^-,IO_3^-)	0.8	PO_3^{3-}	0.057	417	0.00173	1.09

a. 1.0% $NaH_2PO_4 \cdot H_2O$ unless otherwise indicated.

b. See Table I for details.

c. Ground and sieved to 10x16 mesh. Product of North American Carbon Company, Columbus, Ohio.

d. 2.2% KI, 0.6% KIO_3.

e. 0.8% H_3BO_3.

f. 10x16 mesh fraction. Product of Calgon Corporation, Pittsburgh, PA.

g. Witcarb-965 (formerly grade 337). Product of Witco Chemical Corporation, New York, NY.

methyl iodide as effectively as do the other types of carbons impregnated with these HMTA formulations. The fact that penetration values of one percent or less were obtained, however, suggests that specific formulations could be developed for these carbons that would perform as well as some of the commercial TEDA products.

The data also show that the addition of HMTA to the formulation usually improves methyl iodide retention performance over that obtained with iodine compounds alone. The anomalous behavior of Type G-352 carbon with and without HMTA is still under investigation.

Flame retardant experiments included in the data in Tables III and IV are also worth noting. Two samples prepared with H_3BO_3 as a flame retardant (on carbon Types G-210 and G-352) both showed significantly poorer methyl iodide retention than did their companion samples containing monosodium phosphate $NaH_2PO_4 \cdot H_2O$. Examination of ignition temperature data on these same samples shows that boric acid is also less effective as a flame retardant than is the phosphate.

Chemistry of Impregnation Formulations

Choice of Reagents. Preliminary NRL data indicated that an I_2-HMTA reaction, prior to impregnation, is needed to produce a carbon with effective methyl iodide retention. The development of the two-step impregnation technique suggested that the "activation" of the HMTA molecule can take place on the carbon either during or after the impregnation step. During the transition from one- to two-step impregnations, samples were first prepared with I_2 and KI as in earlier studies. The SRL formulations were specifically designed to contain an excess of potassium to achieve a favorable I/K ratio (<0.6:1 atom ratio)[9] and a high pH. As a result, the I_2 incorporated in the solutions was always converted to ionic iodine before the impregnation step. The idealized reaction is[11]:

$$3I_2 + 6OH^- \rightarrow 5I^- + IO_3^- + 3H_2O$$

Other oxyiodides may be formed during the reaction of iodine with caustic as discussed in detail in Part I of this paper[8] and in Reference 12.

To optimize the impregnant formulations for possible commercial use, the cost of reagents and the safety of reagent handling must be considered. Since I_2 is converted to ionic iodides before impregnation, the less costly and less hazardous iodine salt forms were used, rather than I_2. Once dissolved, the same mixtures of iodides and oxyiodides should form in solution as would be formed from dissolution of I_2 in caustic.

Thus, all the later SRL formulations are based on 2% total iodine and derived from KI and KIO_3 in the weight proportion to achieve the ratio $5I^-:IO_3^-$. KOH is added to bring the I/K weight ratio to approximately 2:1 (an atom ratio of <0.6:1) both to maintain the iodine in ionic form and to neutralize the NaH_2PO_4 added.

Preparation of Solutions. Experience has shown that the order of combination of reagents is as important as the amounts of reagents used. The specific order of combination of reagents for the one-step impregnation was discussed earlier. When solutions were prepared for the first two-step impregnations, I_2 and KI were used rather than the KI-KIO_3 combination. Thus, KOH addition was required early in the

preparation phase in order to dissolve the I_2. The phosphate was added last, and the solution remained clear and colorless after KOH addition through the time the solution was added to the carbon. Test data show that the two methods produce carbons with essentially the same methyl iodide retention (compare Sample 7 in Tables I and II with the first sample of Type G-210 carbon in Table III).

When the KI-KIO_3 combination was tested, the first samples were prepared in the same manner. That is, the KI, KIO_3, and KOH were dissolved first, and the phosphate salt was added last. Again a clear, colorless solution was formed and remained up to the time of addition to the carbon. In later experiments with custom-designed solutions for different base carbons (base carbon pH's vary as a function of the natural potassium content), the KI, KIO_3, and phosphate salt were combined first, and the solution was titrated with a known concentration KOH solution.

Addition of the NaH_2PO_4 to the KI-KIO_3 salt solution resulted in the formation of the I_3^- ion because of the lower solution pH (the pH typically dropped from about 8.6 to 7.2 with the addition of NaH_2PO_4). Solutions are typically deep red in color after phosphate addition. The intensity of the color varies with the volume of solution used for a particular carbon. Back-titration of dummy solutions showed that a pH in excess of 13 is required to decolorize the solution once the I_3^- ion is formed. KOH addition required to adjust solution pH to 13 or more corresponds to addition of 0.8-1.0 weight percent KOH to the final product and lowers the ignition temperature substantially (especially on coconut carbons). KOH additions to the red solutions corresponding to 0.4-0.7% addition to the final product result in a solution ranging from red (0.4% addition, solution pH = 10.0) to straw yellow (0.7% addition, solution pH = 12.2).

Samples prepared from colored impregnating solutions show significantly higher methyl iodide penetration as well as exhibiting a lower pH. Typical data on two base carbons are shown in Table V.

Experiments currently in progress involve dissolution of caustic and phosphate together in a concentrated buffer solution (molar ratio KOH:$NaH_2PO_4 \cdot H_2O \approx 2:1$). Addition of buffer solution to the KI-KIO_3 solution brings the pH of impregnation Solution 1 to about 12.4. The solution remains colorless during the buffer addition indicating that the I_3^- ion is not formed. Preliminary data show that this solution preparation technique results in a more satisfactory product (carbon pH's are in the 9.2-10.3 range, ignition temperatures are all above 340°C, and the carbons all have high-temperature iodine penetration values less than 0.002%). Methyl iodide penetration data were not available when this paper was being prepared.

Table V Effect of impregnation solution on methyl iodide penetration.

Basic Formulation: Solution 1 2.18% KI, 0.56% KIO_3, 1.0% $NaH_2PO_4 \cdot H_2O$ + KOH

Solution 2 2.0% HMTA + KOH[a]

Type of Carbon	Total KOH, wt %	Solution pH	Carbon pH	Ignition Temp., °C	CH_3I Penetration, %	Solution Color
G-210	0.41	10.0	9.70	375	3.57	Bright red
	0.48	11.1	10.30	337	2.59	Bright yellow
	0.81	Unknown[b]	10.48	320	0.46	Colorless
Witcarb 965	0.67	11.2	9.62	445	2.08	Bright yellow
	0.65	11.3	9.77	432	1.10	Pale yellow
	0.81	Unknown[b]	10.10	415	0.44	Colorless

a. KOH added to HMTA solution to bring solution pH to same value as Solution 1.

b. KOH added before $NaH_2PO_4 \cdot H_2O$. Solution pH not measured.

Service Aging Studies

Samples of six of the HMTA-impregnated charcoals have been installed in the CTF at SRP for service aging studies. Base carbons include Types G-210, Witcarb 965, G-352, MBV*, and GX-202. Other samples will be included in the evaluation program as test positions become available in the CTF. Particular emphasis is being placed on both the iodine retention properties and the mechanical stability of the carbons.

Observations made during the impregnation of several of the base carbons show that most of the non-coconut charcoals "dust" badly in the rotary drum impregnator used at SRL. This dusting characteristic raises the question as to how well the carbons will withstand the stress of air flowing through the carbon beds in service.

HEPA filters placed ahead of the backup beds used in the SRL high-temperature test accumulate more carbon dust during the testing of coal carbons than during testing of other types of carbons even though all test beds are blown out with an air jet prior to testing. No settling of the test beds has been observed during these tests, but the test period (4.17 hr) is not of sufficient duration to cause much loss of carbon. The longer exposure periods anticipated in the CTF (6-18

* Product of Union Carbide Corporation, New York, N.Y.

months of continuous air flow at a face velocity of 55 ft/min) should be sufficient to ascertain whether attrition is a problem in tightly packed beds.

Conclusions

Several solutions containing HMTA and iodine salts have been used on a variety of base carbons to produce impregnated charcoals for trapping methyl iodide. Test data show that some of these charcoals retain methyl iodide as well as or better than commercial charcoals containing TEDA. Coal carbons retain methyl iodide better with HMTA formulations, but acceptable trapping efficiencies have been achieved with coconut and petroleum carbons as well. The performance of the product also is sensitive to both the chemicals used in the formulation and the techniques used during the preparation of impregnation solutions.

Acknowledgment

The author wishes to express his appreciation to V. R. Deitz of NRL for furnishing methyl iodide penetration test data for this paper and to C. H. Blachly of NRL for performing the methyl iodide tests.

References

1. D. A. Collins, L. R. Taylor, and R. Taylor. "The Development of Impregnated Charcoals for Trapping Methyl Iodide at High Humidity." Proceedings of the Ninth AEC Air Cleaning Conference. USAEC Report CONF-660904, Vol. 1, p 154-198 (1967).

2. A. G. Evans and L. R. Jones. Confinement of Airborne Radioactivity - Progress Report: January 1971-June 1971. USAEC Report DP-1280, E. I. du Pont de Nemours and Company, Savannah River Laboratory, Aiken, SC (1971).

3. A. G. Evans and L. R. Jones. Confinement of Airborne Radioactivity - Progress Report: July 1971-December 1971. USAEC Report DP-1298, E. I. du Pont de Nemours and Company, Savannah River Laboratory, Aiken, SC (1971).

4. R. E. Adams, R. D. Ackley, and R. P. Shields. "Application of Impregnated Charcoals for Removing Radioiodine from Flowing Air at High Relative Humidity." Treatment of Airborne Radioactive Wastes, Proceedings of a Symposium, New York, NY, August 26-30, 1968, IAEA, Vienna p 398 (1968).

5. A. G. Evans. Confinement of Airborne Radioactivity - Progress Report July 1972-December 1972. USAEC Report DP-1329, E. I. du Pont de Nemours and Company, Savannah River Laboratory, Aiken, SC (1973).

6. A. G. Evans. Confinement of Airborne Radioactivity - Progress Report: January 1973-June 1973. USAEC Report DP-1340, E. I. du Pont de Nemours and Company, Savannah River Laboratory, Aiken, SC (1973).

7. J. L. Kovach and J. E. Green. "Evaluation of the Ignition Temperature of Activated Charcoals in Dry Air." Nucl. Safety 8, 41 (1966).

8. V. R. Deitz and C. H. Blachly. "New Charcoal Impregnants for Trapping Methyl Iodide, Part I, Salts of the Iodine Oxyacids with Iodide or Iodine in Basic Solution." Paper presented at the Fourteenth ERDA Air Cleaning Conference, Sun Valley, Idaho, August 2-4, 1976. Naval Research Laboratory, Washington, DC (1976).

9. A. G. Evans. "Effect of Alkali Metal Content of Carbon on Retention of Iodine at High Temperatures." Proceedings of the Thirteenth AEC Air Cleaning Conference, San Francisco, CA, August 12-15, 1974, USAEC Report CONF-740807 (1975).

10. A. H. Dexter, A. G. Evans, and L. R. Jones. Confinement of Airborne Radioactivity - Progress Report: January 1974-December 1974. USERDA Report DP-1390, E. I. du Pont de Nemours and Co., Savannah River Laboratory, Aiken, SC (1975).

11. Therald Moellar. Inorganic Chemistry. John Wiley & Sons, Inc., New York (1952).

12. A. J. Downs and C. J. Adams. The Chemistry of Chlorine, Bromine, Iodine and Astatine. Pergamon Texts in Inorganic Chemistry, Vol. 7, Pergamon Press, New York (1973).

DISCUSSION

R. J. WILLIAMS: One question I have is how well any of these charcoals will perform if one gets an iodine release after a fire. Do you have any information on the effect of the accumulation of combustion products on iodine retention?

EVANS: Not to my knowledge. Perhaps Dr. Deitz has some data on the effects of pollutants on HMTA-impregnated charcoals.

DIETZ: The results that we have today are on new impregnated charcoals. We have, at present, a whole series of weathering experiments where pollutants are being added to the charcoal and we will, maybe at the next charcoal meeting in Washington, be able to report on some of the results.

EVANS: In addition to Dr. Deitz's studies, we have some of the HMTA-impregnated charcoals installed in a weathering facility at Savannah River.

KOVACH: Rather than a question, I would like to make a comment regarding HMTA. At about 380°C, it decomposes and the major decomposition product is HCN, so if you are running ignition temperature studies or any secondary hazard studies, even on a laboratory scale, the quantity of cyanide generated is rather high. I caution you to try not to do away with your lab technicians if you are running decomposition studies.

EVANS: For obvious other reasons, tests that we run are performed in a fumehood. If the carbon itself ever gets exposed to 300°C of more, you might just as well forget its effectiveness. The iodine is gone, anyway, from a practical point of view.

DIETZ: Tomorrow afternoon, we will show that iodine is rather volatile. It will start coming off around 180 to 190°C, depending on the impregnation.

WILHELM: I have a feeling that in most of the containment systems constructed to date, the charcoal filters won't work. Both the primary containment and the secondary containment will work and they will work properly. If the primary containment doesn't fail, the secondary containment will work properly. But what happens when the primary containment fails? I think the secondary containment will fail, too, because it will "see" conditions it can't handle. In this situation, we can't claim safety, we don't normally have the safety, and this situation is strictly not allowed.

THE BEHAVIOR OF HIGHLY RADIOACTIVE IODINE ON CHARCOAL IN MOIST AIR*

R. A. Lorenz, S. R. Manning, and W. J. Martin
Oak Ridge National Laboratory
Oak Ridge, Tennessee 37830

Abstract

The behavior of highly radioactive iodine adsorbed on charcoal exposed to moist air (average partial pressure of water vapor, 110 torr) was investigated in a series of six experiments. The amount of radioactive ^{130}I on a well-insulated 28-cm^3 bed ranged from 50 to 570 Ci. The relative humidity was 47% at the bed inlet temperature of 70°C.

Radioactive iodine was released from the test beds at a continuous fractional release rate of 7 to 10 x 10^{-6}/hr for all types of charcoal tested. The chemical form of the released iodine was such that it was very highly penetrating with respect to the nine different types of commercial impregnated charcoals tested in backup collection beds. Two types of silver nitrate-coated adsorption materials behaved similarly to the charcoals. Silver-exchanged type 13X molecular sieve adsorbers were 20 to 50 times more efficient for adsorbing the highly penetrating iodine, but not as efficient as normally found for collecting methyl iodide. The chemical form of the highly penetrating iodine was not determined.

A species behaving like methyl iodide was released from the main test beds only during the period that the radioactive iodine was being loaded onto the test beds. An exception was a sample of charcoal that had been in service for four years in an air cleaning system associated with a reactor building at Oak Ridge National Laboratory. This charcoal, which contained 108 mg of adsorbed atmospheric contaminants per gram of charcoal, released a methyl iodide-like material continuously at a fractional rate of 80 x 10^{-6}/hr in addition to the highly penetrating iodine form. A different type of charcoal, which had been exposed for nine months at the Savannah River Laboratory and was found to contain a much lower concentration of adsorbed organic impurities, released only the highly penetrating form of iodine.

When the velocity of the moist air was decreased from 28.5 fpm (25°C) to as low as 0.71 fpm (25°C), the temperature of the charcoal bed rose slowly and reached the ignition point in three of the experiments. At 0.71 fpm (25°C), the ignited charcoal beds reached maximum temperatures of 430 to 470°C because of the limited oxygen supply. The charcoal exposed for four years at Oak Ridge ignited at 283°C compared with 368°C for unused charcoal from the same batch.

Two of the experiments used charcoal containing 1 or 2% TEDA (triethylenediamine) and a proprietary flame retardant. The oxidation and ignition behavior of these charcoals did not appear to be affected adversely by the presence of the TEDA.

*Research sponsored by the Energy Research and Development Administration under contract with the Union Carbide Corporation.

I. Introduction

We have completed a series of experiments which had the primary objective of determining whether the ignition of charcoal can occur from the decay heat of highly radioactive iodine before the iodine desorbs. The second objective of our program was to provide supportive data for the calculation of charcoal bed temperatures, and the third objective was to study the movement of iodine within charcoal beds and the desorption of iodine from these beds during exposure to intense radiation fields and elevated temperatures. Seven experiments conducted with dry air have been reported previously;[1] six experiments conducted with moist air are reported here.

We used four types of charcoal in our moist air experiments, Runs 8-13 (see Table I). All of them are coconut-based charcoals except for WITCO Grade 42, which is petroleum-based. Each batch had performed satisfactorily in other iodine or methyl iodide adsorption tests. Because some large differences in iodine desorption and oxidation rates or ignition temperature have been observed from batch to batch of a given manufacturer's type number, we caution that the experimental results presented here apply only to the particular lots of material tested.

Our experimental apparatus is shown schematically in Fig. 1. The charcoal is contained to a depth of 2-1/8 in. (5.4 cm) in a quartz Dewar flask with an inside diameter of 1.03 in. (2.62 cm). A heater on the outside of the flask is adjusted to follow the temperature of the center of the bed in order to further reduce the chance for heat loss through the side, in simulation of an essentially semi-infinite reactor adsorber system. Except for a small heat loss via conduction and heat radiation, the only cooling mechanism is the forced flow of air upward through the bed. Thermocouples measure the temperature distribution in the charcoal. The inlet temperature was controlled at 70°C in simulation of an accident ambient temperature, while the charcoal reached a higher temperature, depending on the amount of radioactive iodine present and the air flow rate.

II. Experimental Procedure

The radioactive ^{130}I was obtained by irradiating a mixture of 86% ^{129}I--14% ^{127}I in the chemical form PdI_2 packed as powder in quartz ampoules and seal-welded in an aluminum capsule. We irradiated this material for 30 hr (except Run 13) in the High Flux Isotope Reactor (HFIR) at a thermal flux of 2.5×10^{15} neutrons/cm^2·sec, which resulted in specific activities of 5.7 Ci ^{130}I/mg I and 1.4×10^{-3} Ci ^{131}I/mg I at the time of removal from the reactor.

After irradiation, the capsule was transported to the hot cell and sealed into the recirculating loop system. The tips of the capsule and ampoules were then sheared off, allowing the ampoules to fall into a quartz-lined furnace where the PdI_2 was thermally decomposed at 600 to 700°C to palladium metal and I_2. Air circulating at the normal flow rate carried the radioactive iodine through two layers of Cambridge 1G HEPA filter medium into the test charcoal bed.

A collimated radiation detector was moved in 1/8-in. increments to follow the distribution of iodine in the bed as the experiments progressed. The collimator, located 6 in. from the bed, contained a slit that was 1/16 in. wide and 8 in. long (8-1/2 in. long beginning with Run 10).

Iodine that penetrated or was desorbed from the test bed was collected in sequentially operated traps. HEPA filters (Cambridge 1G) were used to collect particulate matter, and charcoal and silver-exchanged zeolite were used to collect

Table I Characteristics of charcoal investigated

Charcoal type	ORNL lot No.	Experiment No.[a]	Dry mass in each experiment (g)	Dry density (g/cm^3)	Apparent density[b] (g/cm^3)	Mean surface particle size[c], D_p, (cm)	K[d] (%)	I[d] (%)	pH[e]
MSA 85851[f]	51969	1, 2, 3, 4, 8, 13	11.2	0.420	0.45	0.161	2.85	4.41	9.1-8.6
BC-727[g]	1683	5	13.1	0.461	0.562	0.169	1.87	3.79	8.2-8.2
WITCO Grade 42[h]	62469	6, 9	10.9	0.384	0.389	0.171	0.90	3.07	8.3-7.8
		10 (first in.)	6.77	0.513	0.564	0.168	0.83	2.72	3.6-3.3
		10 (second in.)	6.14	0.449	0.513	0.174	0.96	3.32	7.1-6.8
GX-176[i]	SR-7	7, 11	14.7	0.524	0.563	0.151	1.26	1.30	9.1-8.8
G-615[j]	SR-6	12	14.9	0.539	0.626	-	1.0	1.3	7.3-7.1

[a] Experiments 1-7 reported in ref. 1.
[b] Apparent density of the moist charcoal according to the method of ASTM D-2854-70.
[c] Particles collected on 8-mesh or passing 16-mesh (U.S.) screens eliminated. $D_p \doteq W/\Sigma (W_i/D_{pi})$.
[d] Weight percent based on apparent density of moist (as-received) charcoal. Moisture content varied because of different storage conditions.
[e] First value obtained from 5 g charcoal in 20-ml water for 30 min at room temperature. Second value after heating to boiling and cooling to room temperature in covered container.
[f] Product of Mine Safety Appliances Company, Pittsburgh, Pa.
[g] Product of Barnebey-Cheney, Columbus, Ohio. Charcoal obtained from A. G. Evans, Savannah River Laboratory.
[h] Product of WITCO Chemical Corporation, New York, N.Y.
[i] Product of North American Carbon, Inc., Columbus, Ohio. This charcoal also contains 1% TEDA (triethylenediamine) and a proprietary flame retardant. Charcoal and chemical analyses obtained from A. G. Evans, Savannah River Laboratory.
[j] Product of North American Carbon, Inc., Columbus, Ohio. This charcoal also contains 2% TEDA and a proprietary flame retardant. The charcoal was obtained from A. G. Evans after 9 months service at Savannah River Laboratory.

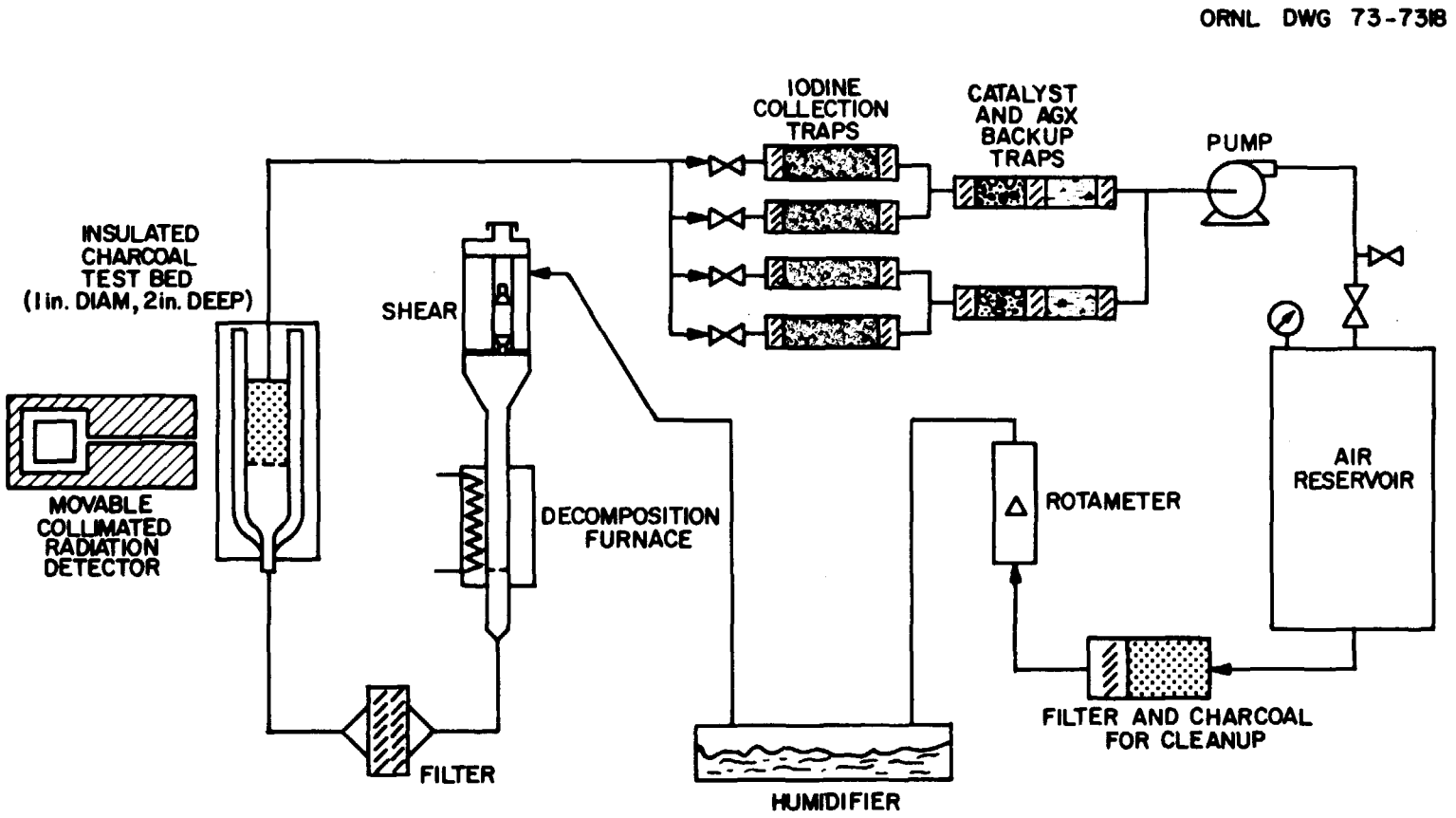

Fig. 1 Flow diagram for experiments with moist air.

both elemental iodine and the more penetrating organic forms of iodine. We examined the distribution of iodine among the cartridges to determine the relative amounts of elemental and organic iodine present.

The experimental procedure can be described as follows. The installed collection traps and heated loop were purged with dried and filtered air, using a once-through mode and a flow rate of 4.9 liters/min for 2.5 hr to dry the loop and remove volatile contaminants. A 28-cm^3 volume of the test charcoal in the as-received moisture condition was then poured into the insulated bed through the outlet tube. (The presence of many thermocouples and the restricted fall resulted in a packing density somewhat less than that measured by the method of ASTM-D-2854-70. Assuming a void fraction of 0.43 for normal packing, we estimate a void fraction of 0.45 for the test bed.) Subsequently, the loop heaters were turned on, the irradiated capsule installed, air circulation started, and the capsule sheared when the desired bed temperature was reached. The humidifier was heated to 54 or 55 °C to maintain proper humidity.

The air inlet temperature to the bed was controlled at 70 °C, and the charcoal bed was heated by the decay heat to some higher temperature, depending on the level of radioactivity and air flow rate, as shown in Tables II-VII. The period of operation at normal air flow rate at the beginning of each experiment enabled observation of the iodine movement and desorption at nearly constant-temperature conditions. The air flow rate was subsequently reduced allowing the temperature to rise, in simulation of an accident situation (except in Run 13). The operating conditions are also summarized in Tables II-VII.

III. Oxidation of Charcoal

The temperature behavior during several of the runs is shown in Figs. 2-5. The accelerating temperature rise during a period of each of these experiments was the result of an increasing rate of heat release from the oxidation of charcoal as the temperature rose. The rate of rise depended on the amount of radioactive iodine decay heat, the oxidation characteristics of the charcoal, and the air flow rate. We calculated the heat balance for the test bed, described in more detail previously,[1] and obtained the rate of heat release also shown in Figs. 2-5. At the very low air flow rates employed in these experiments, the rate of heat release decreased following ignition, possibly due to consumption of the chemically active sites and poisoning of the charcoal surface.

Figure 6 shows the calculated rate of heat release from oxidation as a function of temperature. The heat release data prior to ignition can be correlated for each experiment using the Arrhenius-type equation

$$H = H_o e^{-A/RT} , \qquad (1)$$

where

H_o = a constant (cal/min·g charcoal),
A = an activation energy (cal/mole),
R = 1.987 cal/mole·°K,
H = the rate of heat release by oxidation (cal/min·g charcoal).

The values of H_o and A are given in Table VIII. The experimental heat release data are fairly accurate within the range of 0.5 to 20 cal/min·g charcoal; however, the accuracy of extrapolations beyond this range is uncertain.

The rate of heat release for MSA 85851 during Run 8 was only approximately one-third that observed during Run 4, which was conducted in dry air with charcoal

Table II Summary of conditions and radioiodine release, Run 8 – type MSA 85851 charcoal

Time interval (min)	-340 to -240[a]	-240 to -120	-120 to 0	0 to 150	150 to 465
Main bed activity (Ci ^{130}I)[b]	465	415	370	320	240
Bed midpoint temp. range (°C)	72-93	80-93	79-80	79-147	147-429
Flow velocity (fpm at 25°C)[d]	28.5	28.5	28.5	3.8	e
Water vapor partial pressure (torr)	85	95	95	100	105
Iodine form	Fraction of radioactive iodine released (10^{-6})				
Elemental	<0.3	<0.4	0.05	0.13	0.74
Particulate	0.004	0.001	0.001	0.001	1.20
Moderately penetrating	0.5	<0.4	<0.05	<0.1	<0.4
Highly penetrating	~3.0	~8.6	~11.5	f	f
Total[g]	~3.7	~8.6	~11.5	>2.4	>3.4

[a]Loading of 100 mg of radioactive iodine took place during this period.
[b]Activity at end of time period. The half-life of ^{130}I is 12.3 hr.
[c]The ignition temperature (assumed to be 310°C) was reached at 396 min at approximately 0.8-in. bed depth.
[d]Moist air at 0.98 atm.
[e]Velocity was reduced to 1.43 fpm at 150 min (147°C), reduced to 0.71 fpm at 300 min (195°C), increased to 1.9 fpm at 457 min (369°C), and increased to 3.8 fpm at 460 min (412°C).
[f]These collection traps did not contain silver-exchanged zeolite. Total fraction found in the trap charcoal, loop cleanup charcoal, and humidifier was 47 x 10^{-6}. Total of all penetrating iodine released was 68 x 10^{-6}.
[g]Grand total fractional release of radioactive iodine was 71 x 10^{-6}.

Table III Summary of conditions and radioiodine release, Run 9 — WITCO Grade 42 charcoal

Time interval (min)	-465 to -360[a]	-360 to -240	-240 to -120	-120 to 0	0 to 180	180 to 360
Main bed activity (Ci ^{130}I)[b]	535	480	430	380	320	270
Bed midpoint temp. range (°C)	70-92	81-92	80-81	79-80	79-166	166-181[c]
Flow velocity (fpm at 25°C)[d]	28.5	28.5	28.5	28.5	3.8	0.71
Water vapor partial pressure (torr)	95	100	95	95	95	95
Iodine form	Fraction of radioactive iodine released (10^{-6})					
Elemental[e]	~0.4	<0.3	<0.3	<0.3	<0.5	<0.5
Particulate	0.03	0.05	0.06	0.001	0.4	0.002
Moderately penetrating	0.4	0.2	0.2	≤0.2	<0.2	<0.2
Highly penetrating[f]	>1.2	>7.0	>2.6	>12	15	3.1
Total	>1.6	>7.1	>3.2	>12	15.5	3.2

[a] Loading of 123 mg of radioactive iodine took place during this period.
[b] Activity at end of time period. Half-life of ^{130}I is 12.3 hr.
[c] Ignition was not reached because of the low radioactivity and the high ignition temperature of WITCO Grade 42 charcoal.
[d] Moist air at 0.98 atm.
[e] Total fractional release of elemental iodine was probably in the range 0.4×10^{-6} to 1.4×10^{-6}.
[f] The fraction which penetrated the four collection beds used during normal air flow operation and was collected in the backup bed and humidifier was 21×10^{-6}. Total fractional release of penetrating iodine was 63×10^{-6}.
[g] Grand total fractional release was 65×10^{-6}.

Table IV Summary of conditions and radioiodine release, Run 10 — WITCO Grade 42 charcoal from HFIR air cleaning system

Time interval (min)	-470 to -360[a]	-360 to -300	-300 to -120	-120 to 0	0 to 180	180 to 296
Main bed activity (Ci ^{130}I)[b]	485	460	390	345	290	260
Bed midpoint temp. range (°C)	70-88	83-88	78-83	77-78	77-139	139-376[c]
Flow velocity (fpm at 25°C)[d]	25.7	28.5	28.5	28.5	3.8	0.71
Water vapor partial pressure (torr	100	100	110	110	110	110
Iodine form	Fraction of radioactive iodine release (10^{-6})					
Elemental	-	~1.4	-	-	-	1600
Particulate	<0.2	<0.03	2.5	<0.7	<0.03	<1
Moderately penetrating	130	~76	266	156	24	≤630
Highly penetrating	8	~8	25	15	20	18
Total[e]	139	86	294	171	44	2200

[a]Loading of 100 mg of radioactive iodine took place during this period.
[b]Activity at end of time period. Half-life of ^{130}I is 12.3 hr.
[c]Ignition temperature of 283 reached at 275 min at approx. 0.3-in. bed depth. Ignition temperature is based on thermocouple rate-of-rise first reaching 20°C/min. Maximum recorded temperature was 473°C.
[d]Moist air at 0.98 atm.
[e]Grand total fractional released was 2950 x 10^{-6} or 0.295%.

Table V Summary of conditions and radioiodine release, Run 11 – type GX-176 charcoal

Time interval (min)	-470 to -360[a]	-360 to -300	-300 to -120	-120 to 0	0 to 180	180 to 360
Main bed activity (Ci ^{130}I)[b]	570	540	455	410	345	291
Bed midpoint temp. range (°C)	70-93	89-94	80-87	79-80	79-120	120-396[c]
Flow velocity (fpm at 25°C)[d]	26-28	16-26	28.5	28.5	5.8	1.9
Water vapor partial pressure (torr)	105	105	110	110	110	110
Iodine form	Fraction of radioactive iodine released (10^{-6})					
Elemental	<0.3	<0.2	<0.2	<0.2	<0.2	6.4[e]
Particulate	0.05	0.26	3.0	1.5	0.19	0.50
Moderately penetrating	0.34	<0.2	<0.2	<0.2	<0.2	<0.2
Highly penetrating	6.3	5.2	28.1	20.7	27.7	19.7
Total[f]	6.7	5.5	31.1	22.2	27.9	26.6

[a] Loading of 133 mg of radioactive iodine took place during this period.
[b] Activity at end of time period. Half-life of ^{130}I is 12.3 hr.
[c] Ignition temperature of 307°C was reached at 319.5 min after first flow reduction. Maximum recorded temperature was 504°C.
[d] Moist air at 0.98 atm.
[e] This amount of iodine was leached from tubing network between the main test bed and the adsorber traps. Most of the release probably occurred at the high bed temperature and was probably mostly elemental iodine.
[f] Not included were 7.2×10^{-6} found in loop cleanup bed and 0.4×10^{-6} in humidifier. Grand total release was 124.6×10^{-6}, or 0.0125%.

Table VI Summary of conditions and radioiodine release, Run 12 — type G-615 charcoal used 9 months at SRL

Time interval (min)	-491 to -361[a]	-361 to -300	-300 to -120	-120 to 0	0 to 180	180 to 450
Main bed activity (Ci ^{130}I)[b]	480	455	380	340	290	225
Bed midpoint temp. range (°C)	71-85	85-95	80-85	74-80	74-113	113-219
Flow velocity (fpm at 25°C)[c]	21.5	9-22	22	23	5.8	2.9
Water vapor partial pressure (torr)	110	110	115	115	110	115
Iodine form	Fraction of radioactive iodine released (10^{-6})					
Elemental	<0.6	<0.6	<0.3	<0.6	<0.5	6.0[d]
Particulate	0.09	0.06	0.5	0.3	0.02	0.008
Moderately penetrating	0.6	<0.6	<0.3	<0.6	<0.5	<2.9
Highly penetrating	8.5	10.9	44.7	28.8	35.0	73.7
Total[e]	9.2	11.0	45.2	29.1	35.0	79.7

[a] Loading of approximately 110 mg of radioactive iodine took place during this period.
[b] Activity at end of time period. Half-life of ^{130}I is 12.3 hr.
[c] Moist air at 0.98 atm.
[d] This amount of iodine was leached from the tubing network between the main test bed and the adsorber traps. Most of the release probably occurred at the high bed temperature and was probably mostly elemental iodine.
[e] Not included were 10.9 x 10^{-6} found in the loop cleanup bed and 0.3 x 10^{-6} in the humidifier water. Grand total release was 221 x 10^{-6}, or 0.022%.

Table VII Summary of conditions and radioiodine release, Run 13 – type MSA 85851 charcoal

Time interval (min)	-145 to 0[a]	0 to 60	60 to 195	195 to 315	315 to 2895	2895 to 3015
Main bed activity (Ci ^{130}I)[b]	50	47	42	37	3.3	2.9
Bed midpoint temp. range (°C)	70-71	67-71	69-71	70	68-70	70
Flow velocity (fpm at 25°C)[c]	28.5	21.1	28.5	28.5	28.5	28.5
Water vapor partial pressure (torr)	120-150	120-150	120-150	140	140-145	140-145
Iodine form	Fraction of radioactive iodine released (10^{-6})					
Elemental[d]	<0.2	<0.05	<0.06	<0.1	<20	<0.6
Particulate	0.001	0.003	0.008	0.0006	0.004	0.007
Moderately penetrating	0.2	<0.05	<0.06	<0.1	<20	<0.6
Highly penetrating	8.3	6.6	13.9	15.3	111	1.6
Total[e]	8.5	6.6	13.9	15.3	111	1.6

[a] Loading of approximately 77 mg of radioactive iodine took place during this period.
[b] Activity at end of time period. Half-life of ^{130}I is 12.3 hr.
[c] Moist air at 0.98 atm.
[d] The fraction 0.8 x 10^{-6} was leached from the tubing network between the main test bed and the adsorber traps.
[e] Not included were 2.6 x 10^{-6} found in the loop cleanup bed and 0.3 x 10^{-6} in the humidifier water. Grand total release was 160 x 10^{-6}, or 0.016%.

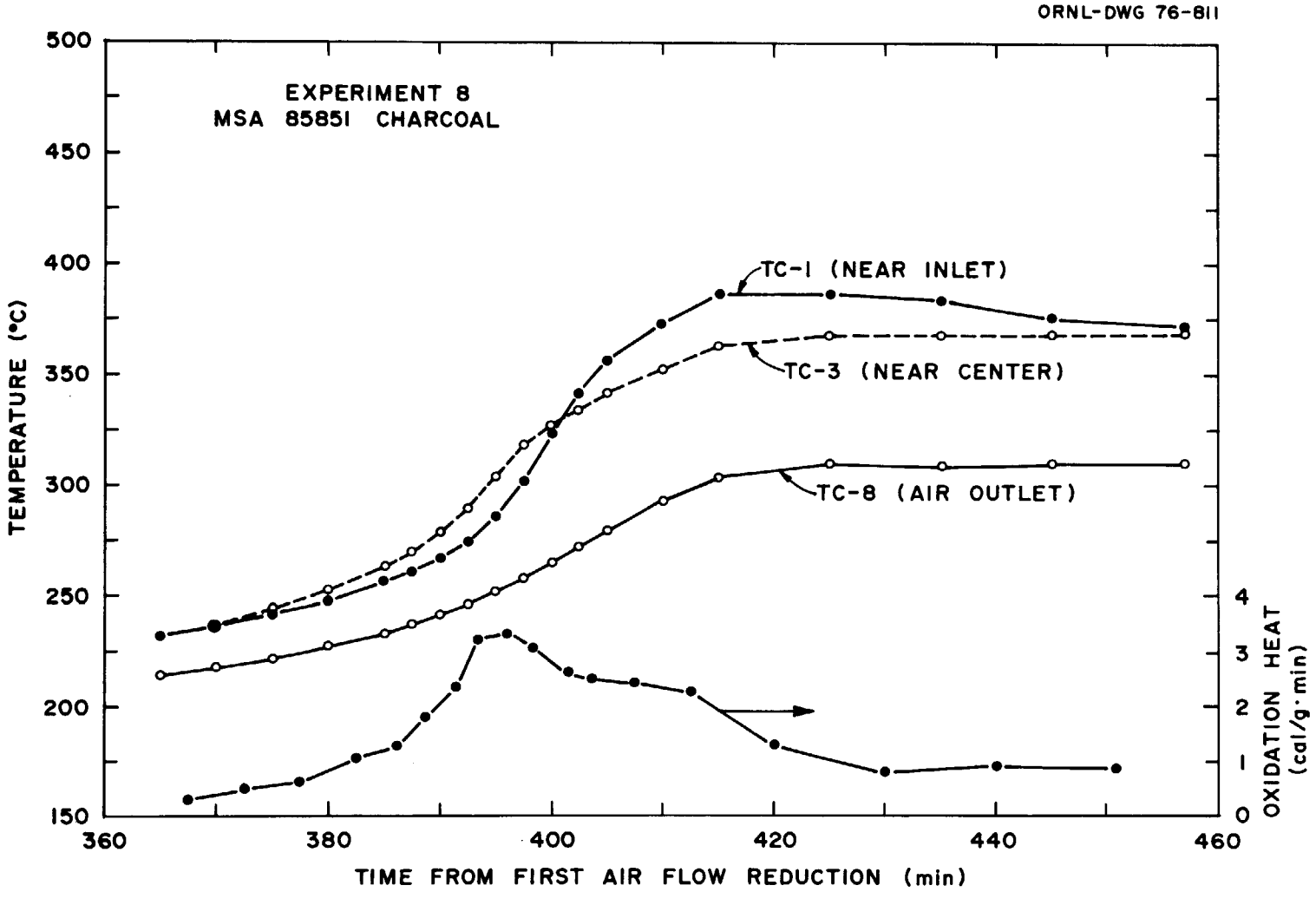

Fig. 2 Temperature behavior during Run 8 with MSA 85851 charcoal.

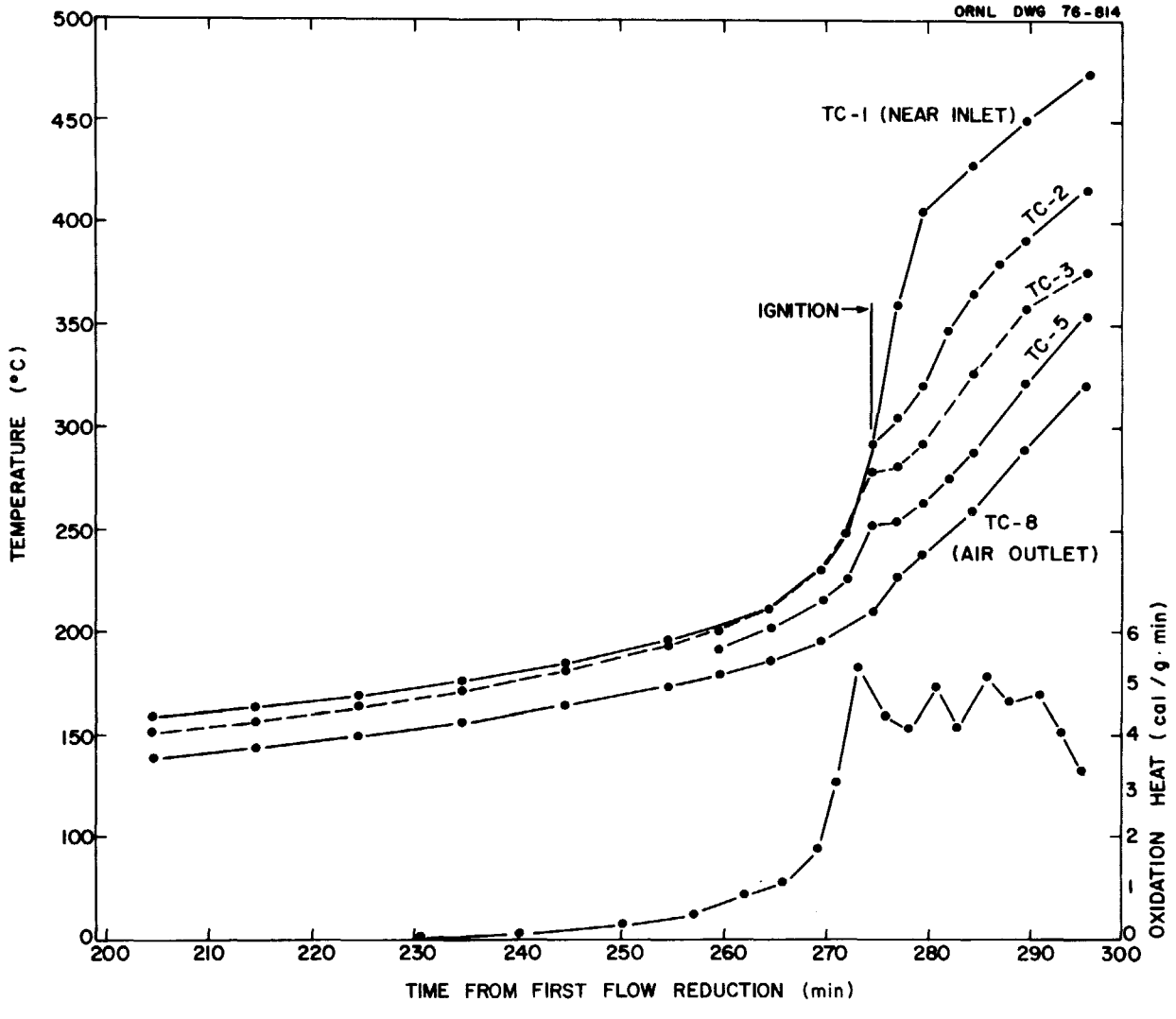

Fig. 3 Temperature behavior during Run 10 with WITCO Grade 42 used four years in the HFIR.

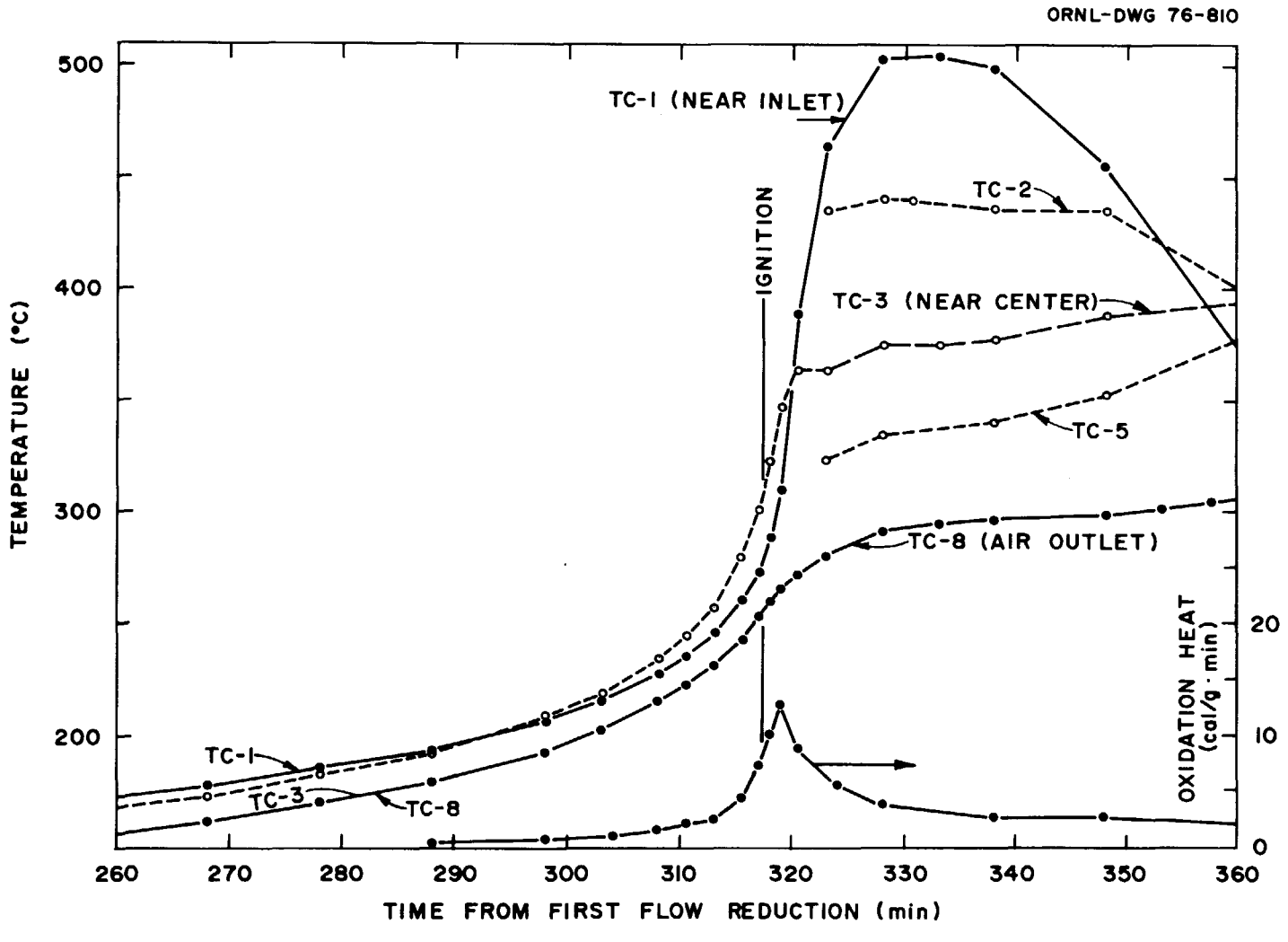

Fig. 4 Temperature behavior during Run 11 with GX-176 charcoal.

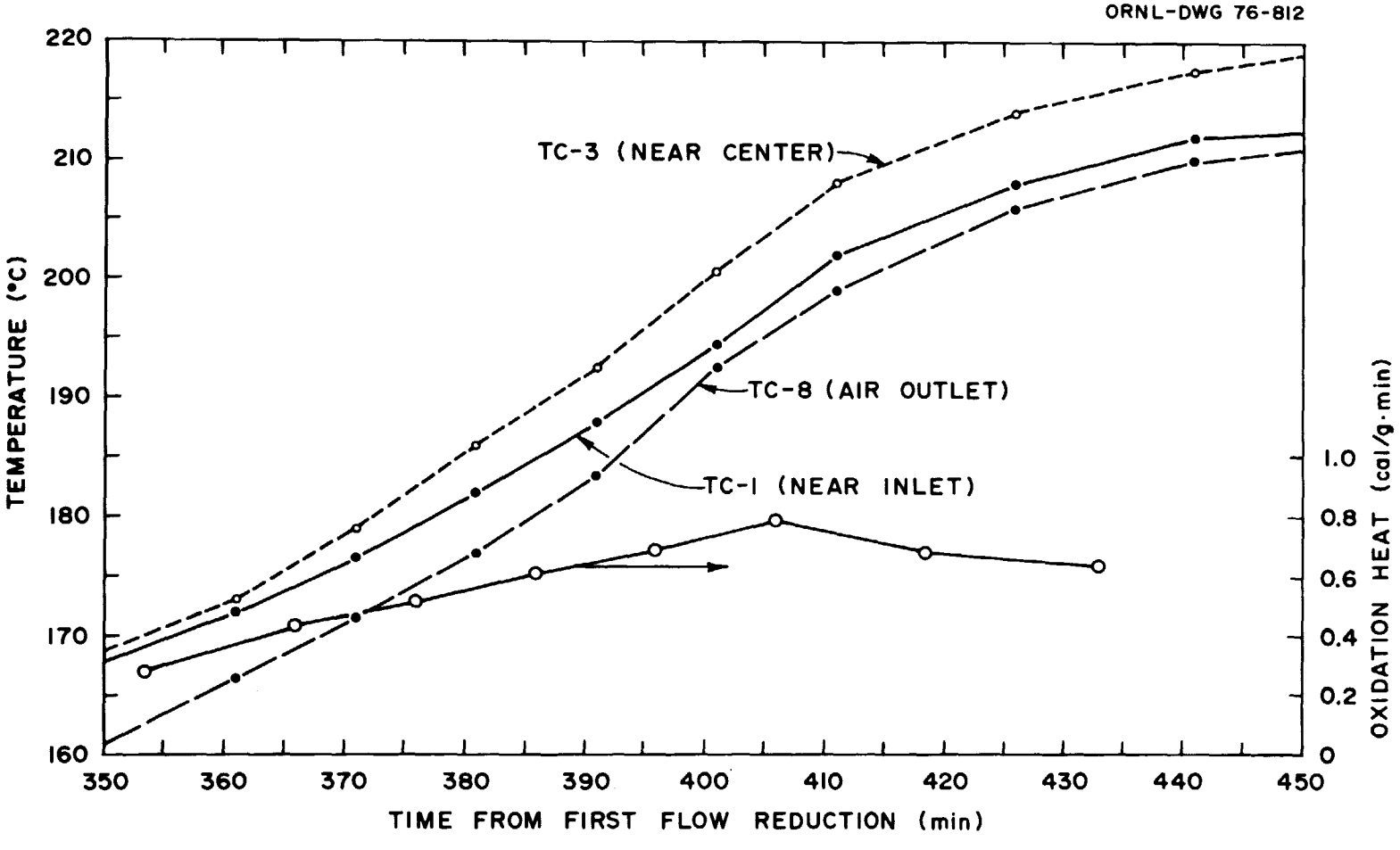

Fig. 5 Temperature behavior during Run 12 with G-615 charcoal used nine months at SRL.

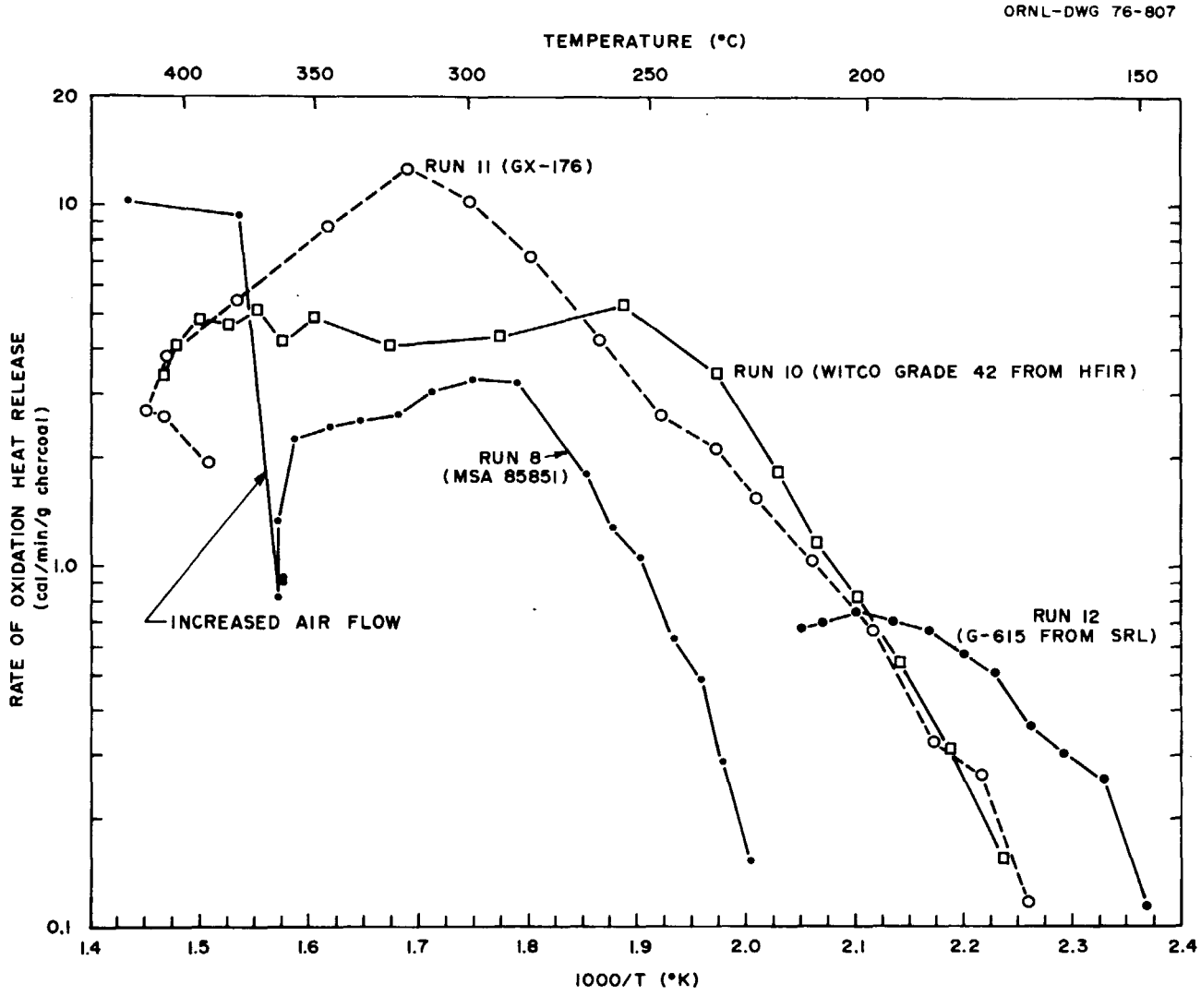

Fig. 6 Rate of oxidation heat release during experiments with moist air.

Table VIII Charcoal oxidation characteristics

Type of charcoal	Run No.	Air velocity (fpm at 25 °C)	Oxidation rate parameters		Ignition temp. (°C)
			H_o (cal/min·g charcoal)	A (cal/mole)	
MSA 85851 Lot No. 51969	8	0.7	2.05×10^8	20,000	a
WITCO Grade 42 HFIR, 4 yr service	10	0.7	1.25×10^9	20,000	283
GX-176 SR-7	11	1.6	3.37×10^6	14,500	307
G-615 (9 mo. service) SR-6	12	2.5	5.41×10^6	14,500	a

[a]Not determined.

from the same batch and nearly three times as much radioactive iodine. We believe that much of this difference resulted from the very slow rate of heatup during Run 8, which allowed consumption of chemically active sites in the charcoal. When the air flow rate was increased for the final 7 min of the experiment, the oxidation heat release rate and the bed temperatures increased rapidly as seen in Fig. 6.

In Run 9, which used WITCO Grade 42 charcoal, a maximum temperature of 184 °C was reached and measurable heat was not evolved from oxidation at that temperature. In Run 10, charcoal from the same purchase lot that had been used for four years in the High Flux Isotope Reactor (HFIR) air cleaning system at Oak Ridge released heat by oxidation at much lower temperatures and ignited at 283 °C. Previous tests with unused charcoal from the same purchase lot indicated an ignition temperature of approximately 368 °C.(1) It is quite clear that the adsorbed atmospheric contaminants promoted ignition of the base charcoal. The first 1-in. depth of our test bed contained charcoal from the first 1-1/8 in. bed in the HFIR system and the second 1-in. depth was taken from the second 1/1-8 in. HFIR bed. Infrared analysis of CCl_4 extracts revealed hydrocarbon concentrations of 145 and 71 mg/g in the respective HFIR charcoals. Based on the reported air flow during the four years of service, the concentration of adsorbed hydrocarbons was approximately 50×10^{-9} g per gram of air. This is compatible with the 290×10^{-9} g/g (excluding methane) concentration found in the HFIR building in 1967.(2) The apparent density of the HFIR charcoal indicates a total weight gain almost twice that given by the CCl_4-infrared method.

The heat from oxidation measured for GX-176 during Run 11 was slightly lower than that measured previously during Run 7.(1) As shown in Fig. 5, the oxidation heat release rate decreased and the bed temperatures stabilized after ignition.

Run 12 was made with type G-615 charcoal that had been in service for nine months at the Savannah River Laboratory (SRL) and contained 16 mg of hydrocarbons per gram according to infrared analysis of a CCl_4 extract. As shown in Figs. 5 and 6, the organic contaminants and/or TEDA impregnant apparently oxidized at relatively low temperatures, but the heat released was insufficient to ignite the base charcoal. We believe that a higher rate of temperature rise provided either by a lower air flow or a higher radiation decay heat could have resulted in ignition of the base charcoal. Both G-615 and GX-176 are reported to contain a proprietary flame retardant that could influence the oxidation heat release rates.

A sophisticated computation of temperatures of a charcoal bed containing organic material would properly assume separate oxidation heat release rate equations for the base charcoal and for the organic material, and provide a maximum total heat release for the organic material, depending on the amount present.

IV. Release and Desorption of Iodine

As mentioned previously, we used sequentially operated traps composed of high-efficiency filters, charcoal cartridges, and silver-exchanged zeolite to distinguish the iodine forms released during the course of the experiments. The results are summarized in Tables II-VII. Identification of the form of the collected iodine was uncertain in some cases. For example, most of the released elemental iodine plated out in tubing common to all of the individual collection traps. Many of our collection beds operated at an unusually low air velocity, a condition for which very little I_2/CH_3I adsorption efficiency data have been reported. For constant residence time, adsorption efficiency decreases when velocity is lowered. Our rather scattered data suggest that, for velocities in the range of 1 to 10 cm/sec, the adsorption (trapping) efficiency for methyl iodide on good-quality impregnated

charcoal will not exceed values extrapolated from the data of May and Polson[3] for nearly dry air. Another departure from conventional iodine adsorption testing techniques was the absence of clean air purging following a collection period. This permitted loosely adsorbed forms of radioactive iodine to be spread throughout the collection bed.

Highly Penetrating Iodine

Our first experiment with moist air, Run 8, revealed that most of the radioactive iodine released from the main test bed was in a chemical form unusually penetrating with respect to impregnated charcoal. For subsequent runs we eliminated the silver-plated honeycombs (used for trapping elemental iodine) and increased the number of cartridges containing silver-exchanged zeolite (AgX).

The highly penetrating nature of the released radioactive iodine is illustrated in Fig. 7. The collection trap from which these data were obtained was operated for 2 hr, beginning 4 hr after loading was completed. The trap temperature was 130°C, the air velocity was 17.3 cm/sec at 130°C, and the total residence time (charcoal + AgX) was 0.43 sec. (The collection traps were heated in order to produce low relative humidity and therefore promote high adsorption efficiency.) With the exception of Run 10, the distribution of radioactive iodine among the charcoal cartridges indicated loosely held or poorly sorbed species. We believe that the large amount of radioactive iodine on the first cartridge in Run 10 was methyl iodide. Under the operating conditions of this collection bed, each charcoal cartridge should collect more than 95% of the entering methyl iodide. In addition to G-618, eight other types of commercial impregnated charcoal were tested in other collection traps without significant difference in adsorption efficiency.

The silver-exchanged zeolite was much more efficient for collecting the highly penetrating radioactive iodine. The decrease in slope between the AgX cartridges (Fig. 7) suggests that at lease two forms of highly penetrating iodine were present. Our AgX material was prepared from type 13X molecular sieves in the 1/16-in.-diam pellet form (mean particle diam, 0.20 cm; void fraction, 0.55) exchanged to > 95% silver content. Two other batches of the same size AgX prepared by others were tried in other collection beds; no efficiency difference was observed. AgX beads in the 10-20 mesh range and granular AgX in the 12-16 mesh range (particle diam, 0.16 cm; void fraction, 0.43) were also tried, and both were found to have higher efficiencies. The mean particle size and void fraction differences could easily account for the higher adsorption efficiency because of improved gas-phase mass transfer.

Beginning with Run 10, we added high-temperature backup beds in the circuits used during operation at normal air flow rates. Beginning with Run 12, all flow lines were routed through these beds which contained a total of 45 cm^3 of Hopcalite, an oxidizing catalyst, MSA lot No. 21215.* This was followed by a total of 42 cm^3 of silver-exchanged zeolite pellets, all in a 2.84-cm-diam tube. Table IX shows the results of most of the high-temperature backup traps. Although the AgX appears to have performed efficiently, a large amount of radioactive iodine reached the loop cleanup filter which contained 550 cm^3 of BC-721, an unimpregnated charcoal.

*Mine Safety Appliances Co.

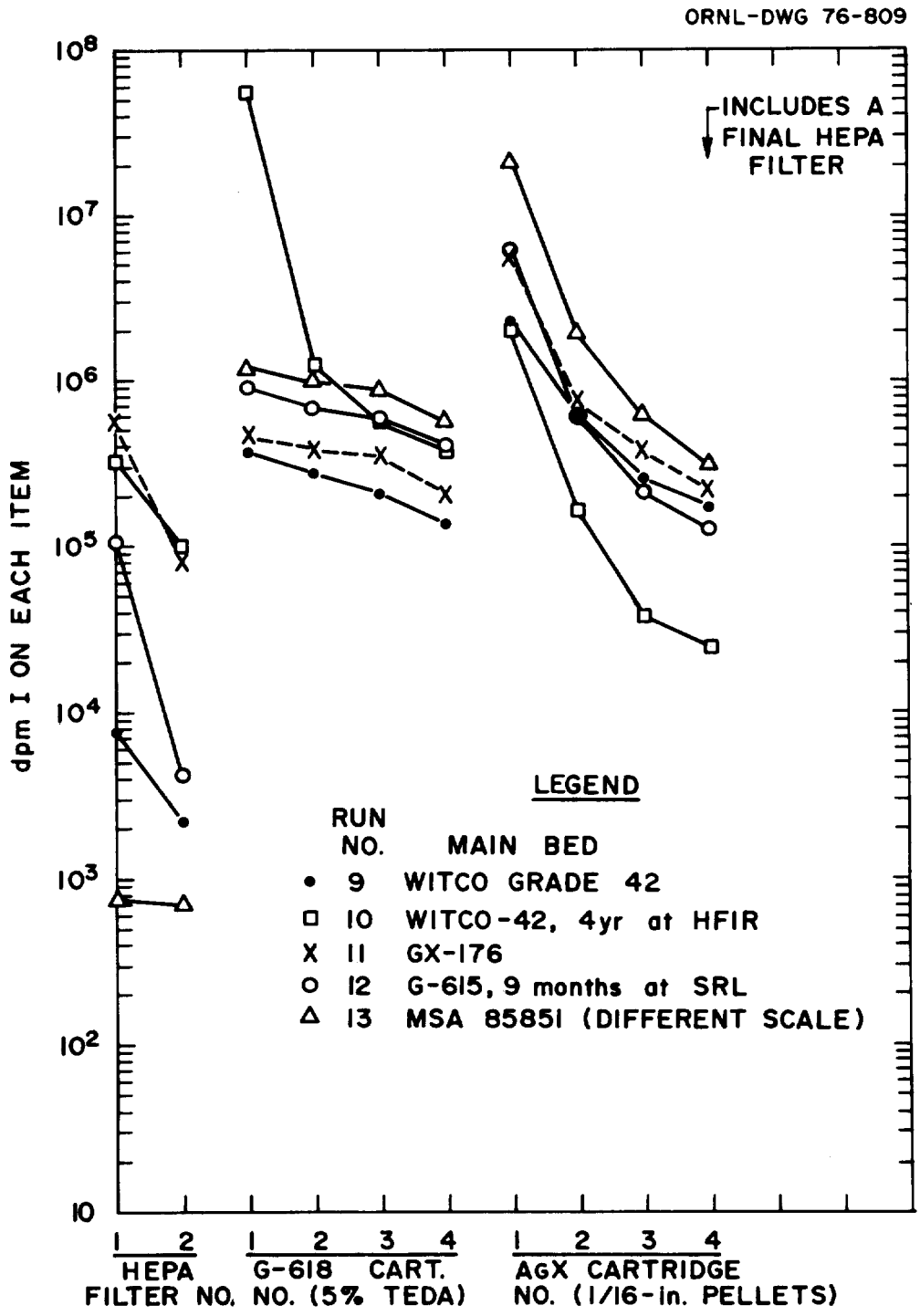

Fig. 7 Distribution of radioactive iodine among components of a collection trap.

Table IX Performance of high temperature backup beds

Component	Approximate temperature (°C)	Run 10 (10^5 dpm ^{131}I)	Run 11 (10^5 dpm ^{131}I)	Run 12 (10^5 dpm ^{131}I)	Run 13 (10^8 dpm ^{130}I)	
HEPA filter	150	0.0005	0.0010	<0.002	0.004	0.0001
1st Hopcalite	280	0.41	0.52	0.34	0.010	0.24
2nd Hopcalite	320	0.52	0.65	0.63	0.009	0.26
3rd Hopcalite	360	0.78	1.64	1.5	0.036	0.30
1st AgX	380	17.7	72.2	1.9	13.2	20.0
2nd AgX	400	0.0034	18.2	0.007	3.3	0.14
3rd AgX	420	0.0069	1.1	0.005	0.0002	0.006
HEPA filter	200	<0.0005	0.0003	Not used	Not used	Not used
Loop cleanup bed[a]	70	16.5	31.8	37.7	5.98	
Time in use (min)		300.0	410.0	491.0	460.0	2700.0

[a]Apparent penetration of above high temperature backup beds.

Such large penetrations are difficult to understand. The distribution of radioactive iodine in the loop cleanup filter was examined to determine whether back-diffusion from the humidifier and main test bed during the 8-day cooldown period could be the source of the iodine. We discovered that some back-diffusion had occurred, but only perhaps 10% of the total on the cleanup bed. Ackley and Davis tested this same catalyst and found it to be beneficial when CH_3I was used but detrimental when I_2 was being tested.(4) A single test with AgX only in a high-temperature backup trap in our system was inconclusive because of possible penetration through a Hopcalite-AgX combination used later in the same run. Our calculations indicate that much of the improved performance of AgX with methyl iodide with increased temperature can be accounted for by improved gas-phase mass transfer.

Two other adsorbing materials were tested for their ability to trap the highly penetrating iodine. AC-6120* is a noncombustible adsorbent which traps I_2 and CH_3I very efficiently.(5) It is a porous form of amorphous silicic acid impregnated with $AgNO_3$. We tested this bead-shaped material in our standard collection beds at 130°C during Run 13. Its performance was shown to be comparable to the charcoals and inferior to AgX for trapping our highly penetrating iodine. Similar results were obtained for GX-135, a granular silver nitrate-coated aluminum silicate-based material which is not currently being manufactured.

The rates of release of highly penetrating iodine and the moderately penetrating form, which behaved like methyl iodide, are summarized in Table X. The release rates for the highly penetrating form were generally within the range 7 to 10×10^{-6}/hr. Release rates during the first time periods shown for each run were lower. This was the period for loading of the radioactive iodine and, on the average, only half of the iodine was on the main test bed available for desorption. Based on the true amount on the bed, these first period rates should be approximately doubled. In Run 13, with reduced radioactivity, the release rates were essentially normal for the first two time periods listed, but then decreased slowly as time progressed and the radioactive iodine decayed to much lower intensities.

Samples of gas taken from the air reservior tank were analyzed by gas chromatography. Methane was always detected and occasionally other hydrocarbons as well. Following Run 9 the reservoir contained 10 ppm methane (CH_4). The sample of gas following Run 10 contained 160 ppm methane, approximately 15 ppm ethane (C_2H_6), and approximately 45 ppm propane (C_3H_8). Gas from Run 11 contained 95 ppm methane and a trace of ethane, and gas from Run 12 contained 16 ppm methane.

Characteristics of the Highly Penetrating Iodine

Beginning with Run 10, we added a sampling circuit (not shown in Fig. 1) in an attempt to collect and identify the highly penetrating iodine form(s). The circuit consisted of two HEPA filters, a condenser at 0°C, a freeze trap at -78°C, and a trap at -78°C containing cartridges of type 13X sodium zeolite, silica gel, Tenax, and Porapac-Q (the latter two are commercial chromatograph packings) alone or in combinations, depending on the experiment. The HEPA filters, condenser, and freeze traps collected only very small amounts of the radioactive iodine. All of the sorbents retained the radioactive iodine efficiently at -78°C, but the Porapac-Q appeared to release the iodine more easily when the sorbents were subsequently warmed for transfer of the radioactive iodine to an evacuated stainless steel holding tank.

*Bayer/Leverkusen.

Table X Rate of release of penetrating forms of radioactive iodine

Run No.	Amount of radioactive iodine (Ci ^{130}I)	Time from first flow reduction (min)	Average temp. (°C)	Partial pressure of water (torr)	Release rate x 10^6 (fraction/hr) Moderately penetrating iodine	Highly penetrating iodine
8	0-465	-340 to -240	82	85	0.3	~2
	465-370	-240 to 0	82	95	<0.1	~5
	370-240	0 to 465	~150	105	<0.1	~6
9	535-380	-360 to 0	81	95	0.2	~7
	380-320	0 to 180	125	95	<0.1	5
	320-270	180 to 360	174	95	<0.1	1.0
10	0-485	-470 to -360	79	100	51	4.4
	485-345	-360 to 0	79	110	83	8.0
	345-290	0 to 180	~110	110	16	13
	290-260	180 to 296	~260	110	<325	9.3
11	0-570	-470 to -360	82	105	0.2	3.4
	570-410	-360 to 0	82	110	<0.1	9.0
	410-345	0 to 180	~100	110	<0.1	9.2
	345-290	180 to 360	~260	110	<0.1	6.6
12	0-480	-491 to -361	78	110	0.3	3.9
	480-340	-361 to 0	80	115	<0.3	14
	340-290	0 to 180	~94	110	<0.2	12
	290-225	180 to 450	~170	115	<0.6	16
13	0-50	-145 to 0*	70	135	0.08	3.4
	50-37	0 to 315	70	135	<0.04	6.8
	37-3.3	315 to 2895	69	142	<0.5	2.6
	3.3-2.9	2895 to 3015	70	142	<0.3	0.8

*For Run 13, time "0" corresponds to end of loading of radioactive iodine.

After several days to allow reduction of the radiation intensity by decay, the contents of the tank were admitted to a mass spectrometer for mass identification. Relatively large amounts of air and CO_2 adsorbed along with the radioactive iodine during the experiment were present in the holding tank and provided a high background which interferred with the iodine-containing mass peaks in the mass spectrometer. A positive peak at mass 130, presumably $H^{129}I$, was observed in the gas from Run 10; however, we believe that this is a result of reaction with some system component. In later experiments we decreased the air + CO_2 background by concentrating the radioactive iodine in a small trap containing cooled Tenax, but the mass results were inconclusive.

The original radioactive iodine loaded onto the main test bed contained ^{129}I and ^{127}I in the ratio of 6:1. The mass spectrometer revealed several paired mass peaks with approximately this same ratio. The larger of the paired peaks occurred at masses 131, 141, 168, 181, 186, 191, and 198. Mass peaks at 262, 278. 281, 331, and 354 were also seen frequently but appeared to be associated with the background emanating from within the needle valve, probe, and mass spectrometer internals.

None of these masses corresponds to a common iodine compound; in reality, we do not know whether any of them actually contained iodine. Since all of the charcoals in the main test bed contained impregnant iodine (^{127}I) in greater quantity than the loaded radioactive iodine, we expected that the highly penetrating iodine leaving our test bed might have $^{129}I/^{127}I$ ratios of much less than 6:1.

Several incidental noniodine-containing masses were observed. From Runs 11 (new GX-176) and 12 (new MSA 85851) we observed masses 101, 103, and 105, corresponding to the fragment $CFCl_2^+$. From Run 12 (G-615 used nine months at SRL) we observed Freon 113 (1,1,2-trichloro-1,2,2-trifluoroethane), Freon 112 (1,1,2,2-tetrachlorodifluoroethane), and a large amount of trichloroethylene.

From the amount of radioactive iodine collected in the condenser in this circuit we could estimate the solubility of the form of iodine present. For Run 10 (which contained predominantly a methyl iodide-like form), as well as later runs (which exhibited only the highly penetrating from of iodine), we calculated partition coefficients $\leq$ 10 g I/cm^3 water/g I/cm^3 air at 0°C. The radioactive iodine in the condensate was readily extracted by carbon tetrachloride. This behavior and the low partition coefficient suggest some organic iodide from(s). Formation and release from the main test bed was essentially independent of air velocity and temperature. Only traces of highly penetrating iodine were observed during the dry air experiments. We observed that most of the radioactive iodine became tightly bound after a long holdup time on most of the mentioned adsorbents (including charcoal). J. G. Wilhelm[6] has shown that aryl iodides exhibit much of the behavior described above, but we have not been able to detect any of this class of compounds.

Release of Methyl Iodide

A small amount of methyl iodide-like material either penetrated through or was released from the main test bed during the loading phase of each experiment. The identification was based only on its trapping behavior on impregnated charcoal. Methyl iodide-like material was not observed later in the runs except for Run 10 in which this type of material was continuously released. With the dry air experiments,[1] most of the form of iodine described as "penetrating" is believed to have been methyl iodide although no positive identification was made. Small amounts of the highly penetrating form were present in at least some of the dry air experiments; however, it was rarely detected because of smaller collection beds, only occasional use of AgX sorbent, and concealment by ^{131m}Xe radioactivity (a daughter of ^{131}I) that accumulated in the recirculating loop.

Desorption of Elemental Iodine

Since very little elemental iodine was released from the end of the main test bed, we used data collected with the collimated gamma scanner to calculate iodine adsorption/desorption coefficients. Gamma scan data are shown in Fig. 8 and in Table XI. A computer program was written to calculate the partial pressure of iodine in equilibrium with the charcoal according to the observed rate of movement within the bed. The rate of mass transfer for elemental iodine is very rapid, so that there is an essentially continuous equilibrium between the charcoal and the vapor phase. Therefore, the extent of movement of iodine should be directly proportional to the air velocity within the bed. The gamma scanner monitored 17 increments, or slabs, along the length of the bed. We assumed that iodine which desorbed from the first (inlet) slab was readsorbed on the second slab, etc. We assumed a linear adsorption isotherm; this means that the partial pressure of iodine is directly proportional to the mass concentration on the charcoal, $P = x/k$, where P is the partial pressure of iodine (atm), x is the total concentration of iodine on the charcoal, and k is the adsorption coefficient.

The calculation is most accurate for the first 1/2-in. of bed depth; hence we correlated experimental k values for this region with the temperature obtained from a thermocouple located in that region of the bed. Results are shown in Fig. 9. For each type of charcoal we can express the value of k satisfactorily with the equation $k = k_o e^{-A/RT}$, where A is the activation energy (cal/mole), R is the gas constant, T is the absolute temperature (°K), and k_o is a constant for each type of charcoal (g I/g charcoal·atm I_2).

The coefficients calculated for these moist air experiments are essentially the same as those determined previously for the dry air experiments.[1] The one exception is Run 10, which used heavily contaminated charcoal that desorbed iodine at a rate approximately six times greater than other charcoals.

When test bed temperatures remained constant, the calculated coefficients generally rose somewhat with longer times indicating stronger adsorption. Therefore, the coefficients shown in Fig. 9 should be used only for short-term situations such as those in our experiments. The relatively large mass of radioactive iodine used in our experiments may have contributed to this behavior.

We had expected that significant differences in adsorption coefficient might be observed for different charcoals since previous observations have demonstrated a strong effect of relative potassium and iodine concentrations on iodine desorption.[1,7,8] Our assumption that the observed movement of iodine within the test bed was simple elemental iodine adsorption/desorption could be in error; the high radiation field could enhance the movement by some yet unrecognized mechanism. The ion chamber gamma scanner readings contained distortions introduced by collimator inefficiency and the inclusion of scattered radiation. No corrections were made for these distortions which made the low-activity readings appear higher than their true levels. F. G. May performed a calibration that demonstrated the type of distortion inherent in the system.[9]

V. Conclusions

Heat from the oxidation of charcoal and organic contaminants is an important contributor to attainment of ignition. Computer programs such as CHART[1] and TOOHOT[10] have demonstrated satisfactory calculation of charcoal bed temperatures, including ignition, when heat release resulting from oxidation of the charcoal was included.

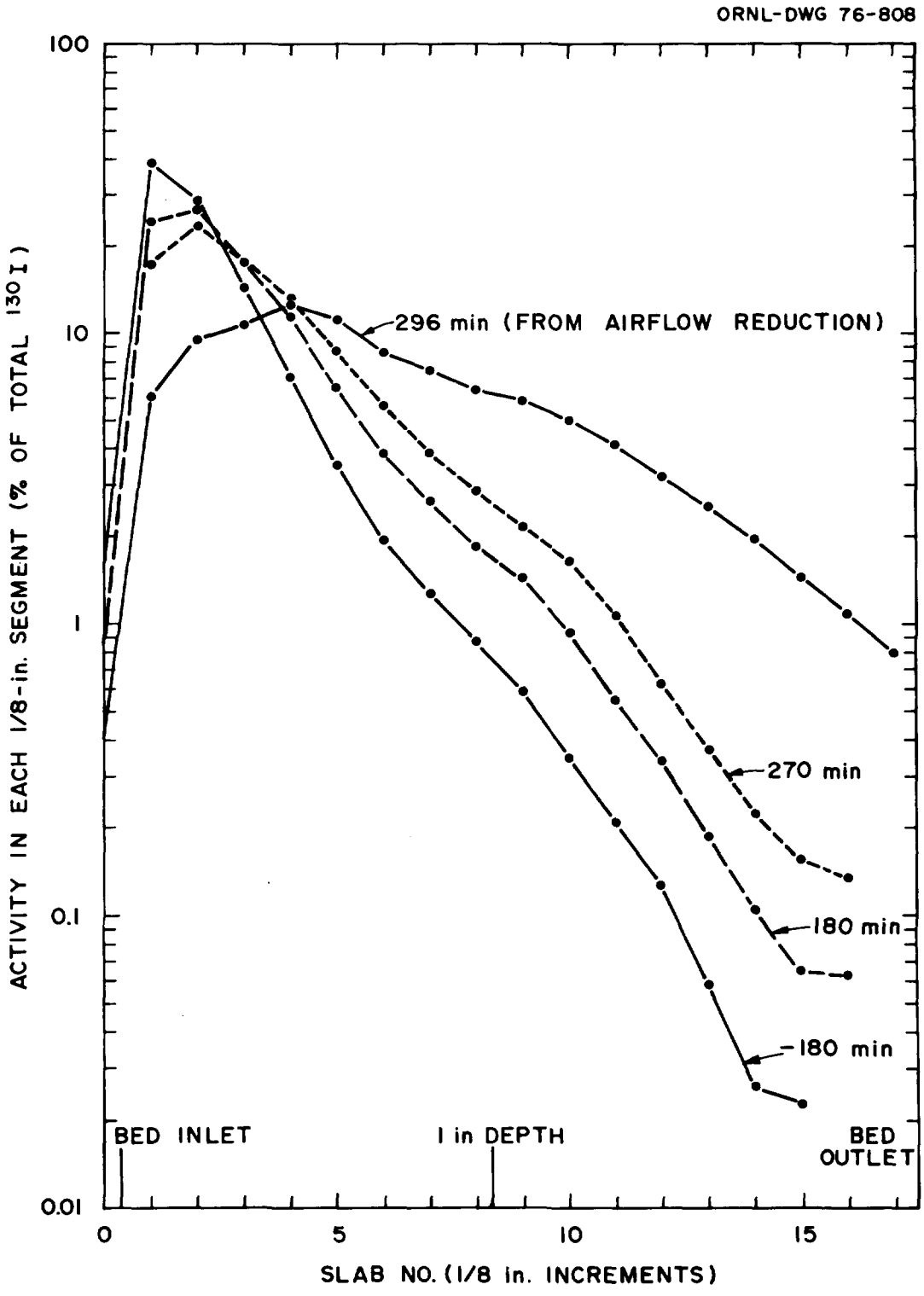

Fig. 8 Distribution and movement of radioactive iodine in the main test bed of Run 10.

Table XI Distribution of radioactive iodine in main test bed

Slab No.*	Percent of total radioactivity in each slab																	
	Run 8				Run 9			Run 11				Run 12				Run 13		
	Time from flow reduction (min)				Time from flow reduction (min)			Time from flow reduction (min)				Time from flow reduction (min)				Time from end of loading (min)		
	-235	0	300	465	-360	0	360	-360	0	180	360	-360	0	180	450	0	1440	2880
1	17.7	12.4	7.5	3.2	16.1	13.9	6.3	6.3	4.7	2.9	0.5	4.9	3.2	2.6	1.4	2.5	2.1	2.0
2	59.7	61.4	57.4	26.2	55.2	53.3	46.8	64.2	61.4	59.7	7.8	59.0	55.3	54.3	37.2	61.3	58.2	56.4
3	13.3	15.9	23.3	22.8	16.2	18.3	26.9	20.2	23.5	26.4	11.2	22.6	25.9	27.0	34.8	25.2	27.9	29.0
4	3.92	4.48	5.93	17.7	5.04	6.33	10.2	4.62	5.37	5.78	11.6	7.36	8.60	8.90	15.2	5.56	6.16	6.46
5	1.62	1.89	2.27	12.7	2.45	3.11	4.21	1.71	1.97	2.07	12.2	2.47	3.01	3.12	5.53	2.12	2.31	2.38
6	0.86	0.95	1.03	7.74	1.01	1.24	1.56	0.91	1.00	1.02	11.8	1.24	1.46	1.49	2.44	1.00	1.06	1.11
7	0.52	0.55	0.55	4.09	0.60	0.75	0.84	0.59	0.61	0.62	10.8	0.75	0.86	0.88	1.23	0.65	0.70	0.72
8	0.39	0.42	0.40	2.34	0.38	0.47	0.55	0.42	0.43	0.44	9.47	0.49	0.54	0.55	0.72	0.44	0.45	0.51
9	0.27	0.28	0.27	1.18	0.23	0.29	0.34	0.30	0.31	0.31	7.59	0.33	0.36	0.36	0.43	0.31	0.31	0.38
10	0.18	0.19	0.16	0.55	0.14	0.18	0.21	0.21	0.22	0.23	6.10	0.24	0.25	0.26	0.31	0.23	0.23	0.29
11	0.13	0.13	0.11	0.28	0.10	0.11	0.14	0.15	0.16	0.16	5.50	0.17	0.19	0.18	0.22	0.16	0.16	0.22
12	0.09	0.09	0.07	0.13	0.07	0.08	0.10	0.10	0.11	0.11	2.75	0.11	0.12	0.12	0.15	0.12	0.11	0.16
13	0.08	0.07	0.04	0.08	0.07	0.07	0.08	0.07	0.07	0.07	1.44	0.07	0.08	0.08	0.10	0.06	0.07	0.10
14								0.04	0.04	0.05	0.61	0.05	0.05	0.05	0.07	0.04	0.04	0.09
15											0.26							
16											0.18							
17											0.16							
Background	0.49				0.56			0.34				0.35				0.37		
Bed midpoint temp. (°C)	85	82	196	429	87	81	178	85	78	120	394	83	78	113	219	73	73	73

*Each slab is determined by collimator movement of 0.125 in. (0.318 cm).

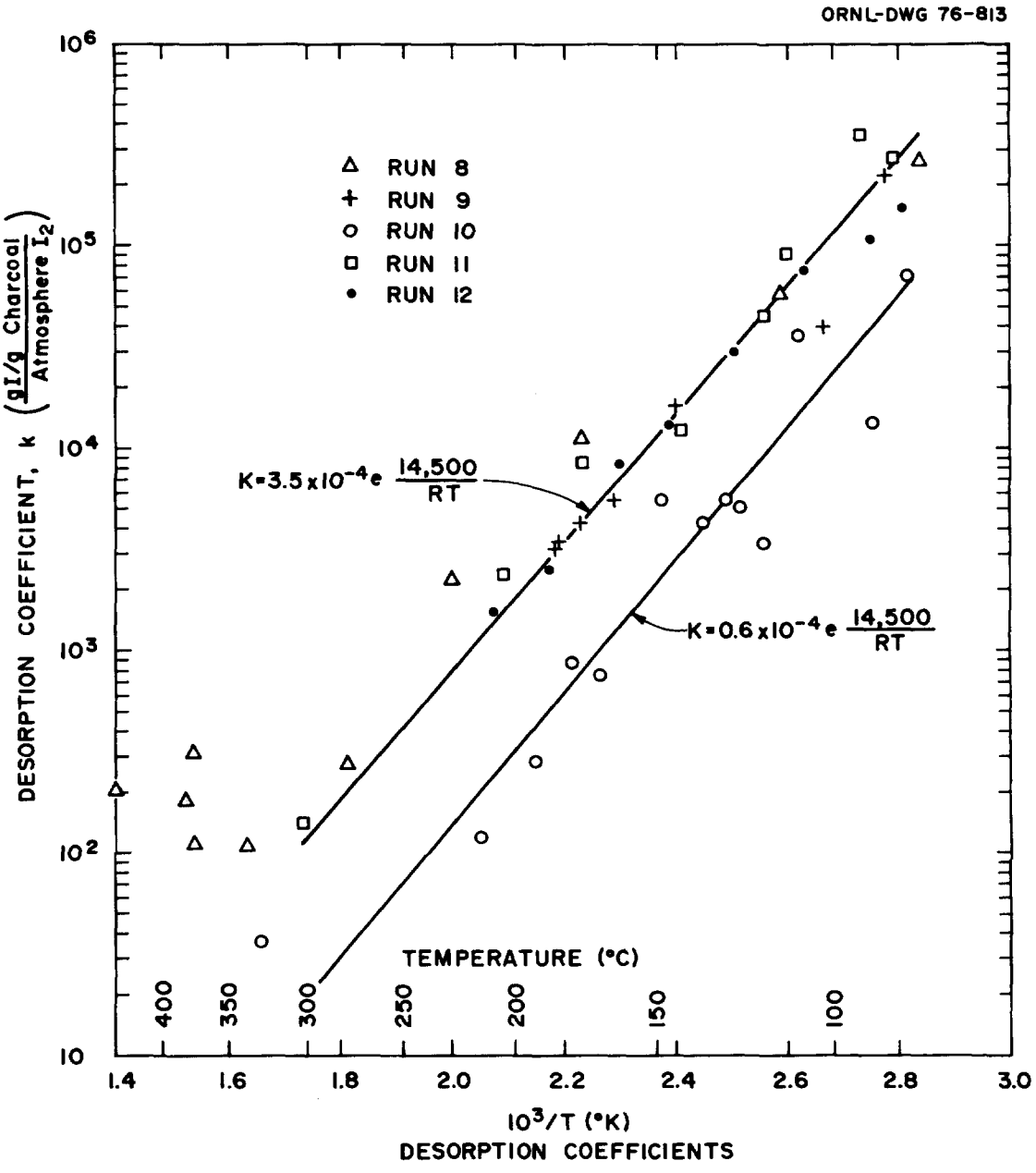

Fig. 9 Desorption coefficients calculated for radioactive iodine in the main test bed of experiments conducted in moist air.

Movement of radioactive iodine within the charcoal bed and desorption from the end of the bed were trivial before ignition at the low air flow rates used in our experiments (0.7 to 3.8 fpm at 25°C reference). Higher flow rates would enhance radioactive iodine movement and desorption to some extent, but unusually large heat sources would be required to reach crucial temperatures.

The decreasing heat release rate, stabilized bed temperatures, and very slow radioiodine desorption rates following ignition when low air velocities prevail provide both time and opportunity for combating the combustion. Increased air velocity or induced turbulence would tend to increase the rate of heat release following ignition.

The formation and release of highly penetrating iodine, although occurring at a very low rate, appear to be promoted by moisture and radiation. The radiation effect apparently saturated above 1.0 Ci $^{130}I/cm^3$ charcoal. Identification and trapping of this material were not completely solved; nevertheless, the use of some silver-exchanged zeolite is recommended in the collection system whenever the highly penetrating form is suspected to be present.

VI. References

1. R. A. Lorenz, W. J. Martin, and H. Nagao, "The behavior of highly radioactive iodine on charcoal," in Proceedings of the Thirteenth AEC Air Cleaning Conference, CONF-740807 (March 1975), pp. 707-35.

2. R. E. Adams et al., Nuclear Safety Program Annual Progress Report for Period Ending December 31, 1967, USAEC Report ORNL-4228 (April 1968), p. 118.

3. F. G. May and H. J. Polson, Methyl Iodide Penetration of Charcoal Beds: Variation with Relative Humidity and Face Velocity, AAEC/E-322 (September 1974).

4. R. D. Ackley and R. J. Davis, Effect of Extended Exposure to Simulated LMFBR Fuel Reprocessing Off-Gas on Radioiodine Trapping Performance of Sorbents (Final Report), USAEC Report ORNL-TM-4529 (August 1974).

5. J. G. Wilhelm and H. Schuettelkopf, "Inorganic adsorber materials for trapping of fission product iodine," in Proceedings of the Eleventh AEC Air Cleaning Conference, CONF-700816 (December 1970), pp. 568-99.

6. J. G. Wilhelm, Kernforschungszentrum Karlsruhe, personal communication.

7. R. O. Lingjaerde and L. Podo, A Study on the Trapping of Iodine at High Temperatures on Activated Charcoal, Dragon Project Report DP-Report-213 (September 1963).

8. A. G. Evans, "Effect of alkali metal content of carbon on retention of iodine at high temperatures," in Proceedings of the Thirteenth AEC Air Cleaning Conference, CONF-740807 (March 1975), pp. 743-57.

9. F. G. May, Comparison of Charcoals in Removing Iodine from Air-Streams at High Temperature, AERE-R4145 (1962).

10. E. A. Bernard and R. W. Zavadoski, "The calculation of charcoal heating in air filtration systems," in Proceedings of the Thirteenth AEC Air Cleaning Conference, CONF-740807 (March 1975), pp. 845-61.

DISCUSSION

WILHELM: Do you think the penetrated compound could be an aryl iodide in which the iodine won't react or isotopicly exchange because of the structure?

LORENZ: I know that you have mentioned this possibility before and have published some experimental results with that type of compound. In our attempts to identify this material, we used the mass spectrometer, but were not successful in finding masses of common iodine compounds, including the type of aryl iodides you described.